ANKARA YILDIRIM BEYAZIT UNIVERSITY

JOURNAL OF OPTIMIZATION AND DECISION MAKING

JOURNAL OF OPTIMIZATION AND DECISION MAKING

YEAR: 2023 **VOLUME:** 2 **NUMBER:** 1

AYBU 15 Temmuz Şehitleri Yerleşkesi, Ayvalı Mah., Gazze Cad., 150. Sokak, Antares AVM Yanı Etlik,
Keçiören / B519, Tel: 0(312) 906 2321, e-mail: berdebilli@ybu.edu.tr/ennacar@ybu.edu.tr
https://aybu.edu.tr/jodm

ANKARA YILDIRIM BEYAZIT UNIVERSITY

JOURNAL OF OPTIMIZATION AND DECISION MAKING

ANKARA YILDIRIM BEYAZIT UNIVERSITY

JOURNAL OF OPTIMIZATION AND DECISION MAKING

Advisory Board / Danışma Kurulu

ANKARA YILDIRIM BEYAZIT UNIVERSITY

JOURNAL OF OPTIMIZATION AND DECISION MAKING

Journal of Optimization and Decision Making (JODM) issued by Ankara Yıldırım Beyazıt University (AYBU) is an international peer-reviewed online academic journal published in Turkish and English in all fields of industrial engineering for any query. JODM addresses the theoretical framework, models, computational studies, and conceptual development of operations research together with current developments and practices. This journal combines the high standards of a traditional academic approach with the practical value of applications. Hence, JODM aims to create an academical platform for the exchange of ideas and the presentation of new achievement in theory and application, wherever engineering and science meet the administrative and economic environment by applying operational research, and constructive suggestions on optimizing the current resources.

Current Publication Schedule

The journal published two times per year (June-December). The journal covers theoretical and some applied aspects of science and technology and informs the reader of new trends in basic science and technology. JODM accepts submissions in the form of research articles, review articles, and short notes.

Open Access Policy

The Journal is an open access journal which means that all content is freely available without charge to the user or his/her institution. Users are allowed to read, download, copy, distribute, print, search, or link to the full texts of the articles in this journal without asking prior permission from the publisher or the author All articles published are available on the journal web page https://aybu.edu.tr/jodm

Publication Fees

There is no submission, evaluation or publication fee for this journal. All accepted articles are freely available online upon publication.

ANKARA YILDIRIM BEYAZIT UNIVERSITY

JOURNAL OF OPTIMIZATION AND DECISION MAKING

CONTENTS / İÇİNDEKİLER

Research Articles / Araştırma Makaleleri

Simulation study for Changing some roundabouts in Karbala government into signalized roundabouts

Ali Fadhlallah Hussein[1] - PhD. Hussein Ali Ewadh[2] - PhD. Raid R.A. Almuhanna[3]

[1] Civil Engineering Department, University of kerbala, karbala, ORCID No: https://orcid.org/0009-0006-9652-5574
[2] Civil Engineering Department, University of Babylon, Babylon, ORCID No: https://orcid.org/0000-0001-5401-7244
[3] Civil Engineering Department, University of kerbala, karbala, ORCID No: https://orcid.org/0000-0002-1426-0044

Keywords

A Simulation Study, Signalized Roundabout, PTV Vissim, Level of Service

Abstract

This research aims to analyze and evaluate some of the main roundabouts in Karbala Governorate after they were converted to signalized roundabouts by the simulation program PTV VISSIM. These roundabouts suffer from large traffic, which leads to a significant decrease in their level of service (LOS), especially at peak times, when it is observed that the traffic police intervene to direct the traffic and reduce congestion. Therefore, one of the proposals was to use the light signal to control the roundabout at peak times.

The results were positive in the first roundabout, as the level of service (LOS) decreased from F to D, and the LOS of the other roundabout also decreased, though to a lesser extent, from F to E due to heavy traffic volumes at peak times and design errors in the roundabout.

Research Article
Submission Date : 09.04.2023
Accepted Date : 02.05.2023

1. Introduction

Iraq's population growth has impacted transportation networks, particularly in Karbala, leading to congestion at roundabouts and delays in traffic flow. Roundabouts are sometimes treated as intersections with traffic signals, and traffic police are needed to manage high volumes during peak times. This highlights the need to study roundabout performance and determine when to convert them into signalized roundabouts for effective traffic management.

2. Problem research

Karbala roundabouts often experience significant traffic congestion, particularly during peak hours, requiring traffic police intervention to manage and alleviate the congestion. This indicates that the roundabouts are not functioning optimally in terms of facilitating smooth traffic flow without stopping, especially during peak times.

3. Aim and Objectives of the research

- Compare functional performance of roundabouts and signalized roundabouts.
- Determine traffic volume threshold for converting roundabout intersection to signalized roundabout.

4. Traffic volumes in Iraq

The population increase in Karbala has led to a significant rise in the number of vehicles on the roads. This has caused congestion, which has become increasingly evident in recent years. The Ministry of Planning has published statistics on the number of registered private sector cars and all types of plates at the Directorate of Traffic between 2016 and 2020.

5. Simulation Concept

Simulation is an essential tool for studying traffic and transportation problems by designing a model close to reality. It helps to analyze issues such as congestion, delay, level of service, and traffic network performance. Traffic simulation programs are necessary for evaluating traffic in all its details.

[1] Resp author; e-mail: ali.f@s.uokerbala.edu.iq

6. Roundabout

Roundabouts are generally defined as a circular intersection in which the velocities are finite and cannot be exceeded. Likewise, the vehicle does not stop moving, but its speed decreases significantly, according to the determinants designated for this type of intersection The vehicles revolve around a median island, and they head as they rotate toward the special exits at the intersection(Ahac and Dragčević 2021)

7. Signalized Roundabout

Combined roundabouts with traffic lights are not common due to the public's reluctance to accept this hybrid system. Most research on roundabouts and traffic lights focuses on them as separate entities. However, a study by Lakouari, Oubram et al. (2018) found that the combination of traffic signals with roundabouts can work effectively for medium traffic volumes. They recommend using the combined system in places with medium to high traffic volumes to address roundabout issues before converting them into traffic signals.

8. Study Area

All roundabouts are located in the urban CKD area These roundabouts contain a high traffic density compared to the other roundabouts, and many violations of priority laws have been noted to eliminate congestion and shorten the travel time as much as possible.

9. Characteristics of Selected Roundabout

The design characteristics of roundabouts greatly impact their performance, and it is important to consider these details when creating simulation models in programs such as Vissim. Key factors include all directions of the roundabout being at the same level as sea level, the absence of heavy truck traffic within the roundabouts, no pedestrian crossings on any roundabouts, and no nearby car parks.

10.layout Roundabout

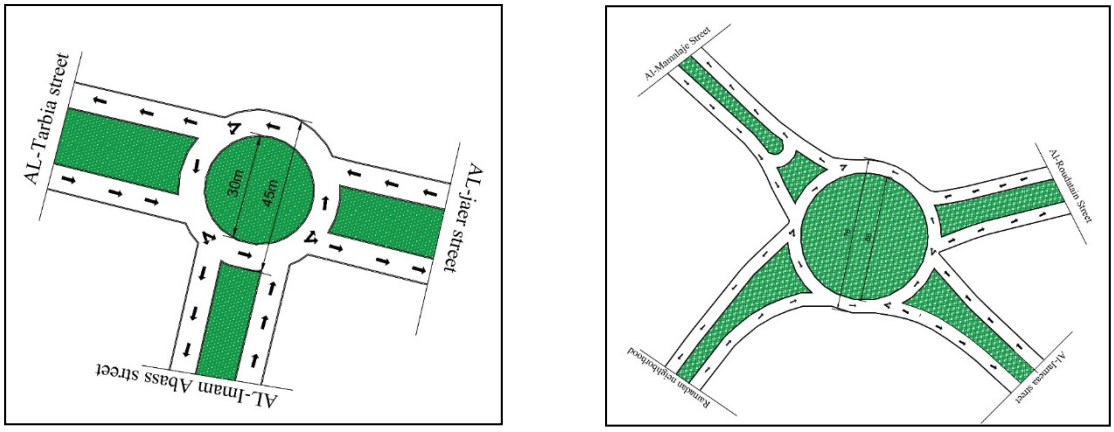

Figure Hata! Belgede belirtilen stilde metne rastlanmadı.**1** Said AL-Assar and AL-Mohafada

11.Data collection

The process of collecting data on traffic volumes is one of the important parts of the process of simulating reality. •forward direction •right turn •left turn •U-turn Traffic volumes are calculated in a way that cameras are installed at the beginning of all streets leading to the roundabout, where five cameras were installed to cover the roundabout completely. Traffic volumes were calculated at peak hour volume 07:30 to 8:30 am, 12:30 to 13:30 am, and 19:30 to 20:30 for a period of four days (three working days distributed over the days of the week and one day off) During the period from Saturday, October 1, 2022, to Friday, October 7, 2022

12.Cycle Length design

The cycle length was calculated based on the Webster equation that provides the optimal cycle length with the least lost time and least delay it Basic equation in many transportation design books and the Result was The optimum cycle length for Said Al-Assar Roundabout is 100 seconds and The optimum cycle length for Al-Mohafada Roundabout is 50 second.

13.Validation Results

The delay values in the Said Al-Assar Roundabout were calculated and compared with the values obtained from PTV Vissim, and according to the regression (R2), the result was as shown below (Figure 1) shows the degree of convergence in the results between reality and the program, with a value of approximately 87.5%.

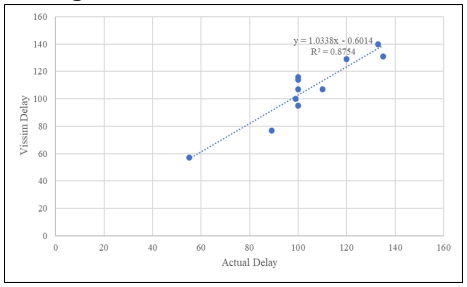

Figure 2 Validation model with regression (r^2)

14.Comparison of Roundabout and signalized Roundabout

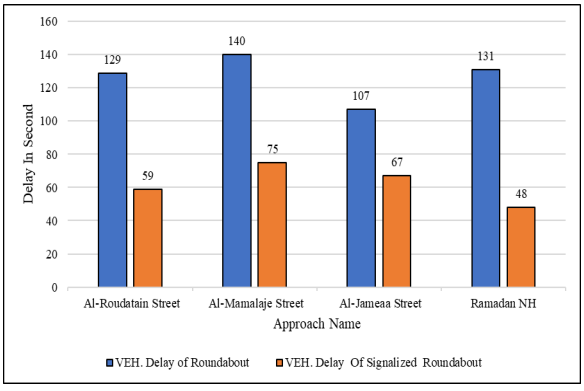

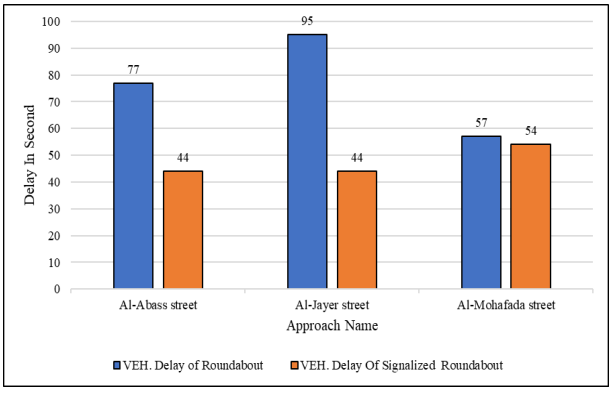

Figure 3 comparison chart between the delay in Said Al-Assar Roundabout and signalized Roundabout and between the delay in Al-Mohafada Roundabout and signalized Roundabout

The delay times for all approaches of Said Al-Assar and Al-Mohafada Roundabout and Said Al-Assar and Al-Mohafada signalized Roundabout were analyzed in Figure(3). The results showed a significant reduction in delay times after the roundabout was upgraded. Approaches such as Al-Roudatain Street, Al-Mamalaje Street, Al-Jameaa Street, Ramadan NH, Al-Abass Street, Al-Jayer Street, and Al-Mohafada Street experienced a substantial decrease in delay times ranging from 5% to 63%. Overall, the roundabout upgrade had a positive impact on traffic flow and reduced delays on all approaches.

15.The general behavior of delay values with an increase in traffic volumes

this part, the relationship between the delay and the traffic volumes entering the roundabout had been discussed, The values were calculated by providing the PTV Vissim with incremental values of traffic volumes and recording the delay values so that the (Figure 4), shows the increase in delay with the increase in traffic volumes, as shown below separately

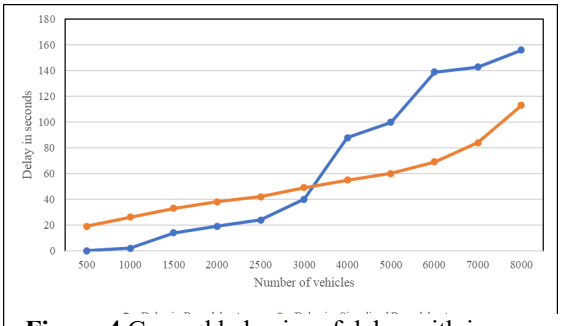

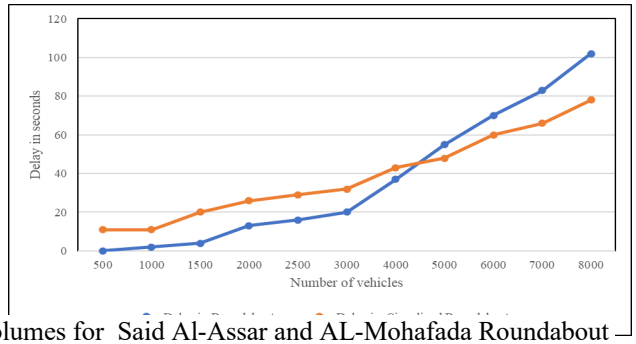

Figure 4 General behavior of delay with increase traffic volumes for Said Al-Assar and AL-Mohafada Roundabout

the roundabout's curve intersects with the Signalized Roundabout curve at the traffic volume in (3300 v/h and a delay value of 55 seconds) and (4500 v/h and a delays value of 48 seconds), which is the value at which it is preferable to put a light signal on the roundabout to control it in case of not wanting to convert it into a Signalized intersection

16.Conclusions

1-Optimal signal times for Said Al-Assar and Al-Mohafada signalized intersections are 100s and 50s, respectively.
2-The model built in PTV Vissim program matches reality by 87%.
3-The level of service in all roundabouts is F with delays exceeding HCM requirements.
4-Converting roundabouts to signalized roundabouts reduces delays and shifts service levels to E for Said Al-Assar and D for Al-Mohafada.
5-At traffic volumes of 3300 and 4500 v/h, converting roundabouts to signalized roundabouts is preferable to regular roundabouts.
6-This case is useful for temporary traffic control or if conversion to traffic light is not desired.

17.Recommendation

Based on the study's findings, it is recommended to install traffic lights on roundabouts to reduce delay times and use them partially during peak hours. It is also important to develop clear plans to solve the issue of traffic congestion in the long term, such as transferring government and service departments from the city center.

18. Conflict of Interest:

The authors declare no potential conflicts of interest with respect to the research, authorship, and/or publication of this paper.

19. Contribution of Authors:

[Author 1's Ali Fadhlallah Hussein]: Conceived and designed the study, collected and analyzed the data, and wrote the manuscript.
[Author 2's PhD. Hussein Ali Ewadh]: research supervisor.
[Author 3's PhD. Raid R.A. Almuhanna]: Assisted with data collection Contributed to the study design, data interpretation, and revised the manuscript for important intellectual content and research supervisor.

20. References

Ahac, S. and V. Dragčević (2021). "Geometric Design of Suburban Roundabouts." Encyclopedia 1(3): 720-743. doi: https://doi.org/10.3390/encyclopedia1030056.

Akçelik, R. (2009). SIDRA INTERSECTION User Guide for Version 6, Akçelik and Associates Pty. Ltd., Melbourne, Australia.

D.C, W. (2005). Highway Capacity Manual TRB, Transportation Research Board. doi:

Garber, N. J. and L. A. Hoel (2019). Traffic and highway engineering, Cengage Learning.

Hummody, M. (2007). A Four-Leg Roundabout Delay Model Using Microsimulation Technique, Ph. D. thesis, University of Technology.

Iraq, C. S. O. o. (2020). Statistics of private sector cars registered in the General Traffic Directorate until 12/31/2020. https://cosit.gov.iq/ar/component/banners/click/2.

Lakouari, N., O. Oubram, R. Marzoug, H. Ez-Zahraouy, J. Velásquez-Aguilar and L. Cisneros-Villalobos (2018). "Simulation study of traffic circle intersection with traffic lights." International Journal of Modern Physics C 29(07): 1850062. doi: https://doi.org/10.1142/S0129183118500626

Muchlisin, I. T. and W. Widodo (2019). "Optimization Model of Unsignalized Intersection to Signalized Intersection Using PTV Vissim: Study Case in Imogiri Barat and Tritunggal Intersection, Yogyakarta, Indonesia." International Journal of Integrated Engineering 11(9): 11-25. doi: https://doi.org/10.30880/ijie.00.00.0000.00.0000

Saleh, H. M. A. (2021). A Surrogate Measure to Assess Safety Condition at Different Signalized Intersections. Master Degree, University of Babylon.

Songchitruksa, P., S. Sunkari, I. Ugalde, J. Rosca and J. Aparicio Ojea (2017). "Interlinking Vissim and ns-3 for Connected Vehicle Simulation: Case Study of Intelligent Dilemma Zone Avoidance." Transportation Research Record 2619(1): 36-43. doi: https://doi.org/10.3141/2619-04

Wu, J., E. Radwan and H. Abou-Senna (2018). "Determination if VISSIM and SSAM could estimate pedestrian-vehicle conflicts at signalized intersections." Journal of Transportation Safety & Security 10(6): 572-585. doi: https://doi.org/10.1177/03611981221075630

Xing, Y., J. Lu, L. Lu, C. Jiang and X. Cai (2014). "Comprehensive safety assessment model of road long tunnel based on VISSIM." Intelligent Automation & Soft Computing 20(4): 501-514. doi: http://dx.doi.org/10.1080/10798587.2014.934595

Guess heat transfer coefficient of forced convection for single-phase flow in a single-phase passage on a vertical tube heat transfer

R.SHAKIR [1]

Department of Petroleum and Gas engineering,University of Thi-qar- College of engineering, Thi-qar,Iraq
ORCID No: https://orcid.org/0000-0001-5413-0861

Keywords

forced convection, laminar zone, turbulent zone, single-phase to coefficient of heat transfer for single-phase passage.

Abstract

Forced convection is difficult to apply to smooth, vertical circular tubes because very low heat fluxes are needed to prevent buoyancy effects from increasing the heat transfer coefficient. Previous research has mainly focused on mixed convection for both laminar and turbulent zones, with limited study conducted on forced convection for heat transfer. The goal of this study was to investigate the heat transfer coefficient characteristics under specific conditions of forced convection, using smooth circular test sections with both upward and downward flows. Water with a Prandtl number of (6.30-7.10) was used for Reynolds numbers ranging from (490.70 to 17219.95), heat fluxes between (0.510-5.01 kW/m^2) were employed and fluid mean velocities of (0.10 to 3.75) meters per second. Heat inputs between (20 – 200)watts were used during the tests.The width of both the laminar and turbulent flow zones in the fully developed zone and developing turbulent zone were determined for all heat fluxes.

Research Article
Submission Date : 14.04.2023
Accepted Date : 04.05.2023

1. Introduction:

The tube can experience either forced or mixed convection when the flow is laminar. It is crucial to differentiate between these two types of convection due to the significance of Reynolds number under various conditions. Buoyancy effects on the liquid cause density to vary radially in mixed convection. Both forced and mixed convection can occur in laminar convective flow through a tube, and distinguishing between them is important because of the Reynolds number's criticality in different conditions. Buoyancy effects on the liquid cause density to vary radially in mixed convection. Several textbooks on heat transfer, including references (Bejan, 2013), (Ya et al., 2015),(Lienhard, 2013),(Holman, 2012), (SevinGumgum NurcanBaykus Savasaneril, 2018) and (M.Alpbaz, 1988) are proceeded method for the 2-D heat equation so the method converts the 2-D heat equation to a matrix equation that was purpose of this study and the origin of the equation for heat transfer interfacial cofficient by their tests.In the absence of empirical data from practical experiments, the study relied solely on predictive analysis using heat transfer equations for hypothetical setups resembling real-world lab tests conducted under the same circumstances.In the absence of empirical data from practical experiments, the study relied solely on predictive analysis using heat transfer equations for hypothetical setups resembling real-world lab tests conducted under the same circumstances.R.Shakir (R.SHAKIR, 2022a, 2022b; Shakir, 2020, 2021b, 2021a, 2022) conducted a numerical analysis on forced convection in mini-channels with fully developed and developing flows, examining both laminar and turbulent flows under various boundary conditions. And, T. L. Bergman (Bergman et al., 2017) possesses valuable resources in the form of textbooks about heat transfer through heat flow in tubes.,state that under a constant heat flux boundary condition, the Nusselt

*R.SHAKIR; e-mail: raed-sh@utq.edu.iq ; shraed904@gmail.com

number in fully developed and laminar forced convection heat transfer on circular tubes remains constant regardless of the value of the Prandtl number or Reynolds number. The primary aim of this investigation is to devise a sophisticated numerical iterative method that employs a prediction software to establish the properties of forced convection heat transfer and fluid flow.

2. The guess set-up

This paper briefly describes the ideal setup for prediction (illustrated in Figure 1), which includes a closed liquid loop, a test bench structure, an inlet section, a test section, and a low-turbulence section. The inclination of the test section can be adjusted depending on the installation of the test bench. As depicted in Figure 1, the test section produced conditions for forced convection when placed vertically. Water was dispensed from a 600-liter storage tank through flow meters, a flow-calming section, the test section, and then returned to the storage tank for redistribution and cooling.

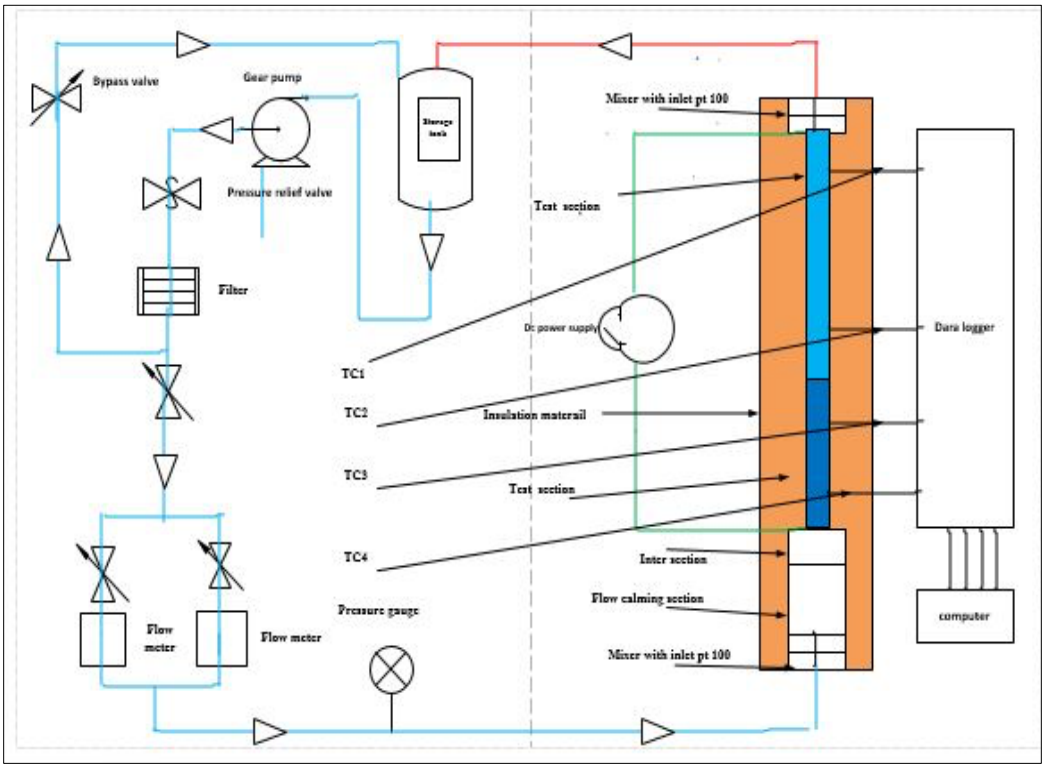

Figure 1.Test section

To maintain a constant temperature and cool down heated water, a chiller unit was connected to the storage tank in the system. A gear pump with a flow rate of 430 liters per hour was used to circulate the water through the test section, and a rubber hosepipe was utilized to prevent vibrations from the pump from affecting the test section. The flow rate of the water was controlled by a personal computer, and a Lab VIEW program was used to adjust the voltage signal to maintain the desired pressure. To prevent flow disturbances, a pressure relief valve was used to bypass the water back to the storage tank. A water bypass line with two flow meters of different capacities was used to increase back pressure.The mass flow rate of the water was measured using two flow meters, one with a flow rate of (330 liters per hou)r and the other with a flow rate of 108 liters per hour. Both flow meters had an accuracy of (±0.07%) of the full scale. The higher flow meter was used to measure the quasi-turbulent and turbulent zones, while the lower flow

meter was used to measure the laminar zone to the quasi-turbulent flow zone. In addition, Pt100 probes were installed downstream of the inlet mixer and outlet mixer, respectively, inside a soft Nylon mesh to measure the water temperature as it flowed axially along the probe.

To ensure a consistent flow rate in the test segment, a flow-calming segment made of a clear acrylic tube with a diameter of 200mm and a length of 620mm was installed before the test segment, as shown in Figure 1. The flow-calming segment also had three air bleed valves located at the top to remove any trapped air.Figure 1 shows a graphic representation of the test segment, including the locations of two pressure taps, four thermocouple stations, and the orientations for upward and downward vertical flows. The test segment was made of a smooth copper tube with an inner diameter of 5mm and an outer diameter of 50mm. It had a length of 5m, resulting in a higher length-to-diameter ratio (x/Di) of 500.

The test section was mounted on a 5.9m long test bench, which was placed on a rigid frame with a height of 2.9m and dampening pads to prevent vibrations from the floor. The test bench was pivotable at the center, allowing for testing in both upward and downward vertical directions. Tightly secured cables kept the test bench upright and rigid, and a grilled inclinometer was attached to the test bench to confirm the test section's inclination angle.To minimize heat transfer to the surroundings, the flow-calming segment, inlet segment, test segment, mixers, and tubes were insulated using an insulation substance with a thermal conductivity of 0.04 W/m.K. The insulation around the test segment had a thickness of 70mm, and the heat loss was estimated using 1-D heat transfer accounts, taking into account the medium's measured wall and outside insulation temperatures and insulation resistance to be less than 3% if possible.

To reach a steady state, a guessable procedure was employed. Steady-state conditions were assumed when there were no significant changes in mass flow rates, energy balance, temperatures, currents, and pressure drop readings, which took about two hours after the first start-up of the day. The lowest mass flow rate was used as the starting point, with the pump velocity adjusted via a Lab view program on a computer lab to reduce flow pulsations. The bypass and provide valves were continuously adjusted to enable the pump to work at higher mass flow rates. Heat fluxes were generated by a DC power supply by stratifying the requested currents and voltages on the system.Guess readings were taken at higher mass flow rate periods in the laminar and turbulent flow zones, but more time (approximately 25-40 minutes) was needed to reach steady-state conditions in the transitional flow zone. Once steady-state was achieved, approximately (390-410) data points were logged at a frequency of (22 Hz), including inlet and exit temperatures, wall and circumference temperatures, mass flow rates, and pressure drops. The water temperature in the storage tank was monitored to maintain a constant temperature in the test segment. All data collected were saved and analyzed using a separate program.

3. Mathematical processes

The fluid temperatures, T(p), at any axial position,

$$T_p = T_{in} + (T_{out} - T_{in}/L)\, x \tag{1}$$

It appears that over (600) heat transfer equations were utilized by Guess software, and then these equations were sent to Excel software using an iterative method. Based on **Figure 2**, Creation concluded that there is only one spot where heat can flow at the interface of the solid and water. The 2-dimensional array is arranged in such a way that it primarily affects the wall line, while the 1-dimensional array is perpendicular to the water flow and the 2-dimensional array is parallel to the water flow. It is necessary for thermal conductivity to adhere to the process illustrated in **Figure 2.** (Shakir, 2020), (Shakir, 2021b).

$$\delta^2 T/\delta y^2 + \delta^2 T/\delta z^2 = 0 \quad (2)$$

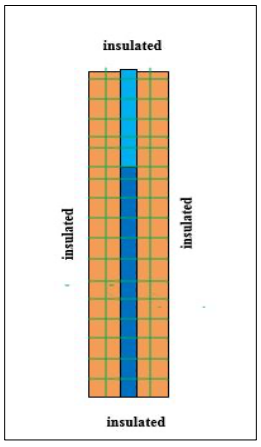

Figure 2.Test segment

The temperature (T) on the copper wall and the perpendicular direction (y) to the axis of water flow were used to obtain the heat transfer in equation (3). This was achieved by dividing the equation by the area of the square cell (0.05 m) squared.(Shakir, 2020), (Shakir, 2021b).

$$T_{i,j} = \delta y^2 \left(T_{i+1,j} + T_{i-1,j}\right) + \delta z^2 \left(T_{i,j+1} + T_{i,j_1}\right)/2\,(\delta y^2 + \delta z^2) \quad (3)$$

To get the area of tube flow,

$$A = \pi {D_h}^2/4 \quad (4)$$

The hydraulic diameter can be found by:-

$$D_h = 4A/P \quad (5)$$

To calculate the fluid of mean velocity by,

$$u = m/\rho\, A \quad (6)$$

To obtain the (Re) by,

$$Re = \rho u D_h/\mu \quad (7)$$

To get the (Pr) by,

$$Pr = C_p \mu/K_f \quad (8)$$

To obtain the (St) by, (Holman, 2012)

$$S_f = E_{st} {R_e}^{-0.205} {P_r}^{-0.503} \quad (9)$$

To obtain the (E-St) by, (Holman, 2012)

$$E_{st} = -0.0225\, exp^{(-0.0225\,(\ln Pr)^2)} \quad (10)$$

To obtain the (Gz) by, (Holman, 2012)

$$G_z = mC_p/K\,L \quad (11)$$

To obtain the (Nu-L) by, (Holman, 2012)

$$Nu = 1.75 G_z^{\frac{1}{3}} \quad (12)$$

To obtain the (Nu-T) by, (Holman, 2012)

$$N_U = 0.023\, R_e^{0.8} P_r^{0.4} \quad (13)$$

To obtain the (h-L) by, [4]

$$h_L = K_C N_u / D_h \quad (14)$$

To obtain the (h-T) by, (Holman, 2012)

$$h_T = \rho\, u C_p S_t \quad (15)$$

4. Results

To examine how buoyancy affects fluid temperatures, **Figure.3** compares temperature data at different heat flux conditions, as a function of Reynolds number, for vertical upward flow in the test section. The figure illustrates that at a heat flux of (3.6, 4.07, 4.6, and 5.10 kW/m^2), the minimum fluid temperature was (20.17, 20.16, 20.15, and 20.14°C), respectively, which was statistically significant, indicating the presence of buoyancy effects that caused flow and mixed convection. This led to a reduction in the Reynolds number with an increase in fluid temperature at the inlet and outlet locations for vertical flow, as well as higher outlet data than inlet data.

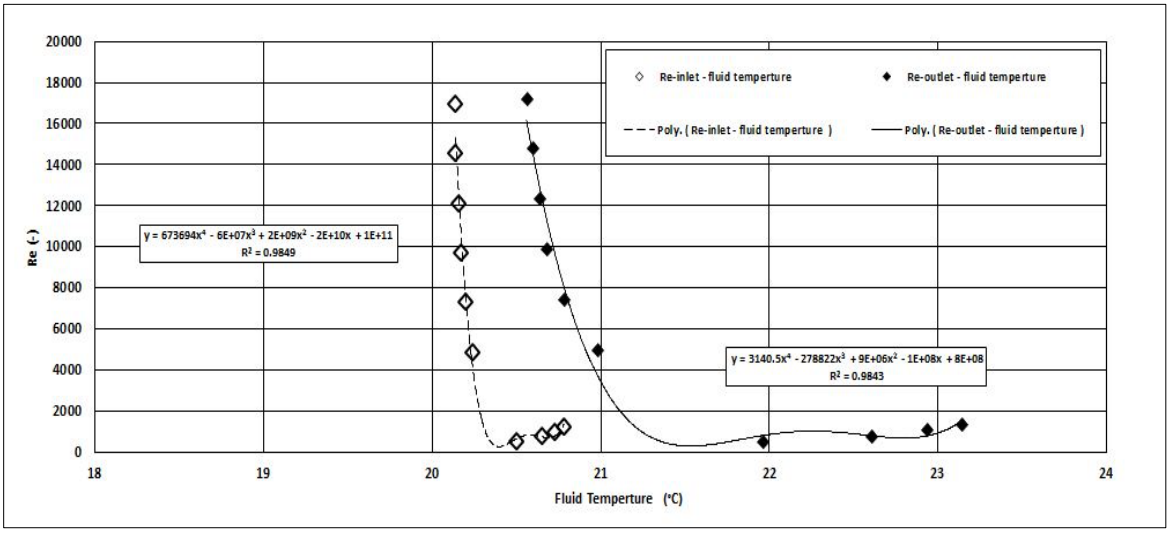

Figure.3. Variation to (Re) versus (Tf)

A correlation was obtained for fully developed laminar and developing turbulent forced convection Reynolds number, which takes into account the increase in Reynolds number with axial location for vertical flow orientation. This correlation was obtained by fitting a simple polynomial curve to all the results for forced convection heat transfer for vertical upward and downward flows (refer to **Figure.4**).

$$Re_{in} = 0.0003(x/D_i)^3 + 0.2955(x/D_i)^2 - 47.53(x/D_i) + 2386.4 \quad (16)$$

$$Re_{out} = 0.0003(x/D_i)^3 + 0.2951(x/D_i)^2 - 47.997(x/D_i) + 2381.8 \quad (17)$$

Equations (16 and 17) hold true for Reynolds numbers ranging from (491-1240) at the inlet data and (518.5-1351.5) at the outlet data, provided that no transition occurs. It is worth mentioning that the onset of transition for vertical tubes typically occurs within the Reynolds number range of (4857.3-16933.3) at the inlet data and (4998.7-17214.95) at the outlet data. This range of Reynolds numbers is significantly influenced by the heat flux, tube diameter, and inlet geometry. Thus, the equations accurately depict the dependence of laminar and turbulent forced convection heat flow on Reynolds number along the length of the tube in the entrance zone.

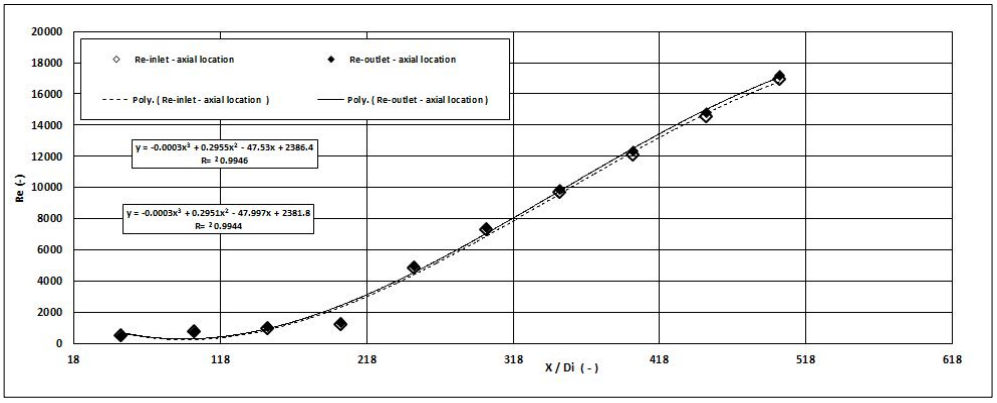

Figure.4. Variation to (Re) as a function of axial location

The coefficient of heat transfer varies with the mass flow rate for different heat fluxes, as shown in **Figure.5.** The data in **Figure.5** reveals that when the mass flow rate is fixed at values of (0.002, 0.003, 0.004), and (0.005) kg/s, an increase in heat flux leads to an increase in the coefficient of heat transfer. Moreover, for mass flow rates higher than (0.005 kg/s), the coefficient of heat transfer increases slightly in a polynomial relationship as the mass flow rate increases. This information is evident from the data presented in **Figure.5**.

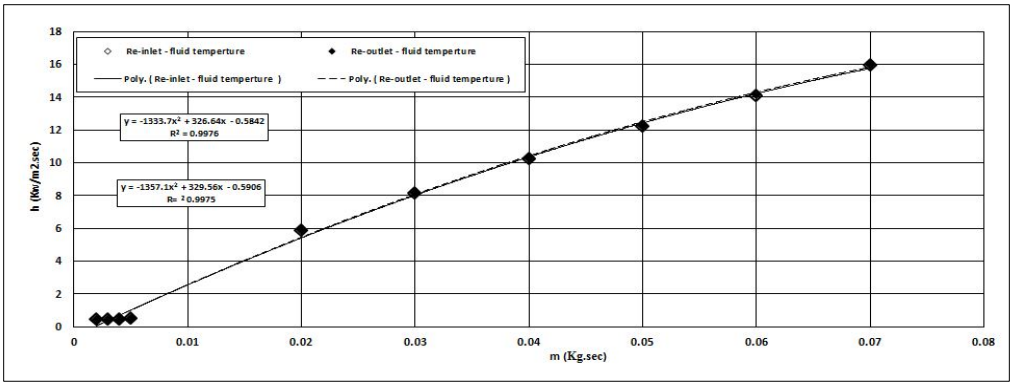

Figure.5. Variation of coefficient of heat transfer as function rate of mass flow

Figure.6. illustrates a comparison between the laminar Reynolds numbers for forced and mixed convection, under different heating conditions and rates of mass flow. The results show that, for vertical flow, the average Reynolds number was approximately the same for all heat fluxes (ranging from 0.510 to 2.04 kW/m^2) at the inlet and outlet locations. However, the forced convection Reynolds number did not fully develop and was not constant at (2.55 kW/m^2) and beyond. Instead, it slightly increased as the rate of fluid velocity increased for all heat fluxes, following a power relationship.

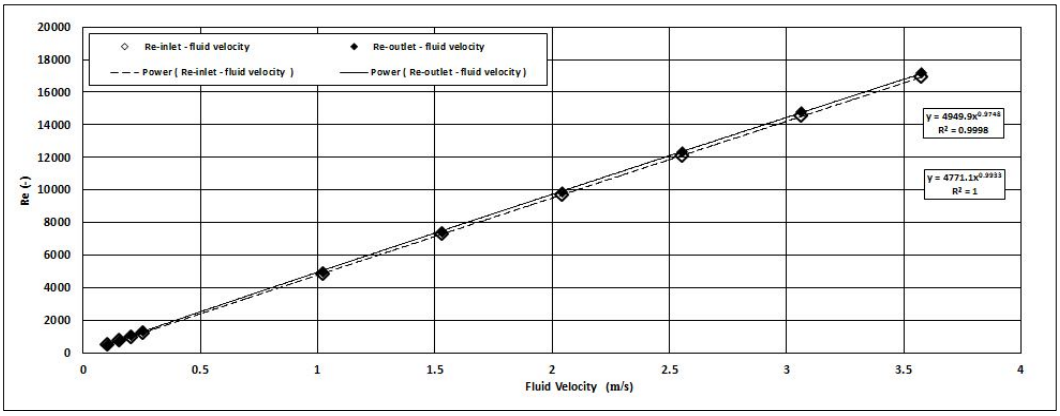

Figure.6. Variation of coefficient of heat transfer as function rate of mass flow

5. Conclusions

Previously, there has been limited research on forced convection in both the laminar and turbulent zones. To ensure that forced convection and buoyancy effects were minimized, experiments were conducted in both upward and downward directions. The value of (Reynolds number) at which the transition from laminar to turbulent flow occurred increased with increasing heat flux in both the fully developed and developing zones. To conduct uncertainty analysis in this paper, it is recommended to increase the (Reynolds number) by increasing the heat flux, which in turn increases the temperature and reduces viscosity. The onset of laminar flow and the cessation of turbulent flow in the fully developed region occurred at higher Reynolds numbers as the heat flux increased for pure forced convection conditions. Additionally, the width of the flow regime varied for different heat fluxes. Equations were derived to establish the boundaries of the laminar, transitional, and turbulent flow regimes for pure forced convection. The findings revealed that the transition occurred at different mass flow rates for all heat fluxes, similar to the isothermal flow case. Nevertheless, the Reynolds numbers increased as the heat flux increased, which was attributed to the reduction in viscosity as the temperature increased.

Nomenclature

A	area of tube flow (mm2)
Cp	specific heat of water,(kJ/(kg .K)
Dh	hydraulic diameter, mm
E-st	factor of Stanton number (-)
Gz	Graetz number (-)
hL	laminar coefficient of heat transfer, (W/(m2.K)
hT	turbulent coefficient of heat transfer, (W/(m2.K)
Kf	thermal conductivity of fluid, (W/(m .K)
Kc	thermal conductivity of copper, (W/(m .K)
L	tube length (m)
m	mass water flow rate,(kg/s)
Nu	Nusselt number (-)
Pr	Prandtl number (-)
St	Stanton number (-)
Re	Reynolds number (-)
T	temperature,(K)

V	water velocity,(m/sec)
ρ	water density, (Kg/m2)
μ	dynamic velocity (N s/m2)

Conflict of Interest

The author's involvement in this study was completely free from any conflicts of interest. There has been no receipt of financial support, and there are no circumstances that would result in financial or personal gain.

References

Bejan, A. (2013). Convection heat transfer. John wiley & sons.

Bergman, T. L., Incropera, F. P., & DeWitt, D. P. (2017). Fundamentals of Heat and Mass Transfer; Bergman, TL, Lavine, AS, Eds. John Wiley & Sons, Inc.: Hoboken, NJ, USA.

Holman, J. P. (2012). Heat Transfer (ten editio). McGRAW-HILL'S.

Lienhard, J. H. (2013). A heat transfer textbook: Courier Corporation. Massachusetts Institute of Technology.

M.Alpbaz. (1988). THE ORIGIN OF THE EQUATION FOR THE İNTERFACİAL COEFFICIENT OF HEAT TRANSFER. Journal, 34(01.02), 114–128.

R.SHAKIR, R. S. (2022a). Investigate the Flow of Boiling Heat Transfer in a Complex Geometry Flat Channel. University of Thi-Qar Journal for Engineering Sciences 25–21 ,(1)12 ,مجلة جامعة ذي قار للعلوم الهندسية.

R.SHAKIR, R. S. (2022b). Pressure Drop Effect on Mini-Scale Heat Sink by Multi-phase: Review & Prediction. University of Thi-Qar Journal for Engineering Sciences ,(1)12 ,مجلة جامعة ذي قار للعلوم الهندسية 20–15.

SevinGumgum NurcanBaykus Savasaneril, E. (2018). Chebyshev collocation method for the two-dimensional heat equation. Journal, 3(2), 1–8.

Shakir, R. (2020). Boiling Heat Transfer in a Micro-Channel Complex Geometry. IOP Conference Series: Materials Science and Engineering, 928(2), 22129.

Shakir, R. (2021a). INVESTIGATION OF SINGLE-PHASE FLOW CHARACTERISTICS IN A STAGGER PIN-FINS COMPLEX GEOMETRY. Journal of Engineering and Sustainable Development, 25(6), 74–81.

Shakir, R. (2021b). Investigation of Single-Phase Flow Characteristics in an Inline Pin-Fins Complex Geometry. Journal of Physics: Conference Series, 1879(3), 32118.

Shakir, R. (2022). Study Of Pressure Drop and Heat Transfer Characteristics Of Mini-Channel Heat Sinks. The Iraqi Journal for Mechanical and Materials Engineering, 22(2), 85–97. https://doi.org/10.32852/iqjfmme.v22i2.595

Ya, C., Ghajar, A., & Ma, H. (2015). Heat and Mass Transfer Fundamentals & Applications. McGraw-Hill.

Calibration of flow equations through regulators using computational fluid dynamics CFD modelling

Hamid Ahmed Mahdi Alasady

Infrastructure , University Of Kerbala, Iraq
ORCID No: https://orcid.org/0009-0001-9449-8801

Keywords

CFD, flow of water, regulator, flow 3D

Abstract

This study examined a simulation performed using the Flow 3D program and compared the outcomes with general and positional equations for calculating the discharge through water facilities that had been established in earlier studies. and investigated the traits of the flow passing through irrigation regulators and the variables influencing them for the two situations of flow at the total opening and partial opening of the regulator gate. Based on the findings of laboratory measurements, the coefficients and other components in the equations for estimating discharge were calculated, and links between these coefficients and the non-dimensional components impacting the flow calculated in the laboratory were drawn.

Research Article
Submission Date : 22.04.2023
Accepted Date : 03.05.2023

Introduction

The CFD (FLOW 3D) simulation program was utilized in this study's results, together with laboratory measurements to install the parameters and elements required in the program's calculations, which may be used to calculate the regulators' discharge based on straightforward field observations. Weirs, regulators, or other water measuring equipment are used to control the water flow in irrigation canals. In areas with little slope, regulators are utilized. showed that CFD can be a good alternative for problem analysis and solution as opposed to generating a final result, mostly because of the large number of assumptions made in the numerical methods employed in CFD. When the flow is three-dimensional (3D), the modeling method is more difficult. (Ghare et al., 2008). The procedure of managing the flow includes regulating the water level, its quantity, or estimating this quantity, or combining the three cases. And there is Gates, which come in a variety of designs like as the sliding gate, radial gate, and cylindrical gate, control the flow in regulators. The regulator's front and back water levels, as well as the size of the gate opening, both influence the drain. By altering the gate opening, the drain traveling through the regulator can be managed. Of course, when the gate is completely opened, the regulator experiences the largest discharge. It is demonstrated that there is a fair amount of agreement for both pressures and discharges between the physical and numerical models. The accessibility and effectiveness of current numerical techniques give engineers another instrument for the construction and study of models.(Savage & Johnson, 2001).in 2020 (Carrillo et al., 2020) conducted a numerical analysis to demonstrate how the coefficient of discharge over labyrinth weirs is affected by submerged and free flows. Additionally, they examined the free surface flow profile at the labyrinth weir's upstream and downstream reaches. The results showed that for a large sidewall angle, CFD models can fairly accurately forecast the coefficient of discharge on submerged and free flow across labyrinth weirs. In 2022 (Pourshahbaz et al., 2022) they utilized the CFD tool FLOW-3D software. They looked at the hydro-morphology and numerical modeling of

a set of parallel groynes that were positioned vertically. The critical velocity ratio (Vavg/Vcr) and approach Froude number had an effect on the correctness of the simulation of the FLOW-3D model,

Channel for laboratory

The used laboratory channel is rectangular in shape, has a metal bottom, and has glass on both sides. It is 20 meters in length, 0.9 meters in width, and 0.6 meters in height. It is mounted on the laboratory floor and fastened to an iron frame with movable screws so that the channel's transverse inclination can be changed. The center of the truss is supported by two cylindrical bearings that are fastened to the lab floor. . Additionally, it has a pair of screw jacks at each end, which are fixed on the laboratory floor and allow the jacks to alter the longitudinal slope of the channel. utilizing an electric motor that can be managed using the control panel's keypad. The bracket at the back of the channel is secured with a ruler with millimeter divisions. This ruler, which is just loosely attached to the truss, is calibrated to read zero when the channel is horizontal. The sliding cart that transports the measuring devices is made easy to move by an aluminum track that has been put above the canal walls. Spirals connecting the rails to the channel walls allow for level adjustment. The outlet basin, which connects to the front of the channel, is 2 meters long, 1.6 meters broad, and 1 meter high. A tube with a diameter of 0.3 meters supplies it with water. The tube's positioning inside the basin is intended to diffuse the water's energy and provide a tranquil flow. To further assure that the water was calm, a floating board was positioned and attached to the basin. In each experiment, when the level of the overflow hole could be adjusted, the outflow basin was fitted with a drain to dispose of any extra water.

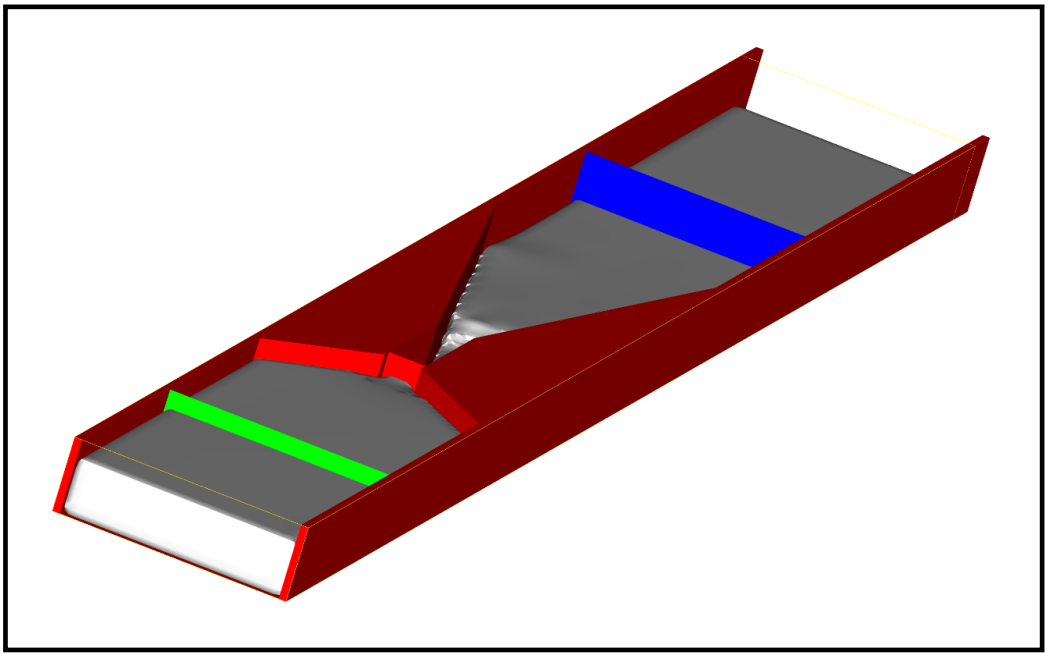

Figure 1. Regulator Channel

Experimental work

The goal of conducting experiments is to obtain measurements that are readily available in the field in order to determine the equation of flow. These measurements include the water level in the front and its level in the back, or the natural depth

of flow and the opening of the gate, and after performing the calibration, they are used to calculate the flow passing through the regulator opening. The same holds true for laboratory tests. The depth of the foreground flow was measured at a distance of 2 m from the model, and the depth of the natural flow was calculated using the natural flow equation at the backside and at a distance of 2 m from the model, assuming a suitable slope for the lands of Iraq, which is 0.002, and a roughness coefficient of 0.018. The relationship between the discharge and the depth of the water at the backside is depicted in Figure 1. The triangular submersible dam also measured drainage. Along with these readings, the distribution of the water's velocity charge in the front and the depth of the water flowing through the regulator were also noted After calibrating the model, measurements are taken of the discharge, height and width of the gate and the water level in the inlet and outlet to be compared later with the results extracted from the program.

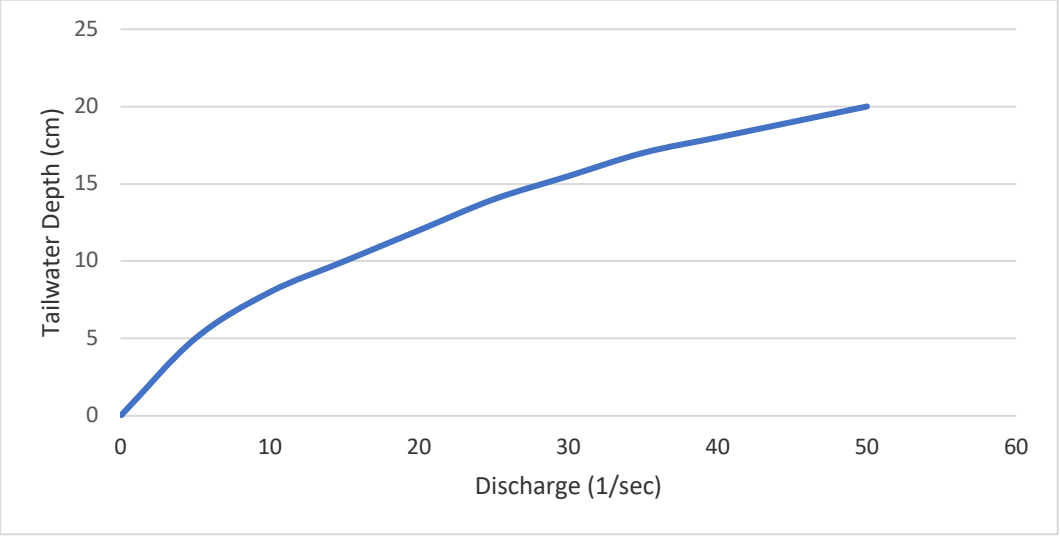

Figure 2. Relationship Between Drainage And Normal Depth At The Outlet

Dimensional analyiıs

Engineers must use translation and base their choices on observations, experience, and experimental data. The method that formulates the problems more effectively is dimensional analysis. The principles of dimensional analysis are used in a theoretical study to connect the relationships between the numerous parameters that affect flow and are affected by changes in the regulator shape, Froude number, change in height of gate, and width of gate in the model. **Table.1** illustrates how the categories of mass (M), length (L), and time (T) can be written.

Table 1. The Affect Parameters on Flow of Water

1-Parameters characterizing the fluid flow		Unit	Dimensions
ρ	Density of the fluid	kg/ m^3	ML^{-3}
Q	The discharge	M^3/l	L^3T^{-1}
g	Gravitational acceleration	m/s^2	LT^{-2}
μ	dynamic viscosity of the fluid N.s/m2	$N.s/m^2$	$ML^{-1}T^{-1}$
Y_1	Depths of the water in upstream flow	m	L
V_1	Velocity of the water in upstream flow	m/s	LT^{-1}

2-Parameters characterizing the model		Unit	Dimensions
S	model bed slop	-	-
L	Length of model	m	L
W	width of model	m	L
N	Number of gates	-	-
B	width of the gate	m	L
H	Height of the open gate	m	L
3-Time		Unit	Dimensions
T	Duration of RUN	Min	T

After using the dimensional analysis using Buckingham's Π theory method and neglecting the non-influential values, and simplifying the equations, discharge's functional relationship can be expressed as follows:

$$Q = g^{0.5} \cdot Y^{2.5} F4(Fr,N,B/Y,H/Y) \quad \text{.....} \quad 1$$

SPSS Program

The statistics package for social sciences (SPSS) version 26 program and an artificial neural network were used to generate the ANN models in the current study (ANN). The discharge (q) was chosen as the output parameter, while the level of water in the inlet (Y), the width of the gate (B), and the height of the gate (H) functioned as the input parameters. The dataset utilized in this study was split into three groups with a random member in each: holdout, testing (validation), and training. The standardized rescaling method was used for covariates. In this rescaling process, the mean is subtracted from the data and the final result is divided by the standard deviation. The rescaling methods normalized, adjusted normalized, and none are also available. These ANN models used the standard methodology. The network was trained using a batch training method in conjunction with the gradient descent methodology. On that, the default SPSS software settings were utilized. When properly trained, an artificial neural network can forecast how a process will behave. After being properly trained, neural networks can deliver accurate results even in situations that they have never experienced due to their exceptional capacity to generalize.(Al-saadi, 2022)

In **Table.2**, the number of layers and the number of neurons in each layer are shown. There are three independent variables in the input layer. Height, width, and intake water level of the gate. The standardized rescaling technique was applied to covariates. The output layer featured a single node for the dependent variable course result, whereas the hidden layer was assigned to a single layer with three nodes via automatic architecture selection. The activation function for the hidden layer was the hyperbolic tangent, which has the form f(x) = tanh (x) within the hidden layer. The output layer's identity function, which has the form i.e. f (x)= x, was used.

Table 2. Network Information

Network Information			
Input Layer	Covariates	1	Height of the gate (H)
		2	Water level in inlet (Y)
		3	Width of the gate (B)
	Number of Units [a]		3
	Rescaling Method for Covariates		Standardized
Hidden Layer(s)	Number of Hidden Layers		1
	Number of Units in Hidden Layer 1[a]		3
	Activation Function		Hyperbolic tangent
Output Layer	Dependent Variables	1	Discharge
	Number of Units		1
	Rescaling Method for Scale Dependents		Standardized
	Activation Function		Identity
	Error Function		Sum of Squares

a. Excluding the bias unit

It can be argued that this model demonstrates very good agreement with the actual observation because its coefficient of determination (R2) is (0.897), as shown in Figure.3.

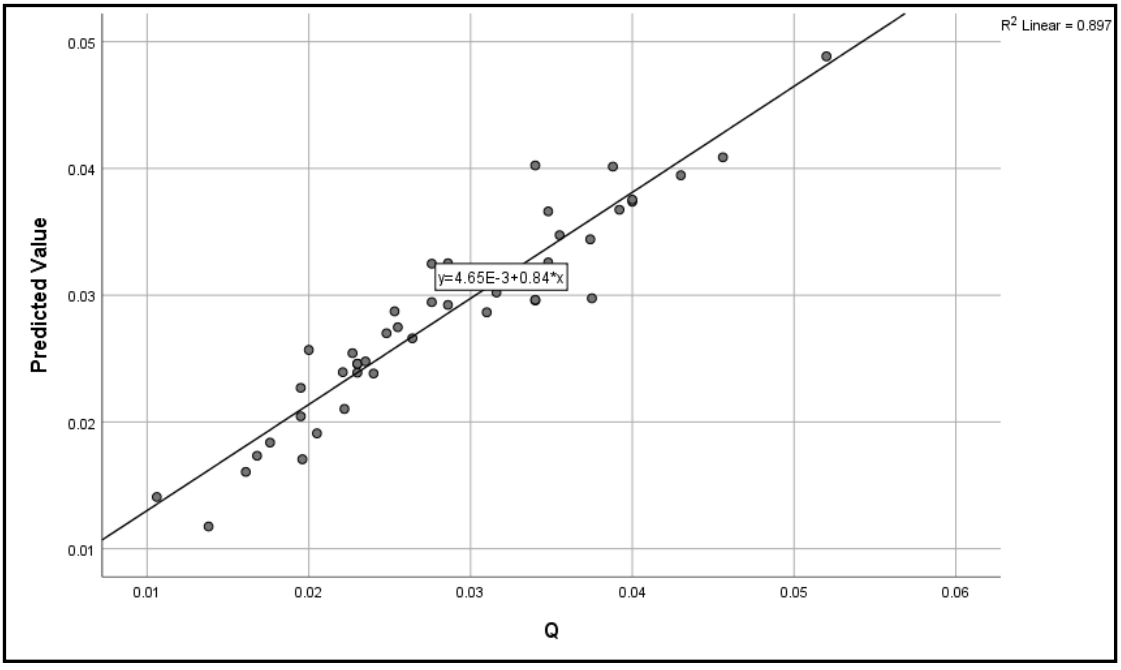

Figure 3. Predicted Value

Analysis and Discussions

Adjusting the discharge rate (Q) and measuring the water level (Y1) downstream of the weir were used to gather data. Measurements weren't performed until a sufficient period of time had passed, which was at least 4 min as advised by (Crookston 2010), in order to ensure the flow is under steady-state conditions. After analyzing and making calculations in the SPSS program, it appeared to us that water level in the intake had the biggest impact on discharge with an importance ratio of about 51.9%, followed by distance with a significance ratio of about 28.7% and height of the gate with a significance ratio of about 19.4%. As shown in the **figure.3**.

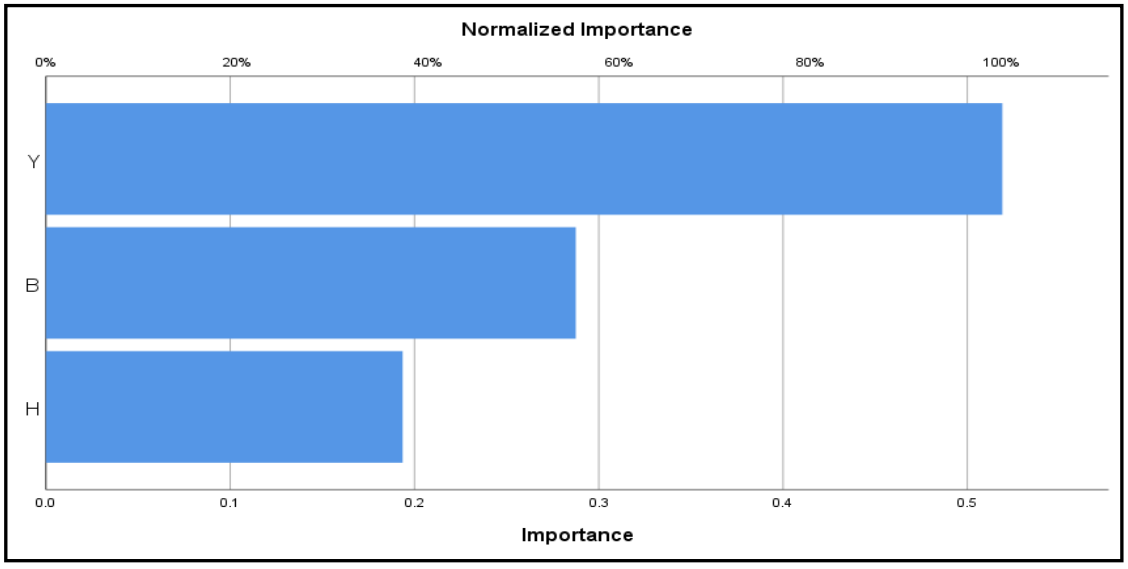

Figure 4. The Effect of Independent Variables on The Prediction of The Discharge Rate

Conflict of Interest

Author declare that there is no conflict of interest.

References

Al-saadi, G. N. H. (2022). Performance evaluation of drip irrigation lateral with different emitters and distances. November.

Carrillo, J. M., Matos, J., & Lopes, R. (2020). Numerical modeling of free and submerged labyrinth weir flow for a large sidewall angle. Environmental Fluid Mechanics, 20(2), 357–374. https://doi.org/10.1007/s10652-019-09701-0

Ghare, A. D., Mhaisalkar, V. A., & Porey, P. D. (2008). An Approach to Optimal Design of Trapezoidal Labyrinth Weirs. World Applied Sciences Journal, 3(6), 934–938. https://pdfs.semanticscholar.org/6cbf/a8d27cd17901217aec339cffe43b834dcad4.pdf

Savage, B. M., & Johnson, M. C. (2001). Flow over Ogee Spillway: Physical and Numerical Model Case Study. Journal of Hydraulic Engineering, 127(8), 640–649. https://doi.org/10.1061/(asce)0733-9429(2001)127:8(640)

Pourshahbaz, H., Abbasi, S., Pandey, M., Pu, J. H., Taghvaei, P., & Tofangdar, N. (2022). Morphology and hydrodynamics numerical simulation around groynes. ISH Journal of Hydraulic Engineering, 28(1), 53–61. https://doi.org/10.1080/09715010.2020.1830000

Importance of communication skills in architectural education to Raise the efficiency of professional practice of graduates

Merna sabree[1], Mozahim Mohammed Mustafa[2]

[1]Department of Architecture, University of Mosul, Mosul
ORCID No: https://orcid.org/0009-0008-8804-5591
[2]Department of Architecture, Mosul University, City
ORCID No: https://orcid.org/0000-0001-9637-3546

Keywords

architectural education, communication skills, professional practice.

Abstract

communication skills are among the most essential skills that architecture graduates need, which help them to engage in the labor market. Communication skills are in visual and verbal formats. After graduation and practicing the profession, many students suffer from a weakness in communication skills for many reasons, despite the emphasis on their importance by the organizing body responsible for practicing the profession such as (NAAB, RIBA, ABET ... etc.).

This study follows the descriptive and analytical approach, whereby the measurement mechanism represented in the questionnaire is used to find out the graduates' proficiency degree in aspects of communication skills, in addition to knowing ways to develop the outputs of architectural education about these skills. The study sample included newly graduated engineers and faculty members who are directly related to the outputs of architectural education and its impact on professional practice and labor market requirements.

The research came out with conclusions, that the graduates have efficiency in some of the aspects of communication skills and lack in other aspects. Based on the conclusions, the research came out with recommendations to cover the lack of knowledge in some aspects of communication skills in architectural education.

Research Article
Submission Date : 28.04.2023
Accepted Date : 04.05.2023

1. Introduction

Architecture is a profession in which the student needs many skills in order to be able to practice this profession, including communication skills, which means the ability of the architect to communicate visually and verbally with all parties related to the stages of the project design and implementation process, such as clients, specialists, users, craftsmen, etc. (Amanda, 2011).

Communication skills are in visual and verbal formats, as visual design skills are represented mostly through architectural and executive drawings, preparation of reports, illustrations, etc., and the architect must be proficient in them and have the expressive ability to communicate his ideas correctly in addition to what is explained verbally, which is the second part of communication skills Which complements and supports the first part of it, and helps the architect explain his ideas to clients, users, and engineers from other disciplines and crafts (Natasha, 2017, p13-15. Waclaw, 2020, p61-62).

Many students, after graduating and practicing the profession, suffer from weakness in some or most aspects of communication skills. This is due to many reasons, including that communication skills are not special courses. Rather,

[1]Resp author; e-mail: merna.sabree@gmail.com

these skills are taught implicitly through practical architectural education courses. his is noticed through the research and survey of the architectural programs of the most important Iraqi universities, although most architectural programs submit to a set of determinants set by the organizing bodies for the practice of the profession, such as (RIBA, ABET, NAAB.... etc.), all of which have agreed that the academic program must include clear courses that develop communication skills as a prerequisite for obtaining a certificate of recognition from them. (Suchismita, 2015, p: 584) (Ahmed, 2019, p: 871) (Kazem, 2017, p. 96) (Abdeen, 2007, p. 9) (Al-Yousef, 2014, p. 167) (Baalusha, 2014, p. 86) (Mohammed, 2015, p. 3) (Badawi, 2009, p. 71) (Esra, 2019, p:148) .

Therefore, this study examines the extent of graduates' competence in possessing communication skills when practicing the profession and the extent of the efficiency of these local architectural programs in achieving the determinants of the authorities regulating the practice of the profession. Where this study follows a descriptive and analytical approach in which questionnaires are used to find out the extent to which graduates are efficient in their possession of communication skills in Iraqi universities. Thus, the research problem and research objectives were generated and its methodology was determined.

1.1 Research problem

There is a lack of knowledge in the extent of the competence of graduates of architecture departments in Iraqi universities with regard to their possession of communication skills.

1.2 Research purpose

The research aims to:

- Knowing the forms of communication skills and their aspects in professional practice.
- Measuring the efficiency of Iraqi university graduates with regard to their communication skills.
- Ways of developing the outputs of architectural education in terms of communication skills.

1.3 Research methodology

The research follows analytical approaches, including:

- Building a theoretical framework that includes the main forms of communication and their aspects by reviewing previous studies and global determinants.
- Determine the study sample.
- Determine the measurement tool and its mechanism.
- Applying the measurement tool to the selected practical study samples
- Analysis of results and conclusions.

2. Theoretical framework

The following is a review of the importance of these skills and their formulas and aspects in Previous studies to get the Theoretical framework vocabulary:

2.1 Previous studies:

2.1.1 David، Simon(2000)

This study dealt with the importance of communication skills and showed how architects are not good listeners and that the gap between the engineer and the client is constantly increasing and requires radical solutions. When conducting interviews with clients, they indicated that architects have ideas that may be great, but they are not good at explaining them.

This study dealt with the importance of communication skills and showed how architects are not good listeners and that the gap between the engineer and the client is constantly increasing and requires radical solutions. When conducting interviews with clients, they indicated that architects have ideas that may be great, but they are not good at explaining them.

And the legal authorities, and the researcher believes that focusing on the design studio and keeping the student for long hours leads to a loss of communication skills with others. Although the design studio includes many forms of visual, verbal, and tactile representation, and sometimes students work as groups, there is a reduction in the systematic development or evaluation of communication skills in engineering.

Finally, in order for the student to learn the ideal professional practice, the student must deal with a real problem, a real reality, with a real customer, go to the community and talk to the users instead of deducing the needs of the users in a drawing board, such as learning how children experience their school environment during their visit to the school.

2.1.2 Amanda, Joseph (2011)

The study dealt with whether communication skills are part of the NAAB program and how important communication skills are for architects. (Writing skills to prepare a business proposal, present prizes, present projects, communicate via e-mail, and promote their products through social media, public speaking skills to present presentations and explain their projects, ideas, and goals to clients, users, contractors, or arbitration committees, marketing, and public relations skills are necessary to market their products winning business and persuading customers). The researcher surveyed architects, deans of faculties, and directors of 49 architecture programs to survey and analyze architects' views on the importance of communication skills in professional practice.

The results indicated that academics differed in their viewpoints regarding the importance of communication skills in the education of architecture.

The results of the survey showed that 100% of the participants agree on the importance of communication courses, and the optional comments emphasized the importance of communication skills for architects, as architecture as a practice is a communication process from beginning to end, and the ability to speak is just as important as the ability to design. Therefore, communication with Customers before, after, and during the provision of services is critical.

2.1.3 Natasha (2017)

This study aims to investigate the changing nature of architectural education and the importance of live projects in developing the communication skills of students in architecture schools. This study hypothesizes that live projects provide students with skills, tools and relationships additional to those acquired during a 'traditional' design project, which will help prepare them for practice. The researcher conducted three case studies, the first is a two-week studio project in Oxford with a real client, the second is a field trip to India and working with communities affected by the Asian tsunami in 2004, and the third is a pavilion project that was built as a competition by the university.

The researcher concluded, after working with real clients, local communities, companies, and the media, that design studios lack practical experience, communication skills, cooperation, and commercial experience, and design studios do not give students an opportunity to share their ideas and develop them with each other unless they work within a group. outside the educational institution and therefore lacks communication skills such as listening, negotiation, explanation and persuasion.

2.1.4 Waclaw (2020)

In this study, the researcher believes that the architect does not have the ability to communicate with the professionals at the construction site while supervising the work and the lack of professional terminology. Speech, persuasion, knowledge of professional terminology and technical knowledge.

The aim of this paper is to analyze the methods of visual communication that are taught in architectural schools based on the curriculum of the Faculty of Architecture at the Krakow University of Technology in Poland in order to improve the level of graphics among students.

The research emphasizes the importance of the practical aspect, and here it does not mean design studios, but rather the construction site. It stresses the need for students to participate in the construction site to learn communication skills with other disciplines, and that this is mandatory in the curricula. The research also emphasized the need for engineers to have free drawing skills to use them quickly on the site. Building to explain ideas because the use of computer graphics is difficult on site and takes time.

After examining the previous studies, it was found that there are many communication skills needed by the architect in the labor market, whether communication skills in the design stage or communication skills in the implementation stage. There are also two types of communication: visual communication and verbal communication as shown in Table 1.

Table 1. communication skills emphasized by previous studies

vocabulary	study(1)	Study (2)	Study (3)	Study (4)
Communication with clients and users	*	*	*	*
listening	*		*	*
negotiation	*		*	*
Communicate with engineers from other disciplines	*	*		*
Explain ideas to the architectural design team		*	*	
Defending their ideas and designs		*		
Speaking in front of an audience to make presentations	*	*		
Outline diagrams				*
Architectural presentation				*
Freehand drawing skills				*
Communication with contractors	*	*		
Communication with professionals	*	*		*
Marketing		*		
Summary preparation	*			
reports writing		*		
Preparing a work proposal		*		
Communication with legal authorities	*			

2.2 Theoretical framework vocabulary

Through the foregoing, a theoretical framework was formed that includes the vocabulary or formulas of communication skills and their most important aspects or the variables they contain, as shown in Table 2.

Table 2. shows the vocabulary of the theoretical framework

Main vocabulary	Sub- vocabulary (Forms of communication)	Variables (aspects of communication skills)
Communication at the design stage	Verbal communication	Communication with customers and users
		Communicate with engineers from other disciplines
		Working with an architectural team
		Dialogue, discussion and exchange of ideas
		Criticize team members in a professional manner
		Public speaking for presentations
		Defending their ideas and designs
		Listening and negotiating
	visual communication	The engineering plans

Communication at the executive stage	Verbal communication	Communication with site engineers
		Communication with contractors
		Communication with professionals
		Marketing
	visual communication	Executive charts
		Summary preparation
		reports writing
		Communication with legal authorities

3. The application framework

3.1 Selection of samples

1. The teaching staff: They are the most important part in the educational process and decision-making.

2. Recent graduates: They were chosen because they have practiced the profession with the knowledge they have and are able to identify what they lack in terms of knowledge of the labor market.

3.2 Determine the measuring tool

The researcher adopted the closed-ended questionnaire format on a five-point Likert scale for most of the questions, and a few open-ended questions were made to survey and analyze the opinions of architects and teaching staff about the importance of communication skills in professional practice.

The questions of the questionnaire were formulated depending on the forms of communication and their aspects that were formed in the theoretical framework, and each of them was coded, whether for teachers or graduates.

The questionnaires were distributed to each of the graduates practicing the profession, and faculty members, each according to his questions. Where the forms were distributed in several Iraqi governorates electronically, and the forms received for the teachers were 42 forms and for graduates 120 forms, and it was processed statistically to avoid discrepancies in the preparation of the forms.

3.3 Application and results analysis

The theoretical framework was applied to the proposed samples, and then the results derived from this application were analyzed as follows:

3.3.1 The statistical description of the results of the questionnaire for the faculty members

After analyzing and tabulating the results (Table 3.), the results showed that 72% of the teachers believe that the courses do not enable students to work with a team from different disciplines due to the lack of joint projects between them, And 73% of them indicated that the courses do not enable students to communicate effectively with professionals on construction sites, and this is due to their lack of extensive exposure to real projects. And 98% of the faculty members indicated that there is a weakness among students in making executive drawings.

On the other hand, the results showed that 98% of the faculty members believe that the courses develop students' skills in defending their ideas and designs, and 95% of them believe that the courses enable them to work with an architectural team and develop their dialogue and discussion skills Also, 93% of them indicated that the courses develop students' ability to speak in front of the public to present projects and information for architectural competitions and to groups of clients and users, and 88% of the teachers

indicated that the courses enable students to criticize works professionally and enable them to listen and negotiate with others, And 86% of them indicated that the courses develop students' conversation skills and persuade customers, while 83% of them believe that the courses enable students to write reports and enable them to manage public relations and marketing for their products.

Table 3. The general average, the frequency distributions, the arithmetic mean, the standard deviations, the coefficient of variation, the response intensity and agreement ratios

variable	Arithm-etic mean	standard deviation	the coefficient of variation	Response measurement										agreement ratios	response intensity
				I strongly agree		I reasonably agree		I slightly agree		neutral		don't agree			
				No.	%	No.	%	No.	%	No.	%	No.	%		
X16	3.357	1.265	37.690	7	16.7	15	35.7	13	31	0	0	7	16.6	83.4	67.142
X17	3.928	0.921	23.446	10	23.8	23	54.8	7	16.7	0	0	2	4.7	95.3	78.572
X18	3.095	1.478	47.766	4	9.5	1	2.3	7	16.6	0	0	30	71.4	28.4	61.904
X19	4.000	1.104	27.608	16	38.1	16	38.1	7	16.7	0	0	3	7.1	92.9	80.000
X20	3.785	1.297	34.285	13	31	19	45.2	4	9.5	0	0	6	14.3	85.7	75.714
X21	4.238	0.849	20.054	18	42.9	18	42.9	5	11.9	0	0	1	2.3	97.7	84.762
X22	3.357	1.284	38.261	8	19	13	31	14	33.3	0	0	7	16.7	83.3	67.142
X23	3.571	1.192	33.384	9	21.4	16	38.1	12	28.6	0	0	5	11.9	88.1	71.428
X24	4.023	1.070	26.601	15	35.8	19	45.2	5	11.9	0	0	3	7.1	92.9	80.476
X25	3.666	1.202	32.808	10	23.8	18	42.9	9	21.4	0	0	5	11.9	88.1	73.334
X26	2.857	1.317	46.105	1	2.3	3	7.1	7	16.6	0	0	31	73.8	26.2	57.142
X5	4.547	0.832	18.302	29	69	9	21.5	3	7.1	0	0	1	2.4	97.6	90.952
General Average	3.70	1.15	32.19		28.77		38.10		20.43		0		12.68	87.31	74.04

3.3.2 Statistical description of the results of the questionnaire for graduates practicing the profession

After analyzing and scheduling the results (Table 4.) below, it turns out that 97% of the graduates have weaknesses in legal matters and communication with legal authorities, and 95% of them have weaknesses in making executive plans, and 90% of them indicate that they suffer from weaknesses in administrative matters. And 71% of them believe that they have weakness in communication skills with a team of various disciplines, and 76% of them believe that they have weakness in communicating with professionals on site.

On the other hand, 95% of the graduates believe that the courses develop in them the skills of defending their ideas and designs, and that 91-93% of the graduates believe that the courses developed their skills of working with an architectural team, dialogue and discussion skills, public speaking skills, listening and negotiation skills, and between 81% -83% of the graduates believe that the courses have developed their skills of persuasion, public relations and criticism in a professional manner, while 74% of them believe that the courses have developed their report writing skills.

Table 4. The general average, the frequency distributions, the arithmetic mean, the standard deviations, the coefficient of variation, the response intensity and agreement ratios

variable I reasonably agree No.	Arithm-etic mean I slightly agree %	standard deviation neutral No.	the coefficient of variation don't agree %	Response measurement										agreement ratios	response intensity
				I strongly agree		I reasonably agree		I slightly agree		neutral		don't agree			
				%	No.	%	No.	%	%	No.	%	No.	%		

y15	**3.142**	**1.424**	**45.309**	**6**	**14.3**	**16**	**38.1**	**9**	**21.4**	**0**	**0**	**11**	**26.2**	**73.8**	**62.858**
y16	**3.857**	**0.951**	**24.676**	**9**	**21.4**	**23**	**54.8**	**7**	**16.7**	**1**	**2.4**	**2**	**4.7**	**92.9**	**77.142**
y17	**2.761**	**1.245**	**45.101**	**2**	**4.8**	**1**	**2.38**	**9**	**21.4**	**3**	**7.1**	**27**	**64.3**	**28.6**	**55.238**
y18	**3.904**	**0.983**	**25.174**	**13**	**31**	**16**	**38.1**	**10**	**23.7**	**2**	**4.8**	**1**	**2.4**	**92.8**	**78.096**
y19	**3.500**	**1.254**	**35.836**	**6**	**14.3**	**23**	**54.8**	**6**	**14.2**	**0**	**0**	**7**	**16.7**	**83.3**	**70.000**
y20	**4.071**	**0.866**	**21.283**	**15**	**35.7**	**17**	**40.5**	**8**	**19**	**2**	**4.8**	**0**	**0**	**95.2**	**81.428**
y21	**3.119**	**1.193**	**38.266**	**3**	**7.1**	**15**	**35.8**	**16**	**38.1**	**0**	**0**	**8**	**19**	**81**	**62.380**
y22	**3.500**	**1.254**	**35.836**	**8**	**19**	**18**	**42.9**	**9**	**21.4**	**1**	**2.4**	**6**	**14.3**	**83.3**	**70.000**
y23	**3.881**	**0.889**	**22.906**	**9**	**21.4**	**23**	**54.7**	**7**	**16.7**	**2**	**4.8**	**1**	**2.4**	**92.8**	**77.620**
y24	**3.714**	**1.088**	**29.303**	**8**	**19**	**22**	**52.5**	**8**	**19**	**0**	**0**	**4**	**9.5**	**90.5**	**74.286**
y25	**2.857**	**1.335**	**46.748**	**2**	**4.7**	**2**	**4.7**	**6**	**14.3**	**0**	**0**	**32**	**76.2**	**23.7**	**57.142**
y9	**4.738**	**0.734**	**15.501**	**35**	**83.3**	**5**	**11.9**	**1**	**2.4**	**0**	**0**	**1**	**2.4**	**97.6**	**94.762**
y10	**4.309**	**1.136**	**26.376**	**27**	**64.2**	**7**	**16.7**	**4**	**9.5**	**2**	**4.8**	**2**	**4.8**	**90.4**	**86.190**
y12	**4.404**	**0.9892**	**22.457**	**26**	**61.9**	**11**	**26.2**	**3**	**7.1**	**0**	**0**	**2**	**4.8**	**95.2**	**88.096**
General Average	**3.696**	**1.095**	**31.055**		**29.06**		**36.75**		**20.7**		**3.7**		**9.7**	**86.55**	**73.9**

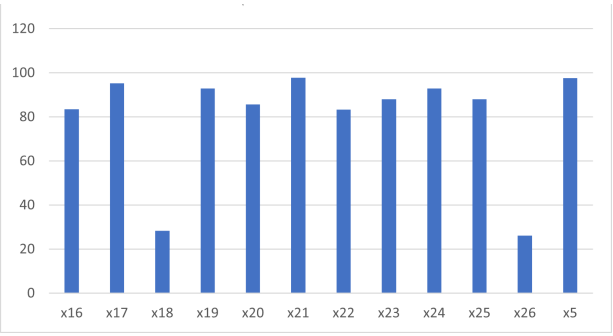

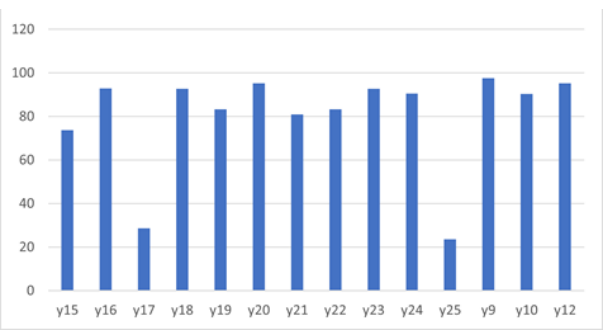

Figure 1. The percentages of agreement for the variables of the teachers. Figure 2. The percentages of agreement for the variables of graduates

3.3.3 Comparison of the results of the questionnaire for teachers and graduates practicing the profession

By analyzing the results for teachers and graduates, it is clear that there is an agreement that architecture graduates do not have communication skills with other engineering disciplines (through the form of visual and verbal communication) because there are no joint projects between them. The teachers and graduates also agreed that they do not have the skills to communicate with professionals in the workplace (both forms of visual and verbal communication), and this is due to the lack of programs for regular visits or to involve them in realistic projects. On the other hand, the teachers and graduates also agreed that there is a weakness in the executive drawings (format of visual communication). The graduates also emphasized that they have weaknesses in visual communication skills related to legal matters and ways of communicating with the legal and administrative authorities.

As for the rest of the communication skills in both their visual and verbal forms, they emphasized that the graduates have these skills, even in varying proportions, and therefore these skills are implicitly present in practical and theoretical courses, but they need continuous improvement to raise the efficiency of these skills further.

4. Conclusions and recommendations

4.1 Conclusions

By analyzing and comparing the results, the research concluded The following conclusions:

1. Graduates cannot communicate effectively with professionals on-site while carrying out supervision activities as a result of the lack of continuous practical training on-site, rather it is limited to one-month training only which is not sufficient.

2. Graduates cannot communicate with the rest of the disciplines in the labor market, such as: (civil, mechanics, electricity.... etc.) due to the lack of joint projects between the different departments and specializations.

3. Graduates suffer from poor communication through executive plans, so there is a need to increase attention to the practical side.

4. The graduates do not know legal matters and how to communicate with government authorities, and this needs to be emphasized in the courses related to aspects of practicing the profession.

5. Most graduates suffer from poor knowledge of administrative matters and how to manage projects, such as preparing a summary, submitting a proposal, and others, as a result of the lack of courses that develop such skills and not including them in practical or theoretical subjects.

6. Most of the graduates have report writing skills, which the student acquires by writing reports on design projects.

7. Graduates have the skills to work with an architectural team, thanks to following the approach of working as a group within some parts of the architectural design course. They also can professionally criticize works, and this is a result of urging courses, especially architectural design, to develop these skills by criticizing the work of their colleagues.

8. The graduates have the skills of dialogue, discussion, and exchange of ideas, as well as the skills of public speaking to present presentations and defend their ideas and designs. This is what the curricula in architectural education, especially architectural design.

9. Graduates can convince clients despite not engaging in real projects and dealing with real clients and real requirements during the years of study.

10. The graduates have knowledge in the field of public relations and marketing for their products, although there are no special courses in project management and marketing.

11. The graduates can listen and negotiate, even though the student did not deal with a real client during his studies, and there are no special courses for learning negotiation methods, but rather he is implicitly trained in the courses.

4.2 Recommendations

1. The need to place greater emphasis on communication skills and increase focus on them in practical materials, or add them as a special course that develops aspects of communication skills, as they are among the basic requirements in the labor market.

2. The need for students to engage in the labor market during their studies by including them in realistic projects to learn communication skills with clients, users, and professionals.

3. Emphasizing and focusing on the subject of executive graphics and strengthening it with modern curricula and

field visits.

4. Set up workshops for students, especially students in the fifth stage, with the administrative and legal authorities responsible for the projects that are implemented to increase their understanding and awareness of the administrative and legal matters related to them and to prepare them for the labor market properly.

5. Holding joint workshops for students with the rest of the engineering departments through the work of joint projects to exchange ideas and raise the efficiency of students in communication with other engineering disciplines.

Conflict of Interest

Authors declare that there is no conflict of interest.

5. References

Al-Yousef, Hamid, Salman, (2014), "Orientation towards quality and reliability in architectural education, the Department of Architecture at the University of Technology as a model", Al-Qadisiyah Journal of Engineering Sciences, Department of Architecture, University of Technology, Baghdad. (Arabic)

Mohamed, Sheeta, Makram, (2015), "Continuous Development of Professional Skills for Architects in Egypt," Mansoura Engineering Journal, Department of Architecture, Future University, Egypt. (Arabic)

Balousha, Al-Mansi, (2014), "The Impact of Developing University Architectural Education on Providing Job Opportunities for Graduates, Case Study - Department of Architecture at the Islamic University of Gaza," Master Thesis, Department of Architectural Engineering, Islamic University, Gaza. (Arabic)

Abdeen, (2007), "Development of Architectural Education for Undergraduate Level", Master Thesis, Faculty of Architecture, Damascus University, Syria. (Arabic)

Badawy, Ashour, Ibrahim, (2009), "The Relationship of University Architectural Education to the Architectural Profession Practice in Egypt," Master Thesis, Faculty of Engineering, Department of Architecture, Ain Al-Shams University, Egypt. (Arabic)

The official website of the University of Mosul http://uomosul.edu.iq/pages/ar/engineering/55301 . (Arabic)

The official website of the University of Baghdad https://coeng.uobaghdad.edu.iq/?page_id=15004 . (Arabic)

The official website of the University of Technology https://ae.uotechnology.edu.iq/images/study%20plan/study%20plan%202012-2017.pdf (Arabic)

Kazem, Ali, Hamid, (2017), "Developing the quality of architectural learning outcomes in Iraq", Iraqi Journal of Architectural Engineering, Department of Architecture, University of Technology, Baghdad.(Arabic)

Esra, B. Kevser, K. (2019). "AN ASSESSMENT OF PROFESSIONAL PRACTICE TRAINING IN UNDERGRADUATE ARCHITECTURAL EDUCATION", The Turkish Online Journal of Design, p 145 -158, İstanbul Kültür University, Turkey.

Amanda, W. Joseph,B .(2011). "MIXED MESSAGES: ASSESSING COMMUNICATION IN ARCHITECTURAL EDUCATION AND PRACTICE". Master Thesis, Department of Public Relations & Advertising, College of Communication, Rowan University, USA.

Natasha,L. (2017). “The Changing Nature of Architectural Education: Do Live Projects prepare students for the realities of architectural practice?”. Master Thesis, Oxford Brookes University,UK.

Wacław,C. (2020). “Architectural education to improve technical detailing in professional practice”. Global Journal of Engineering Education, Cracow University of Technology, Poland.

Suchismita,B . Shivashish,B .(2015). “Comparative analysis of architectural education standards across the world”. University of Oklahoma,OK, Jadavpur University ,Kolkata,India.

David N , Simon P (2000) Changing Architectural Education, London , USA.

Ahmed,A .(2019). “International accreditation of architecture programs promoting competitiveness in professional practice”. Alexandria Engineering Journal, p .877-883, Department of Architecture, College of Architecture and Design, Jordan University of Science and Technology, Jordan, Department of Architectural Engineering, Faculty of Engineering, Alexandria University, Egypt.

Saba,H. Minoo,Sh. (2020). “THE GAP BETWEEN ARCHITECTURE EDUCATION AND ARCHITECTURAL PROFESSION IN IRAN”. Journal of Architectural Research and Education (JARE), p.121-133, Department of Architecture, Faculty of Architecture and Urban Design, Art University of Isfahan, Isfahan, Iran.

Official Website Of ABET Organization https://www.abet.org/ .

Library ,catalogue of RIBA British Architectural www.architecture.

Design and implementation wireless sensors network for monitoring applications using Arduino

Salah Abdulghani Alabady[1*], Sara Raed[2]

[1] Computer Engineering Department, University of Mosul, Iraq
ORCID No: https://orcid.org/0000-0001-9687-2724
[2] Technical Computer Engineering Department, Al-Hadba University College, Iraq
ORCID No: https://orcid.org/0000-0003-0724-9880

Keywords

Multi-hop routing
Wireless Sensor Networks
Internet of Things
Monitoring applications
Energy-aware approach

Abstract

Timely detection of building fires is essential to incident prevention or to reduce the negative impact on human health. This paper presents a Wireless Sensor Networks system for temperature monitoring in a building. In general, sensor nodes in WSN are small, run-on batteries with very limited power resources; it is important to explore power management approaches to enhance network lifetime. The main aim of this system is to save energy costs and reduce power depletion. Through the deployment of many sensors, they collect information about the temperature and send it to the sink. The proposed method is based on multi-hop communication to decrease the transmission energy consumption and increase the monitoring coverage area. Furthermore, we computed the energy usage of the proposed system using Arduino and real sensor networks deployed indoors in the building. The results showed that the proposed system reduced the amount of energy consumed and increased the network's lifetime.

Research Article
Submission Date : 10.04.2023
Accepted Date : 07.05.2023

*Resp author; e-mail: eng.salah@uomosul.edu.iq

1. Introduction

In recent years, a large amount of research has focused on the applications of Wireless Sensor Networks (WSN) in fields like monitoring systems (Gulati et al., 2022). WSN technology is a self-organized network that can provide real-time monitoring by employing many small sensor nodes in the sensing area to collect environmental information (Prabakaran & Kannan, 2017). At the same time, there are many challenges faced by this type of network, like limited energy resources, limited computing capacity, long communication distance, and wireless connectivity, making the sensor network fail most of the time (El-Sayed, Hashem, & Saleem, 2023; Sharma, Prakash, & Roy, 2020). Additionally, when sensor nodes are distributed, the nodes with small batteries should work for a long time without any human intervention (Alabady & Raed, 2018). At the same time, one of the most important design matters in WSNs is to decrease energy consumption by allowing nodes to communicate with each other's and with Base Station (BS) via a multi-hop transmitting schema (Rezaeipanah, Amiri, Nazari, Mojarad, & Parvin, 2021).

Furthermore, nodes must be able to exchange and transmit the monitoring data effectively. In addition, one of the main strategies to reduce energy consumption in WSN technology in wide monitoring fields is multi-hop communication when sending data from remote sensor nodes to the BS (Evangelakos, Kandris, Rountos, Tselikis, & Anastasiadis, 2022; Huang, Ruan, & Meng, 2018). In the general WSN architecture, the end device sensor is located at a large distance from the sink node and transmits the acquired data to the sink (Tiglao, Alipio, Balanay, Saldivar, & Tiston, 2020). The hop means the number of nodes a data packet must pass to reach its destination address. In a single-hop network, when the source packet leaves, take only one hop to the destination without considering the distance. Therefore, using multiple hops in transmission will reduce power consumption by reducing the distance and thus increase the network's lifetime (Yousif, Badlishah, Yaakob, & Amir, 2018). In this paper, we concentrate on maximizing the WSN lifetime by placing intermediate nodes for forwarder between end devisees sensor nodes and BS analysis center for remotely building monitoring systems based on Arduino. The communication used in the proposed model is multi-hop communication.

A significant number of researches using WSN technology have been presented in recent years. For example, the authors (Benammar, Abdaoui, Ahmad, Touati, & Kadri, 2017) suggested a single-hop indoor air quality monitoring system. The gateway is built on the Raspberry Pi 2 platform, while the sensor node is based on the Libelium Waspmote. The system was tested in a school and can sense CO, $CO2$, ozone, clorine, temperature, and humidity. This does not take into consideration the distance between the BS and the sensor node. The authors (Tijani, Almannaee, Alharthi, & Alremeithi, 2018) proposed a building fire system based on WSN for indoor air quality monitoring. The network contains a fixed Arduino and a mobile sensor drone that uses Bluetooth communication technology to send information to a remote smartphone. Then the monitoring data are uploaded to the Cloud via WiFi. The authors (Durrani, Khurram, & Khan, 2019) proposed a smart weather monitoring station to collect weather parameters from the environment and predict them via a combination of the Internet of things (IoT) and deep learning. Numerous sensors built into this system gather information about users' locations and upload it to the cloud. Additionally, they can utilize machine learning techniques to forecast the weather for the future station.

The authors (Qasim, Hamza, Ibrahim, Saeed, & Hamzah, 2020) present a security system for home monitoring based on WSN capable of detecting and sensing a wide range of activities. Specifically, motion detectors, body temperature, humidity, and gas. Moreover, the sensed value sends directly using a single hop from the sensing node to the Arduino. The authors (Mabrouki, Azrour, Dhiba, Farhaoui, & El Hajjaji, 2021) suggested automatic weather conditions monitoring module that provides real-time information about a given area. This system is based on WSN and contains temperature and humidity sensors. Then the sensor node transmits the reading value directly to Arduino. After processing, the Arduino transmits the analyzed values to the server, including a database. Furthermore, the information can be viewed remotely through a web page. The authors (El-Fouly et al., 2022) present an energy-efficient and reliable clustering protocol (ERCP) for WSNs. The suggested routing protocol is based on the idea of an energy-efficient, dependable inter-cluster routing method. The authors in (Behera et al., 2022) summarizes the network's changes to the CH selection threshold value. The article briefly discusses LEACH-based and bio-

inspired protocols, their advantages and disadvantages, underlying presuppositions, and the selection criteria for CH.

As the literature shows, direct communication between sensor nodes and the BS node consumes a high amount of limited energy resources. In this paper, we proposed a wireless sensor system for temperature monitoring based on multi-hop communication. The proposed system is used to remotely and real-time monitor the temperature in a building or home. The module results prove the proposed system's effectiveness in terms of energy consumption. The rest of the paper is organized as follows, section 2 provides the proposed method and the system model, section 3 presents the practical results and results discussion, and section 4 illustrates the conclusion.

2. The Proposed Method and the System Model

This section shows the hardware components used in the proposed system model, and how to connect them to the microcontrollers. In order to have more control over the variables affecting our environment, it is now possible to create systems that gather, analyze, evaluate, and validate data from it. This is made possible by the rapid rise of wireless communications. More flexibility in addressing these environmental issues may be provided by these designs. A wireless sensor system is suggested in this paper for data gathering, processing, and validation. The open-source hardware platform Arduino is the foundation around which the system is built the Arduino Nano as shown in Figure 1 and can be programmed using the Arduino Integrated Development Environment (IDE). The system uses single-wire DHT11 temperature sensors as shown in Figure 2. A single digital pin on the controller can trigger many sensors of this type. As a result, a single sensor node can accommodate numerous single-wire sensors even when the controller only has a few digital pins available.

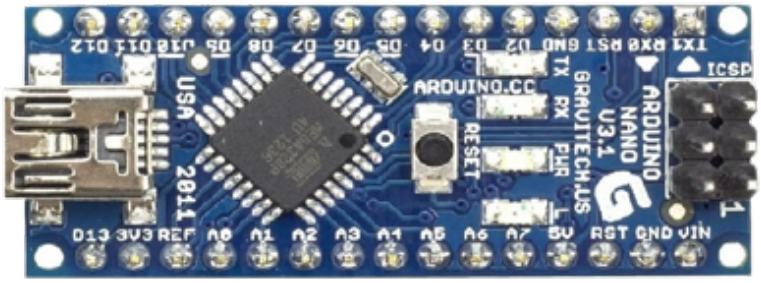

Figure 1. Arduino Nano diagram

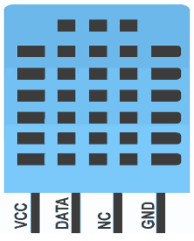

Figure 2. DHT11 Sensor

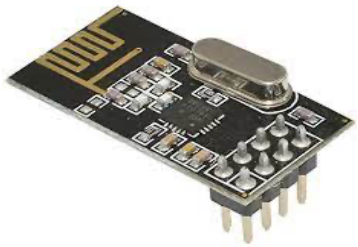

Figure 3. nRF24L01

As a result, sensor nodes are very scalable. The voltage sensor also monitors the battery voltage that powers the sensor node to keep it operating. A mechanism is put in place that instantly connects a new sensor node that enters range with the system base receiving node in order to track data from the sensors. To send and receive data, nRF24L01 (+) radio modules are utilized, as shown in Figure 3. Eight Arduino boards will be used in this system proposal. Figure 4a shows the network topology of the proposal system, and Figure 4b shows practical wireless sensor nodes that are used in the WSN system. The function of nodes 3, 4, and 5 is sensing the environment (temperature, humidity, etc) it works as normal nodes. The function of node 2 is data gathering from the normal nodes (nodes 3, 4, and 5) it works as the cluster head (CH). The function of node 1 is forward the collection data from node 2 to node 0 which in turn works as a sink node or base station that is used to display the sensor results. The function of node 6 and node 7 is to

run the alarm circuit it works as the actuator. The method of communication is through nodes 3, 4, and 5, which sense temperatures as the nodule is distributed in different geographical locations. This node will send data to node 2, which is an intermediate, in turn, will send data to node 1, which is similar to the work of node 2, and node 1 will send data to node 0, which is a base station or the sink through which data will be displayed on the OLED, which will connect to node 6 and node 7 and also connect a switch through which we control the OLED screen and node 0 will send data to node 6 and node 7, which is an alarm attached to it, a buzzer used for the alarm.

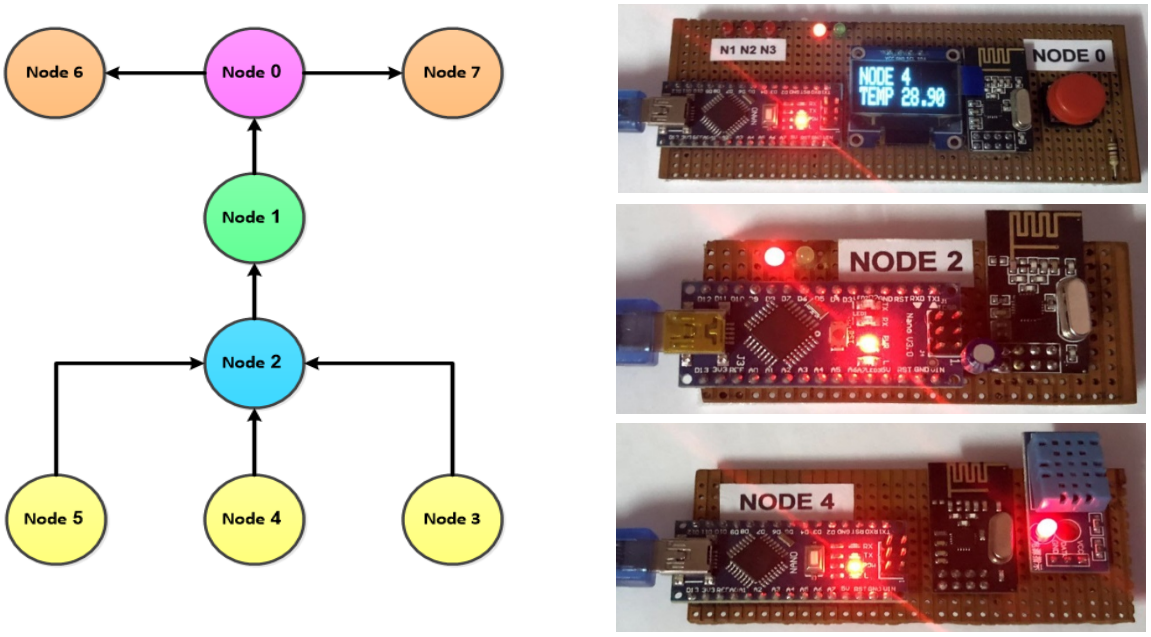

(a) (b)

Figure 4 (a). Network topology of the proposal system **(b).** Practical wireless sensor nodes

The details of the proposed algorithm for sent data and selecting the routing path are as follows:

Pseudo-code:

Notations:

1: SNs: Sensor nodes
2: BS: Base Station
3: D: Distance
4: n: number of nodes
5: T.H: THreshold
6: Temp: Temperature

Network Initialization Phase;

7: START → Initialize for all SNs
8: BS Broadcast Hello_Msg;
9: SNs Broadcast Hello_Msg;
10:Received by SNs = (SN1……..SNn)
11:**for** i=1 to n
12: node-i Receives the Hello_Msg
13: node-i Compute: RSSI Value of Received Signal

14: Node(i) Calculate D for All Neighbors

15: $D = \sqrt{(x_i - x_j)^2 + (y_i - y_j)^2}$
16: Neighbor Table Creation at Each Node
17:**end for**
Information Transmission Phase;

18:SNs Sense Data
19:**if** SNs have Data to Send
20: Send Data Based on Minimum D
21: **else if** BS received a data packet
22: **if** Temp > T.H
23: buzzer ON
24: **end if**
25:**else** Return to Step 16
26:**end if**
27:**end**

2.1. Power Measurement

The power value is determined by the following equation:

$$P = V \times I \qquad (1)$$

Where V represents the voltage, and I refers to the current. The following equation indicates that when the distance increases, the required energy increases. Thus, the small transmission distance reduces the energy consumed by the nodes and improves the network lifetime.

$$E = E_{elec} \times k + (E_{amp} \times k \times d^2) \qquad (2)$$

Where d is the distance, k refers to the amount of data, E is the amount of energy consumption while transmission. E_{elec} is the energy expended to run the transceiver circuit, and E_{amp} is the energy required for the amplification of radio signals (Heinzelman, Chandrakasan, & Balakrishnan, 2000).

3. Results and Discussion

We have set up the sensor nodes for development and testing requirements at the monitoring area. According to Figure 4, the system consists of a coordinator node, two intermediate sensors, and three sensor end nodes. Each sensor node is sent data to the next hop node based on distance. Figure 5 presents sample power consumption results based on collected and routing data from sensors. This data is collected from sensor node 3, sensor node 4, and 5 and sent based on path routing selection to the coordinator node. As can be seen the energy consumed increases as the distance increases, it has significantly reduced the power consumption of monitoring sensor system development.

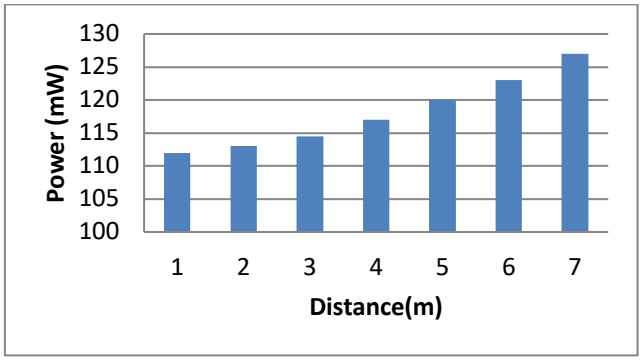

Figure 5. Power consumption in node number 3, 4, and 5

Figure 6 shows the power consumption of intermediate sensors number 1 and number 2. The results show that the power consumption of these intermediate sensors is higher than the end sensors number 3, 4, and 5 because they are always used as forward nodes to deliver data to the coordinator node.The energy consumed by the node that detects an event is shown in Figure 7. According to the graph, there is a relationship between the amount of distance between the source and the destination and the amount of energy used. But we can reduce part of the wasted and consumed energy by reducing the distance by choosing the path based on multiple hops to provide the data to the sink. The results show the reduction of energy consumed through multiple hops to overcome long distances. Figure 8 shows the energy consumption of the sink node. We conclude that the sink is the most energy-consuming compared with previous results, and this is because all nodes send their data to this node and the highest load is on this node.

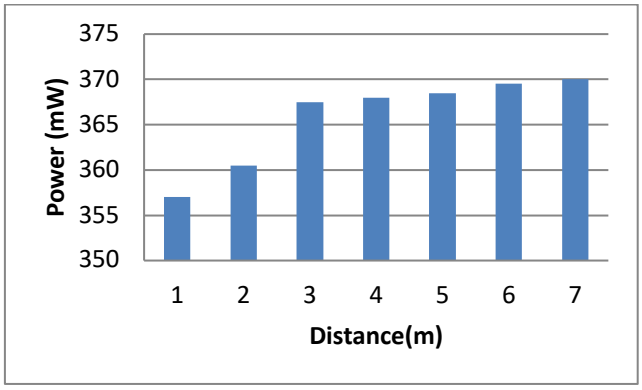

Figure 6. Power consumption in intermediate node number 2, and 1

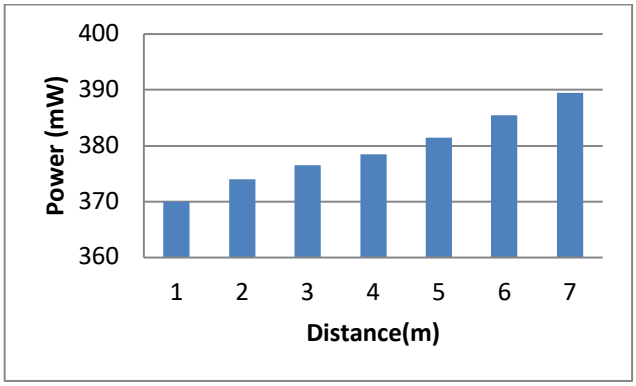

Figure 7. Power consumption of alarm nodes number 6 , and 7

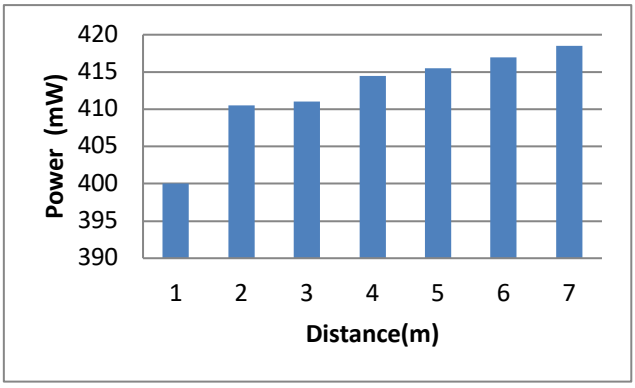

Figure 8. Power consumption of a sink node (node number 0)

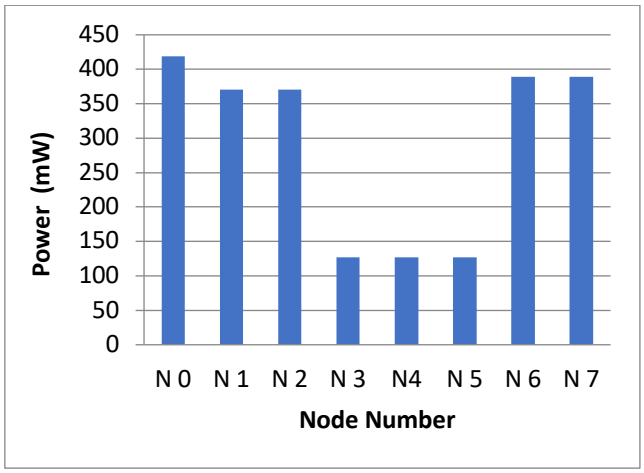

Figure 9. Power consumption of all nodes at distance 7 meter

Figure 9 shows the comparison of the consumed power values for all nodes at a distance of 7 meters. As can be noted in Figure 9 node number 1 and node number 2 consumed a large amount of energy because they were used as the cluster head and intermediate node, respectively. The sink node (Node 0) consumed the highest amount of energy because all nodes in the network send their data to this control node. Furthermore, Table 1 summarizes the power consumption results of all sensor nodes in the proposed system.

Table 1: Power consumption in all nodes

Distance (m)	1	2	3	4	5	6	7
Power consumption (mW) in nodes 3, 4, 5	112	113	114.5	117	120	123	127
Power consumption (mW) in nodes 1, 2	357	360.5	367.5	368	368.5	369.5	370
Power consumption (mW) in nodes 6, 7	370	374	376.5	378.5	381.5	385.5	389.5
Power consumption (mW) in node 0	400	410.5	411	414.5	415.5	417	418.5

4. Conclusion

In this paper, a practical multi-hop wireless sensor network was designed and implemented using an Arduino Nano microcontroller board, a number of sensors, and an nRF24L01+ radio transceiver module. The results show how the power consumption increased when the distance between the nodes increase. The sink node consumes the most energy in comparison to the other nodes. Given that all nodes submit their data to the sink, which carries the heaviest load. The monitoring system is based on small wireless sensor nodes and is dependent on a multi-hop wireless communication paradigm. So, the main aim of this proposed network is to perform continuous and real-time detection of building fires. Furthermore, aims to reduce the power consumption of nodes and increase the lifetime of the network. To reduce energy consumption, each node selects the next hop depending on the minimum distance. Results show the effectiveness of the suggested building monitoring system by increasing the network lifetime and reducing the energy consumption of the sensor nodes. Results show the proposed system saves energy by reducing the power consumption for example from 418.5 mW when the distance 7m to 400 mW when the distance is 1m in case the node 0 (sink node). For future work, network performance will be measured and tested over wide monitoring areas.

Conflicts of interest: The authors declared that there is no conflict of interest.

Authors Contributions: The first author "Salah Abdulghani Alabady" contributed to designing the proposed hardware system and configuring all the components, and collecting the results. In addition to correcting and revising the language, giving appropriate directions on how to write, and analyzing and discussing the results. The second author "Sara Raed" contributed to writing the draft paper and collects all the information in this paper.

References

Alabady, Salah A, & Raed, Sara. (2018). MHUCR: Mutli hop uniform clustering routing protocol for energy efficient WSN. International Journal of Grid and Distributed Computing, 11(6), 95-106, http://dx.doi.org/10.14257/ijgdc.2018.11.6.10.

Behera, Trupti Mayee, Samal, Umesh Chandra, Mohapatra, Sushanta Kumar, Khan, Mohammad S, Appasani, Bhargav, Bizon, Nicu, & Thounthong, Phatiphat. (2022). Energy-Efficient Routing Protocols for Wireless Sensor Networks: Architectures, Strategies, and Performance. Electronics, 11(15), 1-26, https://doi.org/10.3390/electronics11152282.

Benammar, MOHIEDDINE, Abdaoui, ABDERRAZAK, Ahmad, HM SABBIR, Touati, FARID, & Kadri, ABDULLAH. (2017). Real-time indoor air quality monitoring through wireless sensor network. International Journal of Internet of Things and Web Services, 2, 7-13, http://www.iaras.org/iaras/journals/ijitws

Durrani, Areeha, Khurram, Muhammad, & Khan, HR. (2019). Smart weather alert system for dwellers of different areas. Paper presented at the 2019 16th International Bhurban Conference on Applied Sciences and Technology (IBCAST), https://ieeexplore.ieee.org/document/8667190.

El-Fouly, Fatma H, Khedr, Ahmed Y, Sharif, Md Haidar, Alreshidi, Eissa Jaber, Yadav, Kusum, Kusetogullari, Huseyin, & Ramadan, Rabie A. (2022). ERCP: Energy-Efficient and Reliable-Aware Clustering Protocol for Wireless Sensor Networks. Sensors, 22(22), 1-26, https://doi.org/10.3390/s22228950.

El-Sayed, Hamdy H, Hashem, Zainab Mostafa, & Saleem, Mohammed A. (2023). New Proposed Wireless Sensor Network Protocol for Internet of Things Applications. Sohag Journal of Sciences, 8(1), 83-89, https://sjsci.journals.ekb.eg/article_259689.html.

Evangelakos, Emmanouil Andreas, Kandris, Dionisis , Rountos, Dimitris, Tselikis, George , & Anastasiadis, Eleftherios. (2022). Energy Sustainability in Wireless Sensor Networks: An Analytical Survey. Journal of Low Power Electronics and Applications, 12(4), 1-26, https://doi.org/10.3390/jlpea12040065.

Gulati, Kamal, Boddu, Raja Sarath Kumar, Kapila, Dhiraj, Bangare, Sunil L, Chandnani, Neeraj, & Saravanan, G. (2022). A review paper on wireless sensor network techniques in Internet of Things (IoT). Materials Today: Proceedings, 51, 161-165, https://doi.org/10.1016/j.matpr.2021.05.067.

Heinzelman, Wendi Rabiner, Chandrakasan, Anantha, & Balakrishnan, Hari. (2000). Energy-efficient communication protocol for wireless microsensor networks. Paper presented at the Proceedings of the 33rd annual Hawaii international conference on system sciences, https://ieeexplore.ieee.org/document/926982.

Huang, Jianhua, Ruan, Danwei, & Meng, Weiqiang. (2018). An annulus sector grid aided energy-efficient multi-hop routing protocol for wireless sensor networks. Computer Networks, 147, 38-48, https://doi.org/10.1016/j.comnet.2018.09.024.

Mabrouki, Jamal, Azrour, Mourade, Dhiba, Driss, Farhaoui, Yousef, & El Hajjaji, Souad. (2021). IoT-based data logger for weather monitoring using arduino-based wireless sensor networks with remote graphical application and alerts. Big Data Mining and Analytics, 4(1), 25-32, https://ieeexplore.ieee.org/document/9321200.

Prabakaran, N, & Kannan, R Jagadeesh. (2017). Sustainable life-span of WSN nodes using participatory devices in pervasive environment. Microsystem Technologies, 23(3), 651-657, https://doi.org/10.1007/s00542-016-3117-7.

Qasim, HH, Hamza, AE, Ibrahim, HH, Saeed, HA, & Hamzah, MI. (2020). Design and implementation home security system and monitoring by using wireless sensor networks WSN/internet of things IOT. International Journal of Electrical and Computer Engineering, 10(3), 2617, https://ijece.iaescore.com/index.php/IJECE/article/view/20954.

Rezaeipanah, Amin, Amiri, Parvin, Nazari, Hamed, Mojarad, Musa, & Parvin, Hamid. (2021). An energy-aware hybrid approach for wireless sensor networks using re-clustering-based multi-hop routing. Wireless Personal Communications, 120(4), 3293-3314, https://doi.org/10.1007/s11277-021-08614-w.

Sharma, Ravi, Prakash, Shiva, & Roy, Pankaj. (2020). Methodology, applications, and challenges of WSN-IoT. Paper presented at the 2020 International Conference on Electrical and Electronics Engineering (ICE3), https://ieeexplore.ieee.org/document/9122891.

Tiglao, Nestor Michael, Alipio, Melchizedek, Balanay, Jezy Verence, Saldivar, Eunice, & Tiston, Jean Louise. (2020). Agrinex: A low-cost wireless mesh-based smart irrigation system. Measurement, 161, 107874, https://doi.org/10.1016/j.measurement.2020.107874.

Tijani, Ismaila B, Almannaee, Abdulla D, Alharthi, Abdulla A, & Alremeithi, Abdulla M. (2018). Wireless sensor node for indoor air quality monitoring system. Paper presented at the 2018 Advances in Science and Engineering Technology International Conferences (ASET), https://ieeexplore.ieee.org/document/8376839.

Yousif, Yousif Khalid, Badlishah, R, Yaakob, N, & Amir, A. (2018). An energy efficient and load balancing clustering scheme for wireless sensor network (WSN) based on distributed approach. Paper presented at the Journal of Physics: Conference Series, https://10.1088/1742-6596/1019/1/012007.

Various approaches to a bidirectional single-stage single-phase control method PFC-equipped isolated AC-DC converter for EV chargers

S. Gündoğmuş[1*] A. Karaarslan[2]

[1] Electrical and Electronic Engineering, Yıldırım Beyazıt Unıversıty, Ankara
ORCID No: https://orcid.org/0009-0007-1983-8742
[2] Electrical and Electronic Engineering, Yıldırım Beyazıt Unıversıty, Ankara
ORCID No: https://orcid.org/0000-0001-6475-4539

Keywords

PFC, PI Controller, PR Controller, THD, Converter

Abstract

In this study, bidirectional single phase single stage isolated AC-DC converters are controlled using the propotional-resonant (PR) and propotional-integral (PI) control methods. One of the most crucial techniques needed for a system to achieve the ideal circumstances is control. The types of controllers used in power electronics differ depending on the system's structure. Controllers mostly use the open loop and closed loop approaches. For the system to function effectively, closed loop controllers like fuzzy, PI, PID, PR, etc. are typically employed. One of the most widely used controllers for grid-connected inverters to manage the current fed into the grid and reject harmonic disturbances is the PR control approach. The steady state error that occurs while following or rejecting high frequency signals can be completely eliminated by the PR control approach since it has a large gain near the resonant frequency. The Matlab Simulink application is used to compare and verify the PR and PI control strategies that were employed in this investigation.

Research Article
Submission Date : 17.04.2023
Accepted Date : 15.05.2023

1. Introduction

People have started concentrating on technological studies in this direction as the demand for renewable energy sources rises. The trend toward electric cars (EVs) has grown as these studies have as well (Ebrahimi, Taghavi, Tahami and Oraee, 2014). Electric vehicle chargers are prepared to transport both active and reactive power between the grid and EV batteries (Baharom, Salleh, Seroji and Hamzah, 2015), (He, Lu, Wu, Yang, Li and Liu, 2020). Moreover, the non-linear characteristics of DC power sources demonstrate larger harmonic distortions (Prasanna, Singh and Rajashekara, 2017). This leads to numerous issues. Whole harmonic distortion can be fixed as a result of these issues by adjusting power factor (Kisacikoglu, 2013). The outcome of using PFC demonstrates that the choice of controller and the method used are equally crucial to the success of the topology design (Afonso, Freitas and Martins, 2004), (Ortatepe and Karaarslan, 2018), (Karaarslan and İskender, 2011), (Karaarslan and İskender, 2012). The switching elements in the system are switched by utilizing both PI and PR controllers without the use of additional circuits, and when PI and PR controllers are compared,

significant system differences appear (Liu and Lee, 1986), (Prasanna, Rathore and Mazumder, 2013), (Jauch and Biela, 2012), (Busarello, Pomilio and Simoes, 2018), (Lin, Liu and Meng, 2023), (Hornik and Zhong, 2012). In this study, Matlab Simulink was used to observe the performance of the PR and PI controller behaviors using the same topology.

2. Introducing Bidirectional Converter Topology

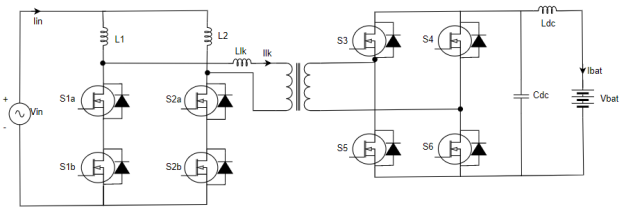

Figure 1. Topology of a single-stage Bidirectional Converter

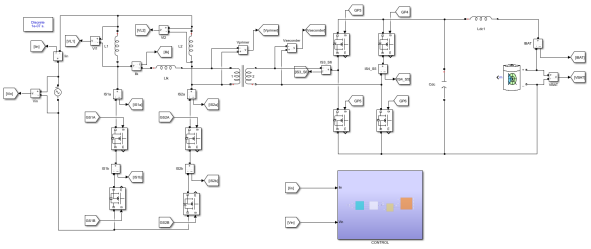

Figure 2. Single-phase Single-stage a Standalone AC-DC converter Topology in Matlab

The polarity of the input voltage and the positive and negative directions of the input current determine the four quadrant modulation. This circumstance leads to the conclusion that the system is acting in both the charge-discharge state and the inductive-capacitive state.

2.1. Four Quadrant Modulation Stage:

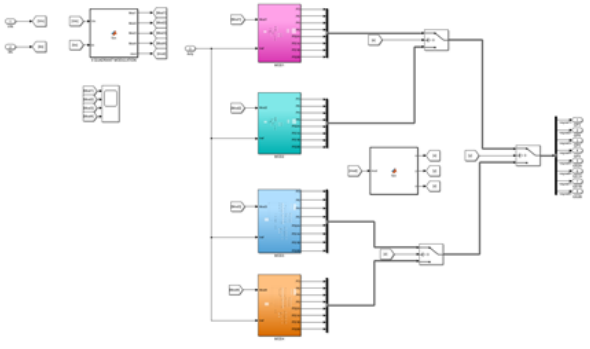

Figure 3. Four Quadrant Modulation Stage

In this section, the polarity of the input voltage and the direction of the input current are used to determine the system's mode of operation. To provide ZVS and ZCS techniques, each mode is configured in its own subsystem.

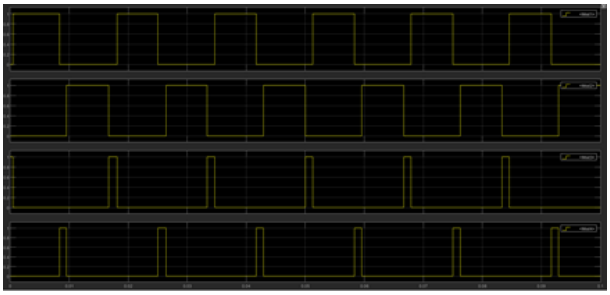

Figure 4. Switching In Mode Transitions

The system's mode of operation is established in this section based on the polarity of the input voltage and the direction of the input current. ZVS and ZCS techniques are provided by each mode, which is configured in its own subsystem.

3. Constructing Circuit and PR Controller

The proposed circuit topology is used to configure the simulation circuit. A PR controller is that the combination of a proportional term and a resonant term given by

$$CPR(s) = Kp + 2Ki\frac{s}{s^2 + \omega^2} \quad (1)$$

The controller transfer function is denoted as CPR(s), where is the resonant frequency. Such a controller can monitor or reject sinusoidal signals with no steady-state error since it has a high gain area around the resonant frequency. The proportional gain (kp) is used with a resonant route to create the digital PR controller. The resonant gain (ki) and transfer function make up the resonant path. Proportional resonant digital control has been used up until this point. In order to provide small steady-state error in the regulated variable, the PR controller operates at such a frequency. As a result, the PR controller works to maintain the current amplitude and frequency at the modified resonance frequency while also responding swiftly to faults.

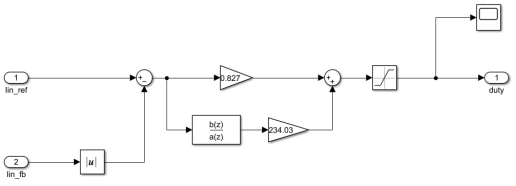

Figure 5. PR Control Topology Matlab Implementation

Input current and output current were taken into account when applying the pr control method. The calculation method of these currents (Iin_ref and Iin_fb) was applied according to the formulas below.

$$\theta = tan^{-1}\left(\frac{Pref}{Qref}\right) \quad (2)$$

$$Ic = \left(\frac{Pref}{V_S * \cos(\theta)}\right) \quad (3)$$

$$Ic = \sqrt{2} * Ic * \sin(\omega t + \theta) \quad (4)$$

The reference values for active and reactive power, as well as the angle between them, are determined. Ic is calculated as the rms value using this angle's value. The angle between the input voltage and current and the first angle value discovered is then added, and its sinus is taken in order to make PFC and determine the Ic reference value.

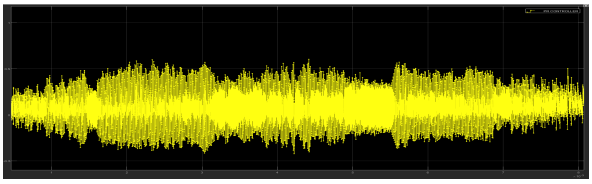

Figure 6. Duty of PR Controller (The PR controller's duty ratio ranges from -1 to -1)

When the PR controller is activated, PWM values are displayed at the output.

3.1. PR Controller Simulation Results:

1- Active power:1000W

Reactive power:-500Var

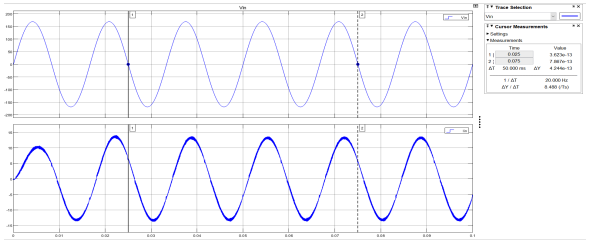

Figure 7. Vin-Iin Graph (Input voltage from Vin and source Iin's current draw)

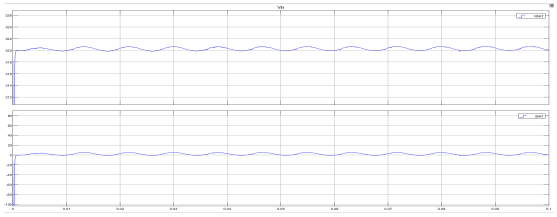

Figure 8. Vbat-Ibat Graph (Simulation results demonstrating battery-side reactive power adjustment)

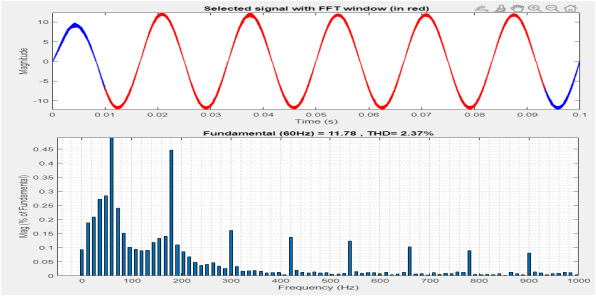

Figure 9. Proposed Converter THD with PR Controller (Input current is controlled to maintain THD at 2.37 percent and be in phase with the voltage)

Even though there is reactive power, the PFC required to adequately charge the battery is carried out as indicated in Figure 8.

4.Constructing Circuit and PI Controller

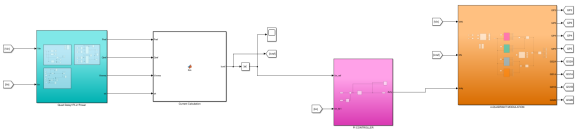

Figure 10. Control Circuit With PI Topology

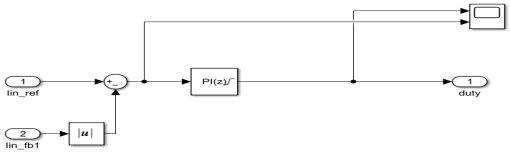

Figure 11. PI Control Topology Matlab Implementation

Non-integrating processes, or processes that eventually produce the same output given the same set of inputs and disturbances, require PI control. The most effective controller for integrating processes is P-only. Integral action, which may be viewed of as an adjustable bias voltage, is employed to eliminate offset. The determined current reference and the feedback reference obtained from the input are compared, and the PI controller is used to compute the PWM duty.

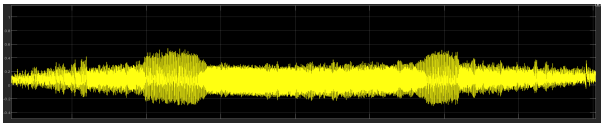

Figure 12. Duty of PI Controller (The duty ratio in the PI controller varies between -1 and -1)

4.1. PI Controller Simulation Results:

1- Active power:1000W

Reactive power:-500Var

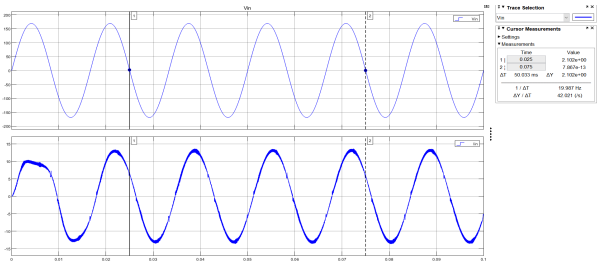

Figure 13. Vin-Iin Graph (Input voltage from Vin and source Iin's current draw)

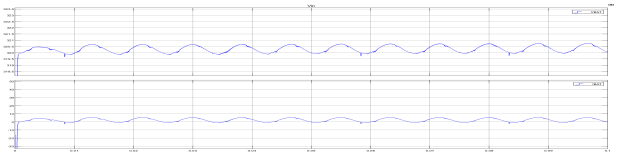

Figure 14. Vbat-Ibat Graph(Simulation results demonstrating battery-side reactive power adjustment)

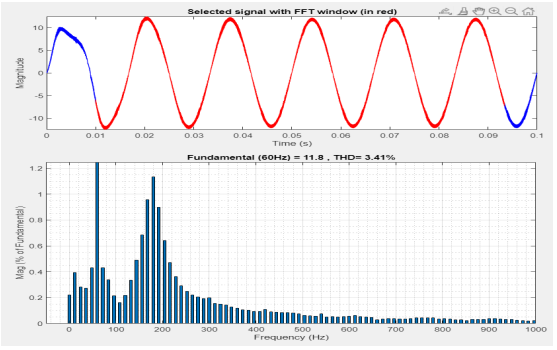

Figure 15. Suggested Converter THD with PI Controller (Input current is controlled to maintain THD at 3.41 percent and be in phase with the voltage)

In Figure 15, the input current is controlled so that it is in phase with the voltage and that the THD remains at 3.41%, which is less than the 5% mandated by IEEE 519.

5. Conclusion

When the output signal is not sent back into the system's input, the control system is said to be in an open loop. As a result, a non-feedback control system is another name for an open loop control system. On the other hand when the output signal is fed back into the system's input, the control system is said to be in a closed loop. As a result, the control action in a closed loop control system depends on the desired output signal. Although open loop controllers are simple, their reliability is lower than closed loop controllers. Because open-loop systems behave according to calibration, while closed-loop systems behave according to feedback signal. A bidirectional single-phase single-stage isolated AC-DC converter topology is studied by comparing and contrasting the two closed loop approaches as a consequence of the comparison.

Yet, PR control is superior to PI control in terms of effectiveness. Because in systems connected to the grid, the frequency and amplitude of the PR controller can be adjusted more stable than the PI controller.

	PI Controller	PR Controller
Complexity	Simple	Complex
Response	Slow	Fast
THD(%)	High	Low
Simulation Time	High	Low
Soft Start	Practicable	Practicable
ZVS	Practicable	Practicable
ZCS	Practicable	Practicable

Table 1. Table of Comparison between PI and PR Controllers

Conflict of Interest

Authors declare that there is no conflict of interest.

6. References

Afonso, J. L., Freitas, M. S., & Martins, J. S. (2003, June). pq Theory power components calculations. In *2003 IEEE International Symposium on Industrial Electronics (Cat. No. 03TH8692)* (Vol. 1, pp. 385-390). IEEE. https://ieeexplore.ieee.org/abstract/document/1267279

Baharom, R., Salleh, M. K. M., Seroji, M. N., & Hamzah, M. K. (2015, June). A high power factor bidirectional battery charger using single-phase matrix converter. In *2015 IEEE 10th Conference on Industrial Electronics and Applications (ICIEA)* (pp. 1397-1402). IEEE. https://ieeexplore.ieee.org/abstract/document/7334327

Busarello, T. D. C., Pomilio, J. A., & Simoes, M. G. (2018, December). Design procedure for a digital proportional-resonant current controller in a grid connected inverter. In *2018 IEEE 4th Southern Power Electronics Conference (SPEC)* (pp. 1-8). IEEE. https://ieeexplore.ieee.org/abstract/document/8636052

Ebrahimi, S., Taghavi, M., Tahami, F., & Oraee, H. (2014, November). A single-phase integrated bidirectional plug-in hybrid electric vehicle battery charger. In *IECON 2014-40th Annual Conference of the IEEE Industrial Electronics Society* (pp. 1137-1142). IEEE. https://ieeexplore.ieee.org/abstract/document/7048645

He, T., Lu, D. D. C., Wu, M., Yang, Q., Li, T., & Liu, Q. (2020). Four-Quadrant Operations of Bidirectional Chargers for Electric Vehicles in Smart Car Parks: G2V, V2G, and V4G. *Energies*, *14*(1), 181. https://www.mdpi.com/1996-1073/14/1/181

Hornik, T., & Zhong, Q. C. (2012). Control of power inverters in renewable energy and smart grid integration. John Wiley & Sons. https://books.google.com.tr/books?hl=tr&lr=&id=m5kWmDIiuxQC&oi=fnd&pg=PT9&dq=CONTROL+OF+POWER

+INVERTERS+IN+RENEWABLE+ENERGY+AND+SMART+GRID+INTEGRATION&ots=99S1jv5Uz2&sig=t6KOIRq1wCHHxVmXrO9HjwOiK6c&redir_esc=y#v=onepage&q=CONTROL%20OF%20POWER%20INVERTERS%20IN%20RENEWABLE%20ENERGY%20AND%20SMART%20GRID%20INTEGRATION&f=false

Jauch, F., & Biela, J. (2012, September). Single-phase single-stage bidirectional isolated ZVS AC-DC converter with PFC. In *2012 15th International Power Electronics and Motion Control Conference (EPE/PEMC)* (pp. LS5d-1). IEEE. https://ieeexplore.ieee.org/abstract/document/6397479

Karaarslan, AHMET, & Iskender, I. (2011). A DSP based power factor correction converter to reduce total harmonic distortion of input current for improvement of power quality. Electrical Engineering, 93(4), 247-257. https://link.springer.com/article/10.1007/s00202-011-0215-5

Karaarslan, AHMET, & Iskender, I. (2012). Average sliding control method applied on power factor correction converter for decreasing input current total harmonic distortion using digital signal processor. IET Power Electronics, 5(5), 617-626. https://digital-library.theiet.org/content/journals/10.1049/iet-pel.2011.0348

Lin, J., Liu, S., & Meng, K. (2023, April). Stability Analysis and Controller Synthesis. In Journal of Physics: Conference Series (Vol. 2479, No. 1, p. 012048). IOP Publishing. https://iopscience.iop.org/article/10.1088/1742-6596/2479/1/012048/meta

Liu, K. H., & Lee, F. C. (1986, June). Zero-voltage switching technique in DC/DC converters. In *1986 17th Annual IEEE Power Electronics Specialists Conference* (pp. 58-70). IEEE. https://ieeexplore.ieee.org/abstract/document/7415546

Kisacikoglu, M. C. (2013). Vehicle-to-grid (V2G) reactive power operation analysis of the EV/PHEV bidirectional battery charger. https://trace.tennessee.edu/utk_graddiss/1749/

Ortatepe, Z., & Karaarslan, A. (2018). The performance analysis of AC-DC bridgeless converter using fuzzy self-tuning and comparing with PI control method. Journal of Intelligent & Fuzzy Systems, 35(4), 4629-4642. https://content.iospress.com/articles/journal-of-intelligent-and-fuzzy-systems/ifs172134

Prasanna, U. R., Rathore, A. K., & Mazumder, S. K. (2013). Novel zero-current-switching current fed half-bridge isolated DC/DC converter for fuel-cell based applications. *IEEE Transactions on Industry Applications*, *49*(4), 1658-1668. https://ieeexplore.ieee.org/abstract/document/6497595

Prasanna, U. R., Singh, A. K., & Rajashekara, K. (2017). Novel bidirectional single-phase single-stage isolated AC–DC converter with PFC for charging of electric vehicles. *IEEE Transactions on Transportation Electrification*, *3*(3), 536-544. https://ieeexplore.ieee.org/abstract/document/7892932

Harmonics elimination of seven phase uncontrolled rectifiers driving Dc motor

Myasar Salim Alttar[1*], Firas Ahmed Aldurze[2]

[1]MechatronicsDepartment, Mosul University, Mosul
ORCID No: https://orcid.org/0000-0001-8725-0448
[2] MechatronicsDepartment, Mosul University, Mosul
ORCID No: https://orcid.org/0000-0001-7709-6731

Keywords
uncontrolled rectifier
THD
seven phase
filters
dc drive

Abstract

Conventional three-phase electrical power systems have great application in industrial and home appliances. An increasing demand for power by consumers has led to the consideration of using different types of power generation units such as solar, wind, and thermal, can be individually used or connected with main the idea network. This driven has engineers to create a modern electrical system with more than three which phases, such as five, six, seven, nine, and more. Using this type of schematic mode helps to achieve better performance of the system in transmitting power, reliability, and stability. Despite these benefits, a generation of harmonics problem appears in the network when using different types of converters such as AC-DC (rectifiers) or DC-AC (inverters). To overcome this problem, a filter design is introduced to eliminate harmonics. In a paper, MATLAB R2020b is used to simulate a seven-phase uncontrolled rectifier driving a DC shunt motor, and a filter is designed and connected with the DC drive. This research presents an analysis of input/output voltage and current waveforms with the THD value of an input current before and after the filter is connected.

Research Article
Submission Date : 14.04.2023
Accepted Date : 21.05.2023

1.Introduction

Multi-phase systems receive wide interest in various domestic and industrial uses. They also have the main role in generation and transmission systems of electric power, especially after the expansion of uses for alternative energies, including solar and wind. Among these three, five, seven, etc. systems, the second type is considered the first development after the traditional triple, where attention has been paid By designing special generators for generating it, as well as designing variables and power converters for changing them into a direct current system, as well as many attempts were made to improve their performance and raise their efficiency through the development of the controlled rate circuit, then the Seven appeared, which consists of seven phases, with a phase difference of 51.428 between them Attention has also increased in many topics related to reducing the harmonics resulting from the rectification process towards the design of different types of active or reactive filters for different types of rectifiers with multiple phases,raising the efficiency of the system (H. Rashıd 2001)(Masoud,2015).)(HeJun,2022).In Figures 1 and 2, different types of multi-phase systems are shown.

*Resp author; myasaralattar@uomosul.edu.iq

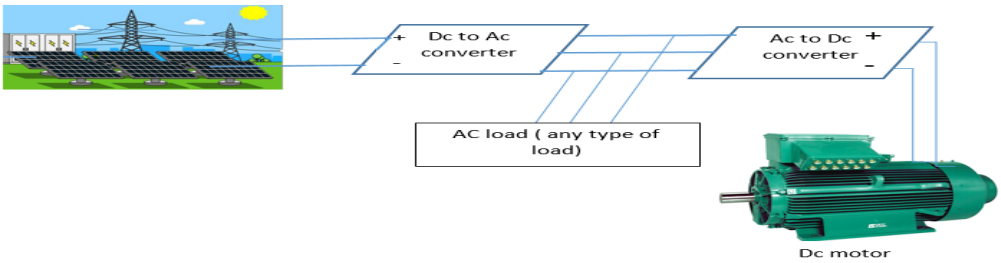

Figure 1. solar schem connected to multiphase system

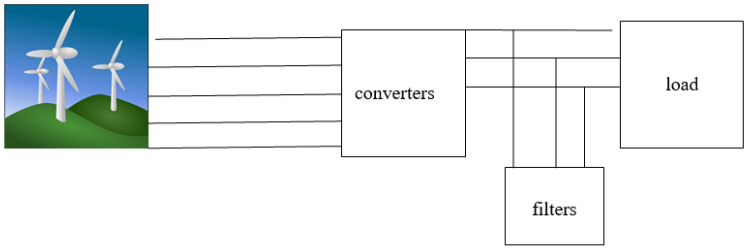

Figure 2. wind turbine schem with multiphase system

2.Model structure:

The studied model in this search consists of multiple stages of components as shown in Figure 3. It can be classified into four parts. The first represents three to seven phase source supply, consisting of a traditional three-phase source connected to a new assembly of transformer winding grouping as three sets. The next presents an alternating to direct current converter (rectifier) which consists of an uncontrolled third part, a DC shunt motor acting as a load connected to the rectifiers. Finally, the last is a filter designed and linked with a circuit to eliminate harmonics generated by power electronic switches in the converter and transformer.

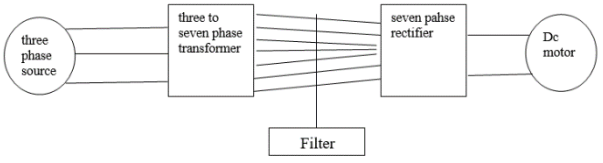

Figure 3. Block diagram of model structure

2.1.Innovative seven phase system using transformer-winding modification

Transformers play a major role in electrical power circuits by changing the number of their turns or the way their coils are wound. Many circuits of power electronics devices depend on traditional three-phase transformers. Because of the need for a three-phase system in transmitting lines, high power converters, DC and AC drives, in recent applications,as as a result of the increasing demand for energy and the difficulty of generating electric power with more than three phases, the need to use renewable energies arose, and to complete the process of transferring power and investing it over long distances, the need to create a multi-phase system that exceeds three appeared, such as five, six, seven or more. Transformers were used as an aid to change the shape of the connection as well as increase the number of phases by using innovative methods of connecting the coils. Figure 4-a represents the schematic diagram of the transformer used in the model with modifications to transform the phases from three (Y) connection to seven phases, while 4-b presents an implementation of the transformer mentioned in the figure above using MATLAB Simulink (Simscape) and its phasor diagram showing the suitable mode for connecting for increasing phases to seven (Chandramohan,2017)

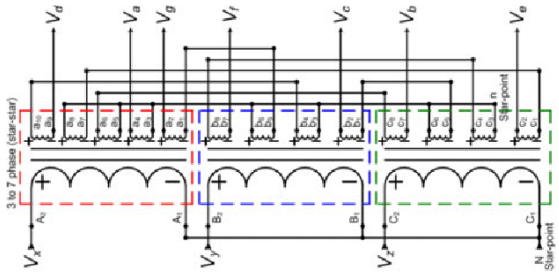

Figure (4-a) represent the schematic diagram of transformer circuit

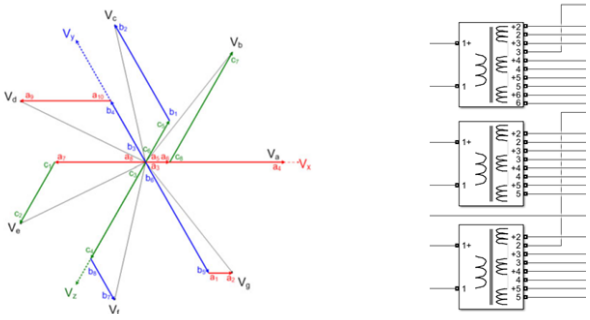

Figure (4-b) block diagram of transformer in matlab Simulink and its phasor diagram

2.2.Rectifier circuit's scheme

The studied rectifier shown in paper, in this Figure 5, consists of uncontrolled power electronic switches (diodes) acting on seven legs representing all phases with 51.428° electrical degree. Its output voltage has fourteen pulses generated by diodes named D1-D7, which denote the upper converter, while D8-D14 refer to the lower, as follows Moinoddin(Shaikh, 2012). (Tabrez, 2017)

$$Vpha1 = Vp \sin(wt) \quad (1)$$

$$Vpha2 = Vp \sin(wt-2\pi/7) \quad (2)$$

$$Vpha3 = Vp \sin(wt-4\pi/7) \quad (3)$$

$$Vpha4 = Vp \sin(wt-6\pi/7) \quad (4)$$

$$Vpha5 = Vp \sin(wt-8\pi/7) \quad (5)$$

$$Vpha6 = Vp \sin(wt-10\pi/7) \quad (6)$$

$$Vpha7 = Vp \sin(wt-12\pi/7) \quad (7)$$

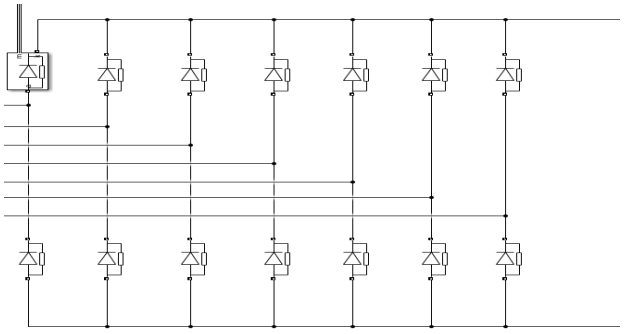

Figure (5). seven-phase rectifier circuit

2.3.Circuit Load

With differen types of loads may be connect to rectifiers dc motor is the common type in many application . In this search dc shunt motor is used as a load shown in figure (6)

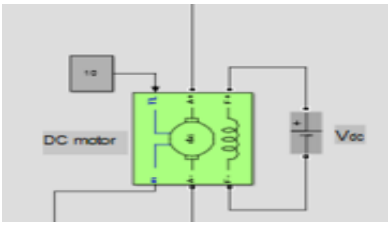

Figure (6) .dc shunt motor (load)

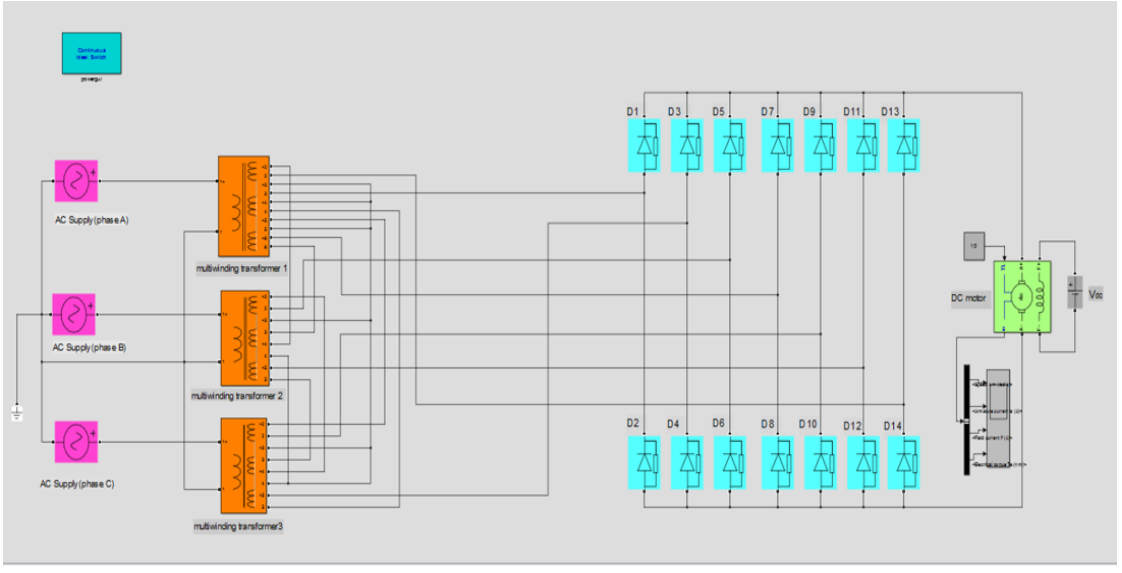

Figure (7). complete circuit model

3.Simulation results The results of this research are divided into two main parts: the first depends on the initial case without any additions, and the second depends on adding a filter to the circuit and its effect on reducing or eliminating harmonics.

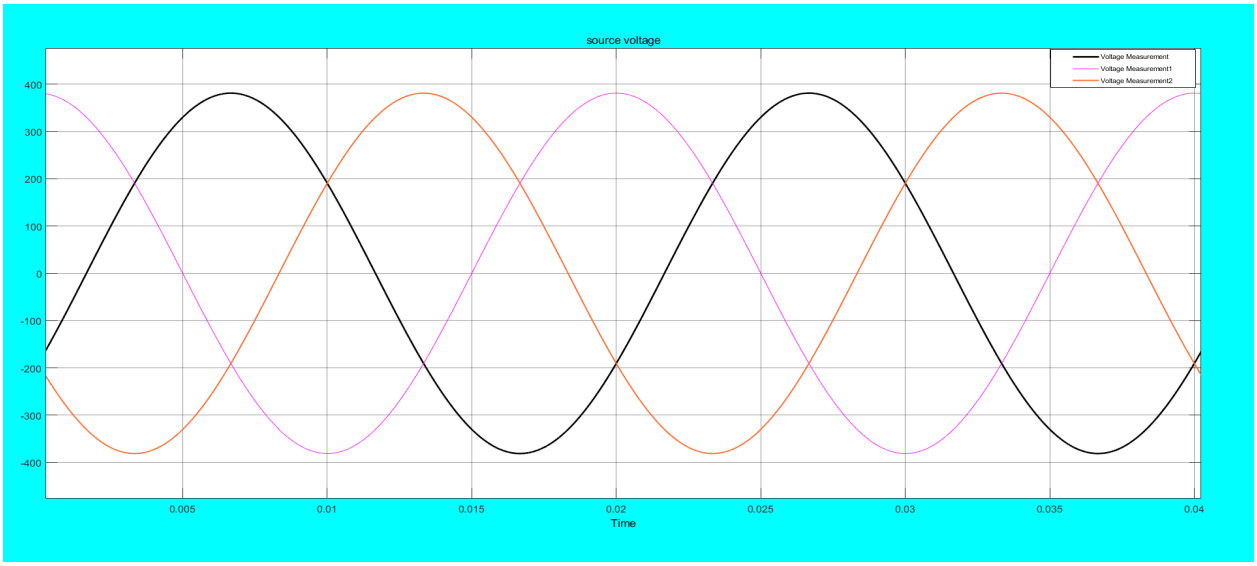

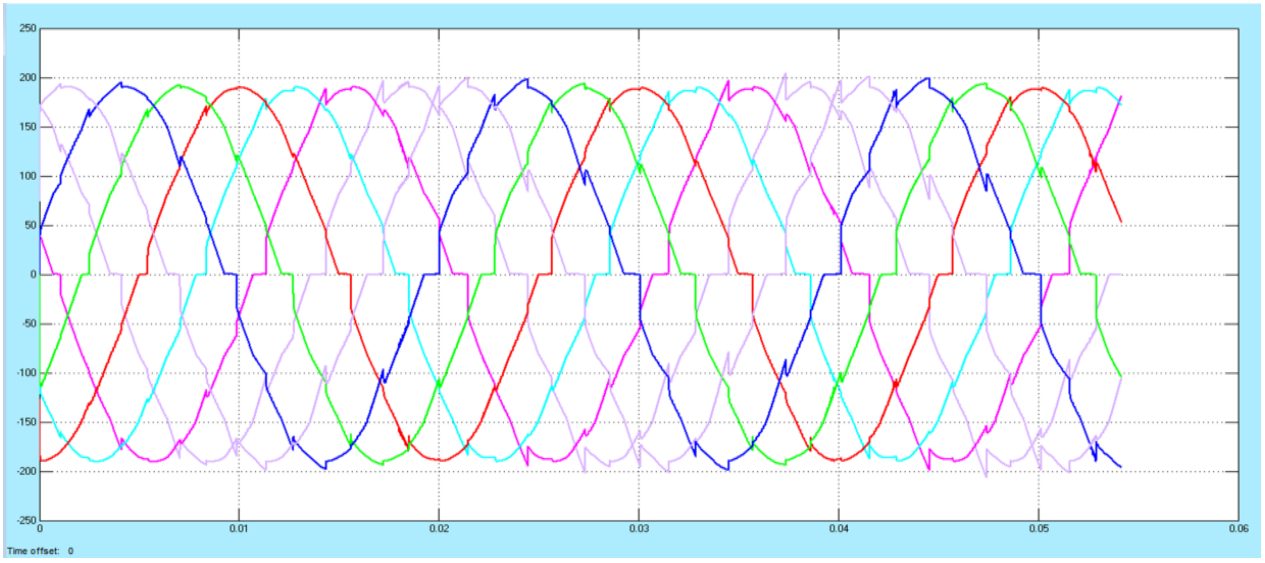

Figure (8).three-phase source voltage

Figure (9).transformer output voltage

The figure 8 shown represents the main three sources responsible for generating the base voltage feeding the transformer sets; these output voltages are purely sine waves. However, the output voltages from the transformers in figure 9 have many harmonic components due to the high reactance in circuits, which leads to unsuitable operating conditions in rectifiers, causing the DC motor to run with unacceptable vibration. The current in figure 10 consists of a seven-wave form with 51.428° electrical degrees, supplying the rectifier with shapes similar to a square wave; this form is due to the effect of circuit and motor reactance.

Figure (10).transformer output current

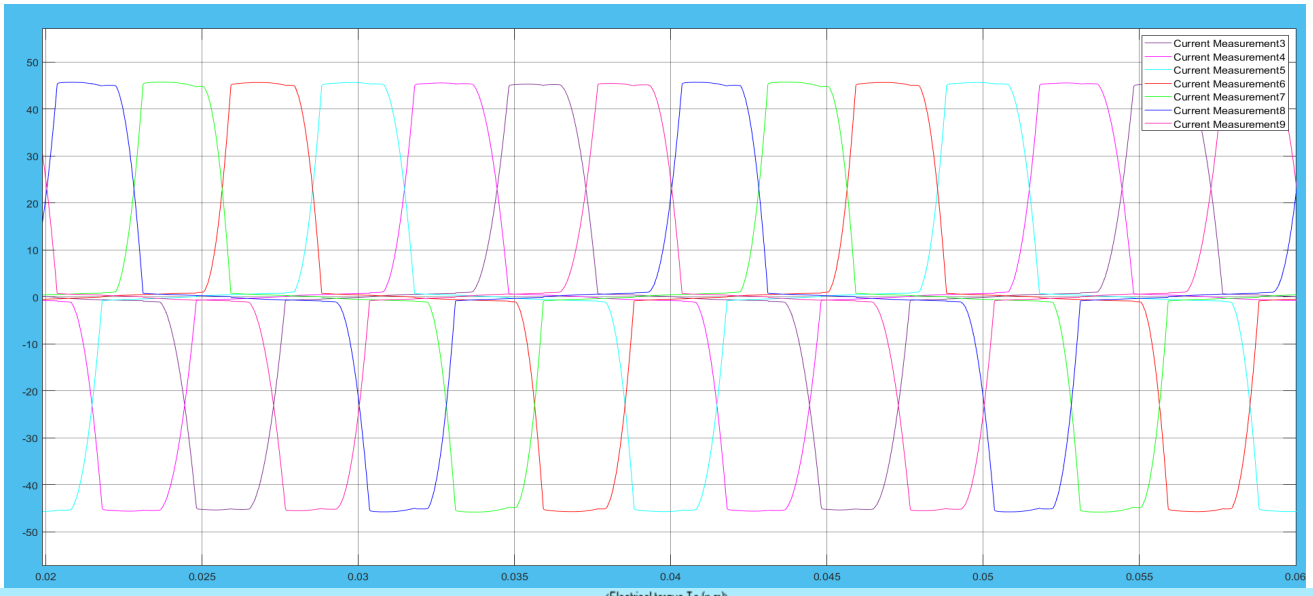

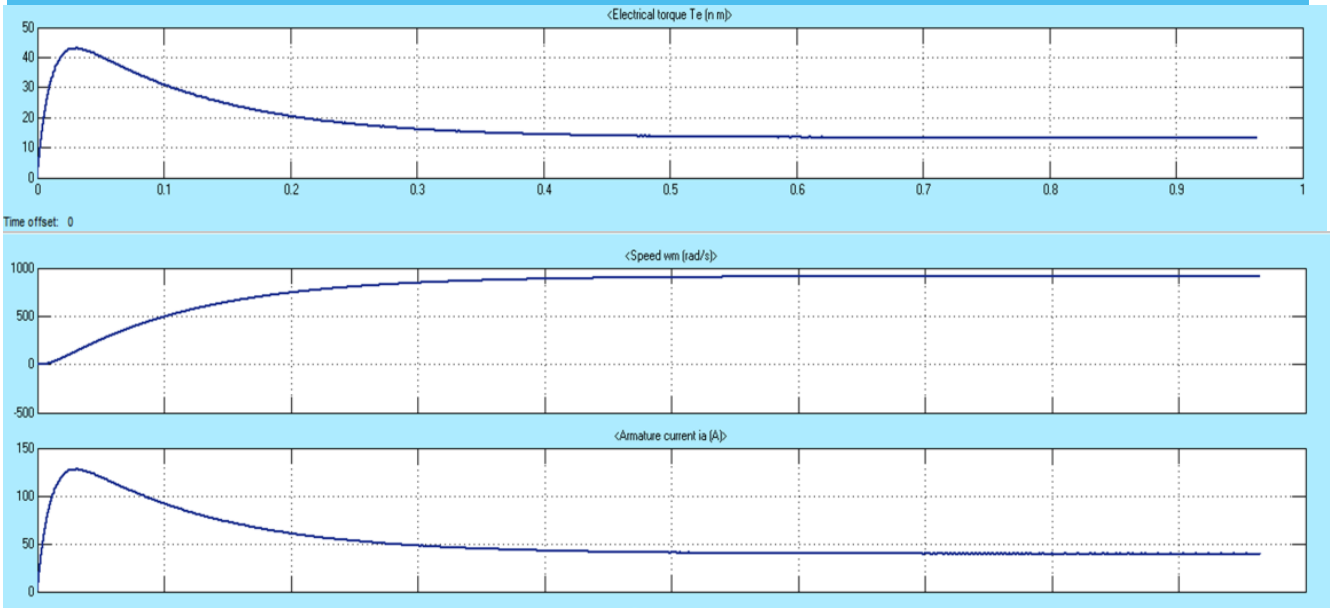

Figure (11).speed, armature current and torque of dc motor

The figure (11) displayed the motor performance, which described by speed in rpm, armature current and torque in Newton. Meter

3.1.Total harmonics distortion

Total harmonic distortion (THD) represents the amount of distortion in each current or voltage wave in power electronics circuits or power circuits as a result of the presence of harmonic components of the sine wave of a frequency of more than 50 Hz as its multiples or at lower frequencies as its parts.

The calculation of THD can be known as the relation between root mean square for current or voltage. It includes all components of frequencies (nth) form, higher than the second to the main component of frequency of the mentioned signals. The following equation presents the

$$THD = \frac{\sqrt{\sum_{n=2}^{\infty} V_n^2}}{V1} \tag{8}$$

mathematical form of this relation.
Vn : represent the all component of voltage higher than main (all values in rms)
V1 : represent the main component of voltage (rms)

In the last equation it can generalize the previous equation to current instead of voltage and for the same definition

$$THD = \frac{\sqrt{\sum_{n=2}^{\infty} I_n^2}}{I1} \tag{9}$$

In : represent the all component of current higher than main (all values in rms)
I1 : represent the main component of current (rms) (H. Rashıd, 2001)

the following figure represented the total harmonics distortion appear on current wave form supplied by transformer to rectifier circuit , it can be shown the effect of high reactance on shape of signal beside the high value of distortion on it .where the odd harmonics component are the dominant ,third and fifth harmonics

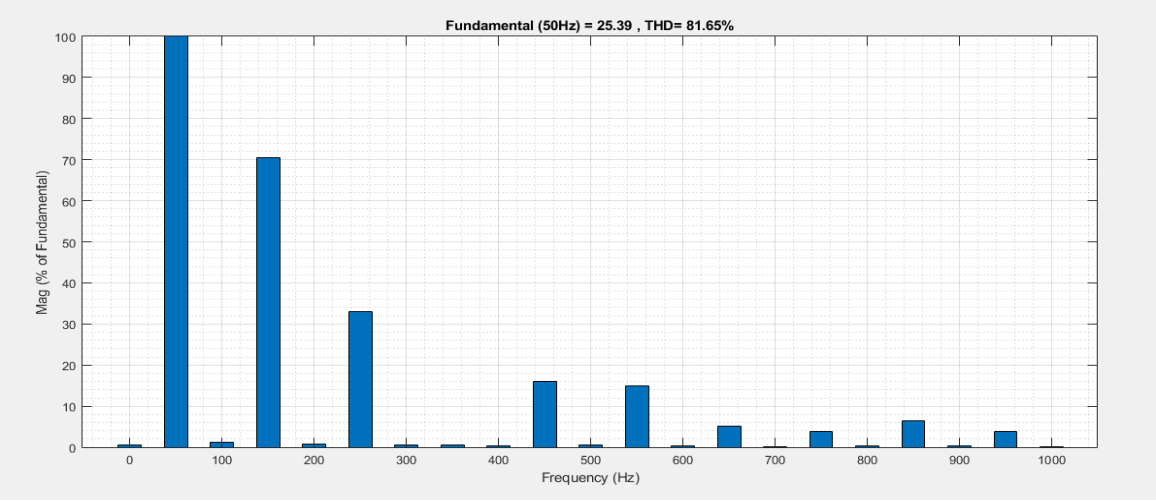

Figure (12). total harmonics distortion (THD) in phase A

The dominant and largest values are followed by the ninth and eleventh, with the seventh disappearing and while the ones vanishing. even This result can used to eliminate or reduce these harmonics as much be as possible, which can be achieved by designing and connecting filters to the circuit. Many types of filters are used for this purpose, which be classified can

into many types according to their type; it may be active depending on designing an to inverter work a filter as or passive associated with the passive and active elements an in electric circuit such as resistors, inductors and capacitors. In this research, passive filters are used to eliminate the There are two kinds of them, harmonics. the of which first will used

3.2.Types of passive filter

Types of passive filter: be 1- Band-Pass Filters: used to reduce the odd harmonics an electric circuit; these types are in used for eliminating one frequency for each circuit (mono-tone filters) or two frequencies (dual-tone filters). designed 2-High-Pass Filters: used for high harmonics. They order also classify into three types (single, dual, high-pass triple) filter. 13 shows the filter types. Figure Represents (a) the single mono-type, or (b) points the to dual band.

The equations needed to design the filter can be written in the following form

$$\boldsymbol{fo} = \frac{\mathbf{1}}{\mathbf{2}\boldsymbol{\pi}\sqrt{\boldsymbol{LC}}} \tag{10}$$

$$\boldsymbol{Qc} = (\sqrt{\boldsymbol{L}}/\boldsymbol{C})/\boldsymbol{R} \tag{11}$$

Where

fo target frequency needed to design filter

QC quality factor ,that can be define as the ratio between the

maximum stored energy and dissipated power at resonance frequency (I.Zynal Hussein & A.Fadeel Bashar.(2014)

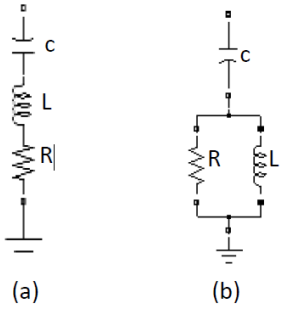

Figure (13). (a) single or monotype. (b) Dual band

The filter designed using previous equation connected to model circuit at transformer side gave result showing the effect of filter total circuit performance by improving the value of total harmonic distortion which decreasing by 8.8%

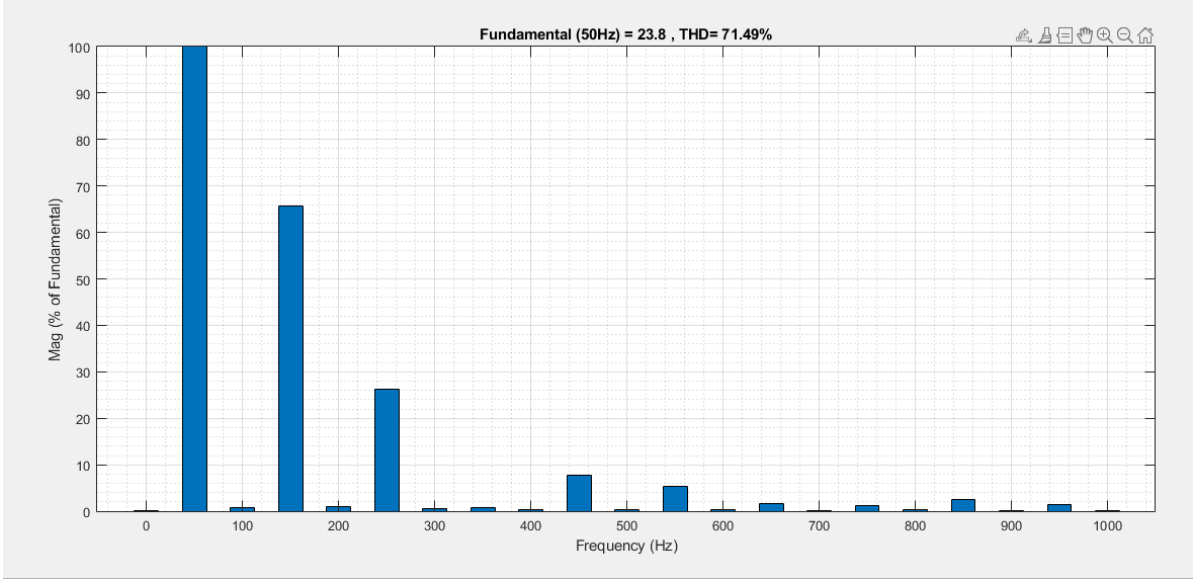

Figure (13) total harmonics distortion (THD) in phase A after filtering

4.Conclusion

The research deals with the operation of a DC motor driven by a rectifier circuit, which consists of a modified three-to-seven-phase transformer. The system suffers from a high amount of harmonic orders due to the high reactances of the circuit and the rectification process. To reduce this amount of THD, a filter was used, in the form of a package of filters (dual band) connected to the transformers for all lines. These packages improved the total harmonic distortion (THD) in the drive circuit by reducing the overall ratio by 8.8%, where before filter insertion it was 81.65%, while after insertion it became 71.49%, decreasing the greatest orders (third and fifth) as main components by 8% and 12.5%, respectively. As a result, the other odd orders were also reduced by 50% at the ninth order and 30% at the eleventh order.For future work to improveme circuit performance an active filters can be used to cover more orders of harmonics eleimination

Conflict of Interest

Authors declare that there is no conflict of interest

5.References

Chandramohan Kalaivani& Padmanaban Sanjeevikumar (2017).Grid Synchronization of a Seven-Phase Wind Electric Generator Using d-q PLL. www.mdpi.com/journal/energies . 10, 926; doi:10.3390/en10070926

H. Rashıd Muhammad, Power Electronıcs Handbook, Academıc Press,2001.

Hu HeJun, Wang JunJia, Huang YiYun & Chen Hui.(2022) Analysis and Suppression of Harmonic Characteristic for Multi-pulse Rectifier Based on Phase-shifting Transformer. Conference Series 2237.doi:10.1088/1742-6596/2237/1/012003

I. Masoud Mahmoud.(2015).Fully controlled 5-phase, 10-pulse, line commutated rectifier. Alexandria University Alexandria Engineering Journal, Volume 54, Issue 4, Pages 1091-1104.
doi: 10.1016/j.aej.2015.07.004

I.Zynal Hussein & A.Fadeel Bashar.(2014). Analysis and Design of Passive Filters to Reduce Line Current Harmonics for Controlled Rectifiers Al-Rafidain Engineering Vol.22 No. 1

Moinoddin Shaikh, Iqbal Atif, Abu-Rub Haitham & Ahmed Sk. Moin .(2012). Three-Phase to Seven-Phase Power Converting Transformer. IEEE TRANSACTIONS ON ENERGY CONVERSION, VOL. 27, NO. 3. **doi:** 10.1109/TEC.2012.2201483

Salim Alattar Myasar & A.Salih Asef.(2022).Analysis of a novel seven phase uncontrolled rectifier system International Research Journal of Engineering and Technology (IRJET). 2395-0056 Volume: 09 Issue: 08

Tabrez M.& Iqbal A. (2017). A Novel Three Phase to Seven Phase Conversion Technique Using Transformer Winding Connections. Engineering, Technology & Applied Science Research. Vol. 7, No. 5, 1953-1961 1953. https://doi.org/10.48084/etasr.1190

Adequate compensation of dstatcom-based fgs for mitigating the impact of source disturbances in radial power systems

Ahmed Samir Alhattab[1*], Dr .Ahmed Nasser B. Alsammak[2], Dr. Hasan Adnan Mohammed[3]
[1, 2, 3] Electrical Engineering Department, College of Engineering, University of Mosul , Mosul-Iraq
[1] ORCID No: https://orcid.org/0000-0002-0334-4736
[2] ORCID No: https://orcid.org/0000-0002-1248-4538
[3] ORCID No: https://orcid.org/0000-0002-5071-0102

Keywords
D-STATCOM, sensitive load, FGS controller, response optimizer, voltage disturbance.

Abstract
Electrical power systems are often exposed to disturbances due to various factors (internal and external). One of these disturbances is source voltage disturbance. The source voltage sags and swells, significantly affecting sensitive loads and the rest of the system's equipment, causing them to work less well or even break down. Because of this, the effects of these disturbances on the power system should be lessened. One of the most effective solutions is to employ modern power electronics technologies such as Distribution Static Synchronous Compensator (D-STATCOM) as one of the custom power devices. Conventional PI controllers are commonly used in D-STATCOM but are not adaptive to large disturbances, which can lead to significant performance degradation. Also, the tuning methods of their parameters are tedious and time consumed. In this work, a fuzzy gain scheduled (FGS) controller integrated with PI parameters was used to provide adaptive performance in a wide range of source voltage disturbances for a radial power system. The optimal parameters were found by the response optimizer tool. Simulation of the system operation was carried out using MATLAB/Simulink software. The simulation results showed adaptive performance and superiority in response speed and overshoot value in the fuzzy control unit compared to the traditional PI units.

Research Article
Submission Date : 13.04.2023
Accepted Date : 30.05.2023

1. Introduction

Previously, consumer equipment was immune to short-term power fluctuations and didn't cause electrical grid problems. But now, the nature of loads in industrial, commercial, and residential facilities has changed as a result of the widespread use of modern technology that relies on computing and microprocessors, so most electrical appliances and equipment are described as sensitive loads, which require feeding them from a high-quality source, in addition to being continuous. The power quality problem refers to any deviation of voltage, frequency, and current from its standard values, which can be a reason for malfunction or poor performance of customer equipment. Among power quality problems, sag and swell in voltage are the most common problems (sag happens up to 80% of the time) (Shahgholian and Azimi 2016). For customers, the economic impact of these electrical power quality disturbances can reach millions of dollars, while for electric utilities, electrical power quality disturbances lead to dissatisfaction with consumers and decreasing income. So, the electrical power quality importance is significantly increasing for both electric utilities and customers (Van den Broeck, Stuyts, and Driesen 2018).

* Resp author ; e-mail: ahmed.20enp53@student.uomosul.edu.iq

The magnitude of supply voltage is a parameter that should be preserved in the overall power system. Any change in the source voltage magnitude results in voltage changes at all system levels. The distribution level is regarded as the most system-level affected by power quality problems due to two reasons: firstly, the increased use of renewable energy sources is interconnected with the distribution system, and these interrupted sources result in several power quality problems that affect the performance of the whole system, and secondly, the end users' power quality problems are coupled with the distribution system. The nature of renewable energy sources or the loads, whether inductive or capacitive, heavy or light, and the nonlinear customer devices that draw non-sinusoidal currents that pollute the supply system, are all these issues regarded as important issues and require creative solutions continuously (Mararakanye and Bekker 2019; Naderi et al. 2018).

Reactive power compensation is one of the most significant power quality problem solutions. It has benefits for improving voltage profile, power factor correction, voltage stability, and increased transfer and operation capacity of lines and devices of the system, in addition to reducing energy losses (Abdelsalam, Ghoneim, and Salem 2022). Conventionally, it has used devices such as capacitor banks, tap changers, and Static Var Compensators for reactive power compensation. however, these devices suffer from many disadvantages, such as slow response, bulky size, resonance, high losses, noise, and require continuous maintenance (Gawande, Khan, and Ramteke 2013). But with the rapid development of the semiconductor industry and control systems in recent decades, fast compensation has enabled using controllable power electronic devices. These compensation devices are the Custom Power Devices (CPD) and Distribution Static Synchronous Compensator (DSTATCOM) is an essential device of this family (Masdi et al. 2004).

DSTATCOM is installed in parallel near sensitive loads to improve power quality. It is broadly used for sag and swell voltage mitigation, power factor correction, harmonic elimination, and voltage or load balancing (Gupta, Fritz, and Kahn 2017). The CPD includes other compensation devices like series type, namely Dynamic Voltage Restorer (DVR) (Danalakshmi, Bugata, and Kohila 2019) and hybrid type, namely Unified Power Quality Compensation (UPQC) (Qasim, Alsammak, and Tahir 2022).

In (Eltamaly et al. 2021) the PI unit is used in DSTATCOM to regulate AC voltage due to its simplicity of installation and ease of implementation. However, during the validation and modification process, the response degraded. Generally, the PI unit suffers from some disadvantages, such as not being adaptive; in other words, its performance is degraded at significant disturbances because its parameters are designed for specific conditions. Also, these parameters are tuned in traditional methods like trial and error, which are tedious and time consumed and do not provide an optimal response permanently (Nguyen, Nguyen, and Le 2020).

In this work, intelligent techniques have been utilized to overcome these disadvantages. An optimization method has been used to find optimal PI parameters for all points of working with the help of the response optimizer tool, and the fuzzy gain schedule was utilized to provide adaptivity in the controller. Two fuzzy units for both (Kp and Ki) controlling were created by Adaptive Neuro Fuzzy Interference System (ANFIS) to override the complication of fuzzy controllers' design.

2. Distribution static synchronous compensator

DSTATCOM mainly consists of a transformer and coupling reactance, a voltage source converter, dc energy storage, a controller, and a harmonics filter as depicted in Figure (1)(Kumar, Kumar, and Akella 2014). The transformer is used to match the output voltage of the converter with the grid voltage, the coupling reactor provides isolation between the grid and converter, the voltage source converter is working to generate three-phase ac voltages from dc voltage, and a filter is used to remove ripples from converter current (Arya et al. 2020).

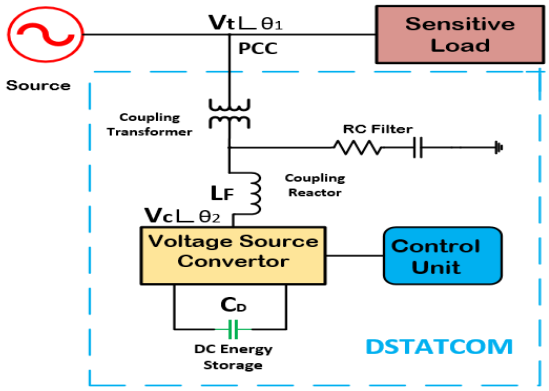

Figure 1. Main parts of DSTATCOM

2.1 Working principle of DSTATCOM

DSTATCOM is connected to the grid at the point of common coupling (PCC) where it is required to address the power quality problem. The compensation of reactive power depends on the voltage difference between the magnitude of grid voltage (V_t) and converter output voltage (V_c), if (V_t) is smaller than (V_c) the reactive compensation will be transferred from DSTATCOM to the grid, but if (V_t) is greater than (V_c) the reactive compensation will be transfer from the grid to DSTATCOM, while there is no reactive compensation transferred if the two voltages are equal (Adnan and Alsammak 2020). Practically, there is a small phase shift between the grid voltage angle (θ_1) and the compensator voltage angle (θ_2) allowing to transfer of small active power from the grid to DSTATCOM to cover the internal losses of the latter, the equations (1), (2), (3) are used to calculate phase shift angle (δ), active and reactive power transferred (Yousif and Mohammed 2021).

$$\delta = \theta_1 - \theta_2 \tag{1}$$

$$P = \frac{V_t V_c}{X} \sin\delta \tag{2}$$

$$Q = \frac{V_t(V_t - V_c \cos\delta)}{X} \tag{3}$$

Where δ is a phase shift angle, θ_1 is a grid voltage angle, θ_2 is a compensator voltage angle, P is an active power, Q is a reactive power, V_t is a grid voltage, V_c is a converter voltage, and X is a coupling reactance.

2.2 Controlling in DSTATCOM

The controller plays a vital role in the functioning of DSTATCOM. Its function is to take samples of the system voltages and currents and compare them with the reference values and resulting in an error value which used to extract the appropriate signals for the pulses generator to trigger switches of the voltage source converter for an adequate compensation of reactive power value to mitigate the power quality problem at this point (Latran, Teke, and Yoldaş 2015). As Synchronous Reference Frame (SRF) or dq theory used in the conventional control of DSTATCOM, it is needed PI units for each AC voltage regulator, DC voltage regulator, and current regulator, as shown in Figure 2 (Bapaiah 2013).

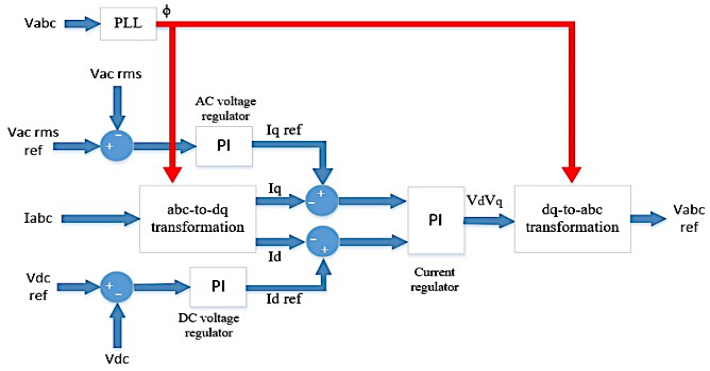

Figure 2. Conventional PI control of DSTATCOM

The response optimizer tool in Matlab was used to get the optimal Kp and Ki parameters at different source voltage values. These (input/output) data sets had downloaded in the ANFIS editor, as shown in Figure. 3, the two fuzzy systems are created to control both Kp and Ki by the intelligent controller, which is a combination of fuzzy and PI units (FGS). This proposed FGS unit is instead with the conventional PI unit in an AC voltage regulator to produce proper reference compensation component and adequate reactive compensation at the different voltage values of the source. Figure. 4 show the proposed control unit in the AC voltage regulator.

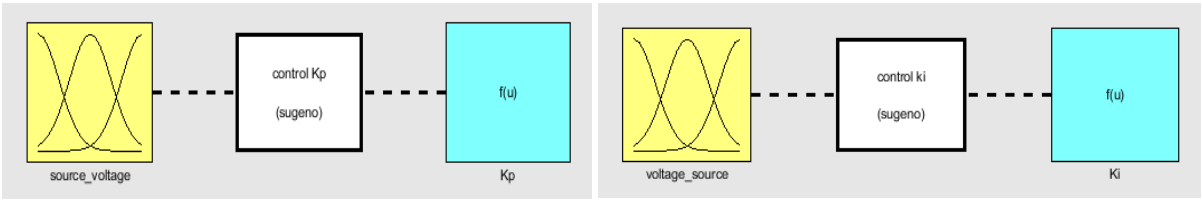

(a) (b)

Figure 3. Proposed fuzzy logic system.
(a) Fuzzy logic control of Kp.
(b) Fuzzy logic control of Ki.

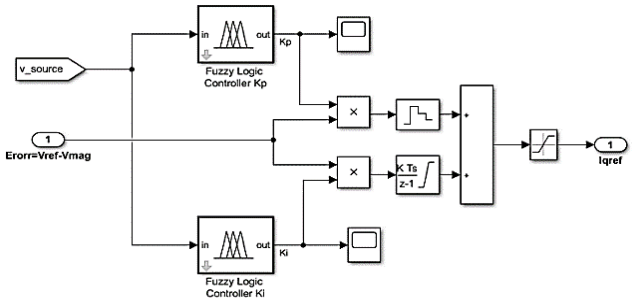

Figure 4. The scheme of proposed control (FGS) unit in the AC voltage regulator of DSTATCOM

3. Simulation result

Simulations were carried out on the radial distribution power system shown in Figure 5. using Simulink/Matlab package. This system consists of a voltage source, three buses, transmission lines between them, and a distribution transformer at bus 3 feeds a sensitive load at its end, in addition to loads at buses 1 and 2. The DSTATCOM is connected close to the sensitive load at bus 3. The simulation is performed with and without DSTATCOM for both the two cases of disturbance in the source voltage shown in the subsections below:

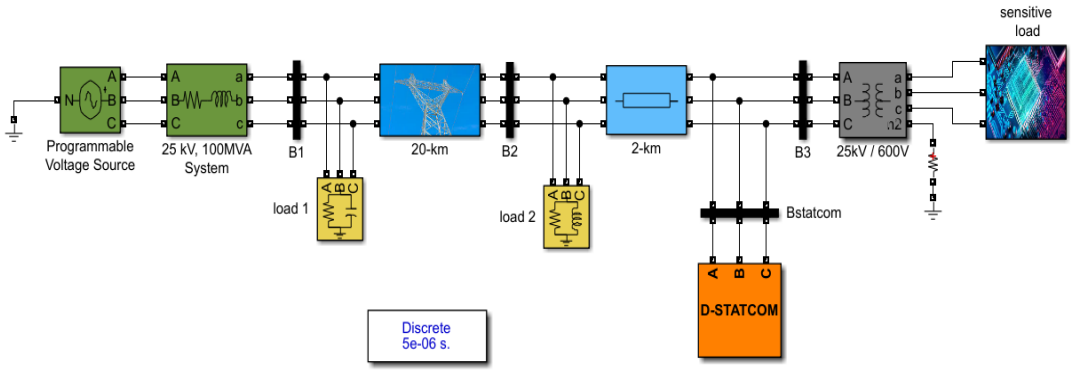

Figure 5. The radial power system simulated in Matlab

3.1. A sag of source voltage

The first disturbance was the source voltage sagging, which was represented by a decrease in the source voltage for the period (0.3 to 0.7 s) by a value of (0.15 p.u). As a result, without using DSTATCOM, the voltage was decreased to (0.85 p.u) at bus 3, as shown in Figure (6a).

DSTATCOM of a PI control unit was connected to the system, and the simulation had a rerun. The voltage at bus 3 is red in Figure (6b). It is clear, through the appearance of continuous voltage fluctuation throughout the disturbance period, that DSTATCOM did not regulate the voltage to the nominal value due to the PI control unit not working correctly, which caused inappropriate compensation and bad performance of DSTATCOM. The simulation had rerun after connecting DSTATCOM with the proposed fuzzy-PI control unit. The apparent improvement in its work and response is noted in mitigating this disturbance and regulating the voltage to the nominal value (1 p.u) within a short time of about 0.08s, as shown in Figure (6b) in blue; the reason behind that is the appropriate compensation through the proper working of the proposed control unit. Figure (7) shows the optimal Kp and Ki parameters of a fuzzy controller provided for the PI control unit continuously when the source voltage changes through the disturbance period.

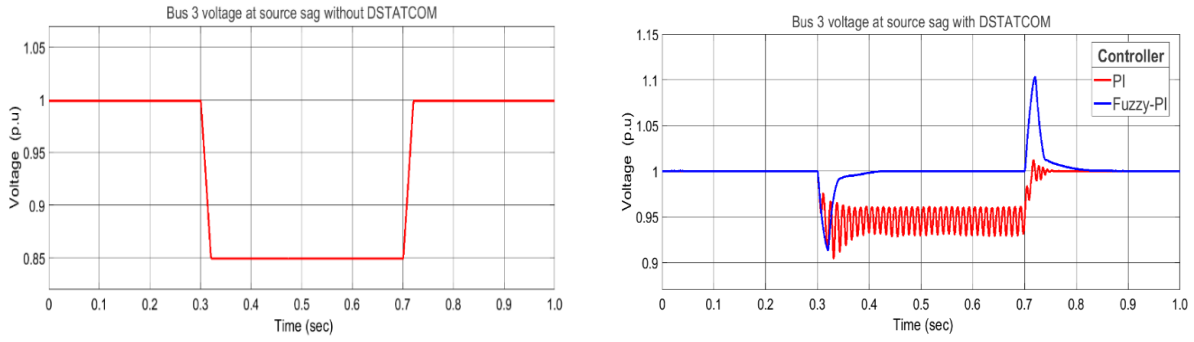

(a) (b)

Figure 6. Bus 3 voltage at source sag (a) without DSTATCOM (b) with DSTATCOM

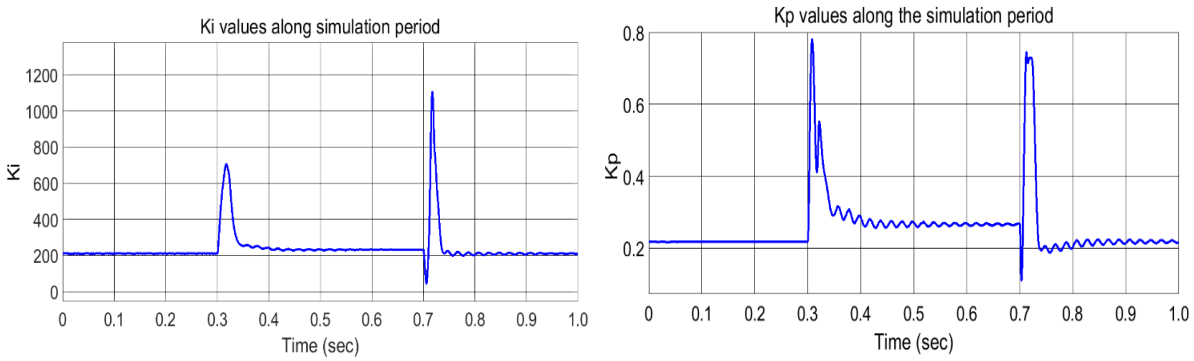

(a) (b)

Figure 7. Fuzzy unit output at source swelling simulation for a parameter of (a) Ki, (b) Kp

3.2. A swell of source voltage

It is one of the disturbances that badly affects the performance of sensitive loads. It may lead to them going out of work, which may have internal causes such as increased excitation of the synchronous generator and poor control prosses, or external such as turning on a capacitors bank or turning off a large inductive load (Al juboori, Al-Younus, and Alrawe 2022). This disturbance was done by applying an increasing source voltage by a value of 0.15 p.u for a period 0.3 to 0.7 s. As a result, without using DSTATCOM, the voltage was increased to (1.15 p.u), as shown in Figure (8a).

DSTATCOM of a PI control unit was connected to the system, and the simulation had a rerun. The performance of the DSTATCOM was bad, as this disturbance was not mitigated, and the fluctuation of the voltage along the disturbance period appeared as a result of the incompatibility of the original PI parameters with the system conditions during the disturbance, as shown in Figure (8b) in red.

The simulation had rerun after connecting DSTATCOM for this case with the proposed fuzzy-PI control unit. The performance of DSTATCOM was significantly improved, as depicted in Figure (8b) in blue color. This intelligent response will provide optimal control parameters at all voltage source values. These optimal parameters are reflected in the compensator's response and, consequently the compensation process's efficiency. Figure (9) shows the optimal values changing of Kp and Ki parameters through the source voltage disturbance period.

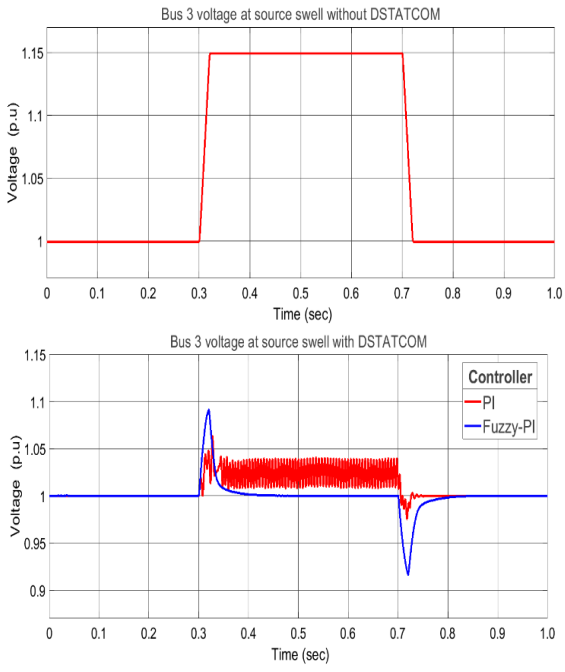

(a) (b)

Figure 8. Bus 3 voltage at the swelling of source (a) without DSTATCOM (b) with DSTATCOM

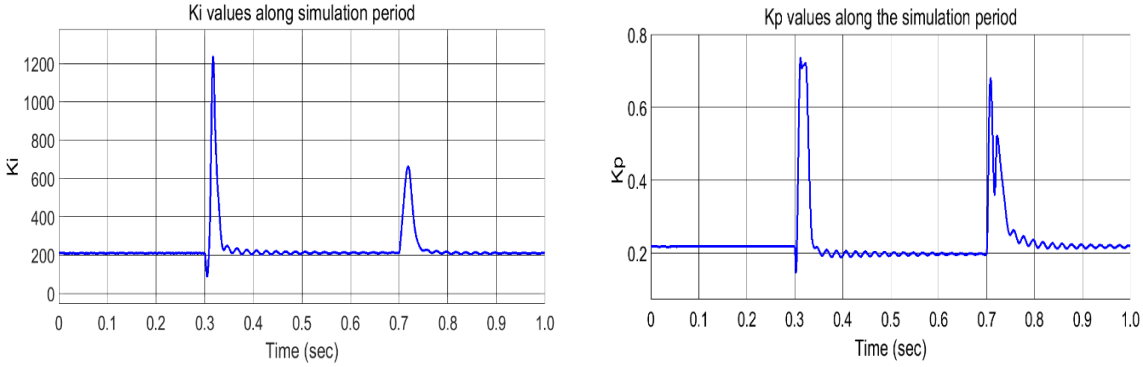

(a) (b)

Figure 9. Fuzzy unit output at source swelling simulation for a parameter of (a) Ki, (b) Kp

4. Conclusion

Voltage source disturbances badly affect the power quality in electric power systems. Sensitive loads require high power quality to operate correctly with high efficiency. Reactive power compensation is one of the most effective solutions to reduce disturbances in electrical power systems. It must be an appropriate value in the shortest time to ensure effective compensation. DSTATCOM is custom power devices broadly used due to its ability to mitigate various disturbances. The traditional PI controller is commonly used, but it suffers from some problems, such as; a lack of adaptation to significant disturbances or changing system conditions and weaknesses in its tuning methods. Optimization with the help of Artificial Intelligent techniques was used to obtain the optimal parameters of Pi controller, in addition to replacing the traditional controller with an intelligent one composed of integrating the fuzzy controller with PI units. The simulation results showed performance and response advancement of a proposed intelligent control unit and a significant improvement in mitigating disturbances of sagging and swelling source voltage compared to traditional unit that suffers from delayed response and oscillation.

Conflict of interest

There was no conflict of interest between the authors during the creation of this study. No financial support has been received and there are no conditions that provide financial or personal benefit.

Contribution of authors

The authors involved in this study are Ahmed Samir Alhattab, Dr. Ahmed Nasser B. Alsammak, Dr. Hasan Adnan Mohammed; contributed to all aspects of the study. All authors contributed to the idea, design, inspection, resources, data collection, literature review, critical review and analysis and interpretation sections of the study.

References

Abdelsalam, Abdelazeem A., Sherif S. M. Ghoneim, and Ahmed A. Salem. 2022. "An Efficient Compensation of Modified DSTATCOM for Improving Microgrid Operation." *Alexandria Engineering Journal* 61(7):5501–16. doi: 10.1016/j.aej.2021.10.061.

Adnan, Hasan, and Ahmaed Alsammak. 2020. "A Comparison Study of the Most Important Types of the Flexible Alternating Current Transmission Systems(FACTs)." *Al-Rafidain Engineering Journal (AREJ)* 25(1):49–55. doi: 10.33899/rengj.2020.126854.1027.

Arya, Sabha Raj, Mittal M. Patel, Sayed Javed Alam, Jayadeep Srikakolapu, and Ashutosh K. Giri. 2020. "Phase Lock Loop–Based Algorithms for DSTATCOM to Mitigate Load Created Power Quality Problems." *International Transactions on Electrical Energy Systems* 30(1):1–26. doi: 10.1002/2050-7038.12161.

Bapaiah, P. 2013. "Power Quality Improvement by Using DSTATCOM." *International Journal of Emerging Trends in Electrical and Electronics* 2(4):1–12.

Van den Broeck, Giel, Jeroen Stuyts, and Johan Driesen. 2018. "A Critical Review of Power Quality Standards

and Definitions Applied to DC Microgrids." *Applied Energy* 229(July):281–88. doi: 10.1016/j.apenergy.2018.07.058.

Danalakshmi, D., Srinivas Bugata, and J. Kohila. 2019. "A Control Strategy on Power Quality Improvement in Consumer Side Using Custom Power Device." *Indonesian Journal of Electrical Engineering and Computer Science* 15(1):80–87. doi: 10.11591/ijeecs.v15.i1.pp80-87.

Eltamaly, A. M., Y. S. Mohamed, A. H. M. El-Sayed, A. N. A. Elghaffar, and A. G. Abo-Khalil. 2021. "D-STATCOM for Distribution Network Compensation Linked with Wind Generation." Pp. 87–107 in *Control and Operation of Grid-Connected Wind Energy Systems*. Springer-Cham.

Gawande, S. P., S. Khan, and M. R. Ramteke. 2013. "Design Consideration for Configuration, Topology & Control Schemes of DSTATCOM Implemented on Distribution Systems." *Lecture Notes on Information Theory* 1(3):89–94. doi: 10.12720/lnit.1.3.89-94.

Gupta, G., W. Fritz, and M. T. E. Kahn. 2017. "A Comprehensive Review of DSTATCOM: Control and Compensation Strategies." *International Journal of Applied Engineering Research* 12(12):3387–93.

Al juboori, Mohammad, Yousif Al-Younus, and Mohammed Ali Alrawe. 2022. "Impact Study of Unequal Voltages of Power Plants (Generators)." *Al-Rafidain Engineering Journal (AREJ)* 27(2):110–16. doi: 10.33899/rengj.2022.134000.1176.

Kumar, Pradeep, Niranjan Kumar, and A. K. Akella. 2014. "A Simulation Based Case Study for Control of DSTATCOM." *ISA Transactions* 53(3):767–75. doi: 10.1016/j.isatra.2013.11.008.

Latran, Mohammed Barghi, Ahmet Teke, and Yeliz Yoldaş. 2015. "Mitigation of Power Quality Problems Using Distribution Static Synchronous Compensator: A Comprehensive Review." *IET Power Electronics* 8(7):1312–28. doi: 10.1049/iet-pel.2014.0531.

Mararakanye, Ndamulelo, and Bernard Bekker. 2019. "Renewable Energy Integration Impacts within the Context of Generator Type, Penetration Level and Grid Characteristics." *Renewable and Sustainable Energy Reviews* 108(October 2018):441–51. doi: 10.1016/j.rser.2019.03.045.

Masdi, Hendri, Norman Mariun, S. M. Bashi, Azah Mohamed, and Sallehhudin Yusuf. 2004. "Design o f a Prototype D-Statcom for Voltage Sag Mitigation." Pp. 112–27 in *Proceedings. National Power and Energy Conference, 2004.* Kuala Lumpur, Malaysia: IEEE.

Naderi, Yahya, Seyed Hossein Hosseini, Saeid Ghassem Zadeh, Behnam Mohammadi-Ivatloo, Juan C. Vasquez, and Josep M. Guerrero. 2018. "An Overview of Power Quality Enhancement Techniques Applied to Distributed Generation in Electrical Distribution Networks." *Renewable and Sustainable Energy Reviews* 93(May 2017):201–14. doi: 10.1016/j.rser.2018.05.013.

Nguyen, Huu Vinh, Hung Nguyen, and Kim Hung Le. 2020. *ANFIS and Fuzzy Tuning of PID Controller for STATCOM to Enhance Power Quality in Multi-Machine System under Large Disturbance*. Vol. 554. Springer International Publishing.

Qasim, Ahmed Yahyia, Ahmed Nasser B. Alsammak, and Fadhil R. Tahir. 2022. "Optimization of Power Quality Using the Unified Power Quality Conditioner (UPQC) with Unbalanced Loads." *Al-Rafidain Engineering Journal (AREJ)* 27(2):101–9. doi: 10.33899/rengj.2022.133962.1175.

Shahgholian, Ghazanfar, and Zahra Azimi. 2016. "Analysis and Design of a DSTATCOM Based on Sliding Mode Control Strategy for Improvement of Voltage Sag in Distribution Systems." *Electronics (Switzerland)* 5(3). doi: 10.3390/electronics5030041.

Yousif, Sabah, and Saad Mohammed. 2021. "Reactive Power Control Using STATCOM for Power System Voltage Improvement." *Al-Rafidain Engineering Journal (AREJ)* 26(2):124–31. doi: 10.33899/rengj.2021.128914.1070.

DQ model of PMSG with the most proficient dynamic analysis in standalone grid

Ammar Shamil Ghanim[1], Ahmed Nasser B. Alsammak [2]

[1]Department of Electrical Engineering, College of Engineering, University of Mosul, Mosul
ORCID No: https://orcid.org/. 0000-0002-3602-5491
[2]Department of Electrical Engineering, College of Engineering, University of Mosul, Mosul
ORCID No: https://orcid.org/0000-0002-1248-4538

Keywords

PMSG, Pico hydro, Modelling İsolated grid, Dynamic model

Abstract

The pico grid implements an essential solution to provide electrical power for isolated areas like villages and remote regions. Wind, tidal or hydropower, etc., may be the energy source for these grids. This application can be effectively served by a permanent magnet synchronous generator (PMSG), which is a very convenient option. In this work, the generator's prime mover is a regular speed source that mimics a pico-hydro turbine. Using park transformation, the dynamic model was built and employed in Matlab/Simulink to study the system's response with different perturbations for operation at constant and variable of load, rotor speed, and flux. The results of the proposed system model show a smooth voltage and current output.

Research Article
Submission Date : 08.04.2023
Accepted Date : 07.06.2023

1. Introduction

Renewable energy sources (RES) consider a solution in terms of providing electricity for isolate societies which located remotely from the national grid (NG)(F. AL Kababjie & H. Hamdon, 2013); also, the case of providing power is a more economical solution than depending on NG(Williamson et al., 2017). another reason for the developed interest in the RES is to preserve the environment from gaseous emissions resulting from dependence on traditional energy sources such as coal and other fossil fuel sources(Ghanim & Alsammak, 2020); also, there are some countries face difficulty to provide fossil fuels, either due to economic difficulties, or because they are not naturally available to them, or due to geopolitical complication, like what happened in the recent crisis between Russia and Ukraine.

Based on what was mentioned above, it is clear that the dependence on the RES maybe not be a choice but a fact, and from that point, the study of that energy source in terms of being more familiar with its weak points to overcome it, or to increase the efficiency of its generation components is a significant concern.

Pico hydro turbine considers a friendly environment source of energy that depends on the flowing of water to produce electricity(Praptodiyono et al., 2021). In this paper, the hydro turbine is assumed to be a pico one in which it produces lower than 5kw(Zainuddin et al., 2009). the main difference between hydro and other RES like tidal or wind, that it is approximately has a constant speed, where the speed of water flow changes seasonally, not like wind turbines where the speed varies in less than a minute, so in this paper, a constant speed source will be assumed as a simulation to the pico hydro turbine.

Various types of generators are used with the hydro turbine, but the most typically used with pico grids is the PMSG generator(Murali Krishna et al., 2022) because it has a permanent excitation, not like a winding rotor, so it needing for maintenance is limited due to the absence of rings and brooms(Fateh et al., 2016); also the development in material science regarded to hard magnetic materials, make the characteristics of PMSG became more efficient and compact(Quintal-Palomo et al., 2021). Another advantage of using PMSG is that the slow rotor speed does not need the gearbox in direct drive machines (Wang et al., 2014).

[1]Resp author; e-mail:ammarshamilhanon@uomosul.edu.iq

The representation with DQ model has excellent importance like the easiness of depending on the constant variable with time(Rotor reference frame), compared with the variable in the ABC stationary frame, which varies instantaneously with time. Hence, designing the control circuit is much easier with this model(Ghanim et al., 2022), also the use of models in the study of PMSG production provides insight into many abnormal situations, such as what happens to the magnet in terms of demagnetizing impact owing to increased temperature or some sorts of defects in general(Uršič & Nemec, 2019).

Many authors dealt with the analysis of PMSG in the previous works of literature; (Mohan & Vittal, 2018), (Hossain et al., 2017), (Bisoyi, 2013)& (Anbarasan et al., 2021); all of them studied the modelling and simulation of standalone PMSG-based wind energy conversion system. The co-simulation approach in dealing with the modelling of PMSG was presented by (Quintal-Palomo et al., 2019) paper. (Chandran et al., 2018) Discussed the existence of PMSG in the small hydro system with a vision to improve the generated voltage. (Fukami et al., 2010) Analysed the behavior of salient pole PMSG in a model derived from the dynamic model. (Williamson et al., 2017) mentioned how to model and simulate the pico-hydro power in an isolated grid. (Zainuddin et al., 2009) Studied the design of a pico hydro generation system using the consuming water distributed to houses. The machine rating used in the paper was taken from (Eduardo & Palomo, 2019), where R_s=5.56**Ω**, L_d=L_q=11.3e-3 H, Npp=2, λr=0.8 wb, 1500rpm.

In this work, Matlab-Simulink will be used to create a DQ model. Then Different simulations will be done under multiple input/output perturbations to provide knowledge about the machine behavior under these perturbations, which can be used later to propose an efficient control algorithm to set the generated voltage at permissible limits.

2. System design:

2.1 Pico hydro turbine:

The hydrolic power available from hydro turbine type undershoot waterwheel is given in Eq (1) :

$$P_{hyd} = 0.5\rho A v^3 \quad (1)$$

So the mechanical power transferred depends on the efficiency of the turbine according to

$$P_m = \eta_{hyd} P_{hyd} \quad (2)$$

In which the turbine efficiency is a function of a constant of the turbine named C given in:

$$\eta_{hyd} = 2C\left(1 - C^2\right) \quad (3)$$

In this context, 'p_{hyd}' represents hydraulic power, 'p_m' denotes mechanical power, 'ρ' signifies water density, 'v' indicates water speed, 'A' represents the swept area by the water wheel, and 'C' is a constant with an approximate value of 1/3 for this particular type of hydro turbine.(Denny, 2004)

2.2 Permanent magnet synchronous generator (PMSG):(Kamruzzaman Khan Prince et al., 2021)

The dynamic model of the PMSG is derived by applying Kirchhoff's voltage law on the circuit of Fig.(1), then the stator DQ voltages are given by Eq. (4) & (5):

$$v_{ds} = -R_s i_{ds} + \omega_r L_q i_{qs} - L_d \rho i_{ds} \quad (4)$$

$$v_{qs} = -R_s i_{qs} - \omega_r L_d i_{ds} + \omega_r \lambda_r - L_q \rho i_{qs} \quad (5)$$

Where v_{ds}, v_{qs}, i_{ds} & i_{qs} are stator DQ axis voltages and current, while R_s, L_d & L_q are the stator winding resistance and inductance for direct and quadrature axis, finally λ_r, ω_r are the rotor flux and mechanical rotational speed.

With some mathematical manipulation, the stator current equations can be written as shown in eq. (6) & (7):

$$i_{ds} = \frac{1}{SL_d}\left(-v_{ds} - R_s i_{ds} + \omega_r L_q i_{qs}\right) \tag{6}$$

$$i_{qs} = \frac{1}{SL_q}\left(-v_{qs} - R_s i_{qs} - \omega_r L_d i_{ds} + \omega_r \lambda_r\right) \tag{7}$$

The electromechanical torque induced in the stator due to the reaction between rotor and stator fluxes is given in Eq(8):

$$Te = \frac{3P}{2}\left(\lambda_r i_{qs} - \left(L_d - L_q\right) i_{ds} i_{qs}\right) \tag{8}$$

for non salient pole machine L_d=L_q, so eq.(8) becomes:

$$Te = \frac{3P}{2}\left(\lambda_r i_{qs}\right) \tag{9}$$

The active power in the DQ frame can be calculated from eq.(10):

$$P = \frac{3}{2}\left(v_{ds}\, i_{ds} + v_{qs} i_{qs}\right) \tag{10}$$

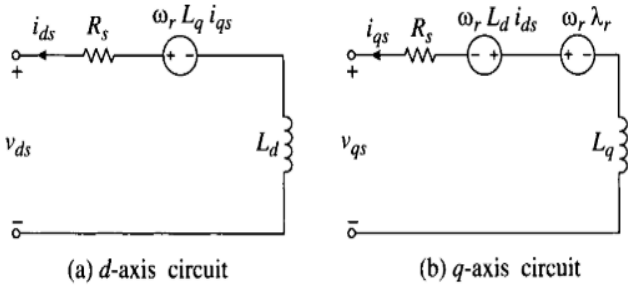

Figure 1. PMSG's dynamic equivalent circuit in the quadrature axis

The Matlab Simulink software was utilized to create Fig. (2) by employing the Simulink Library, incorporating equations (1) to (10) into the simulation.

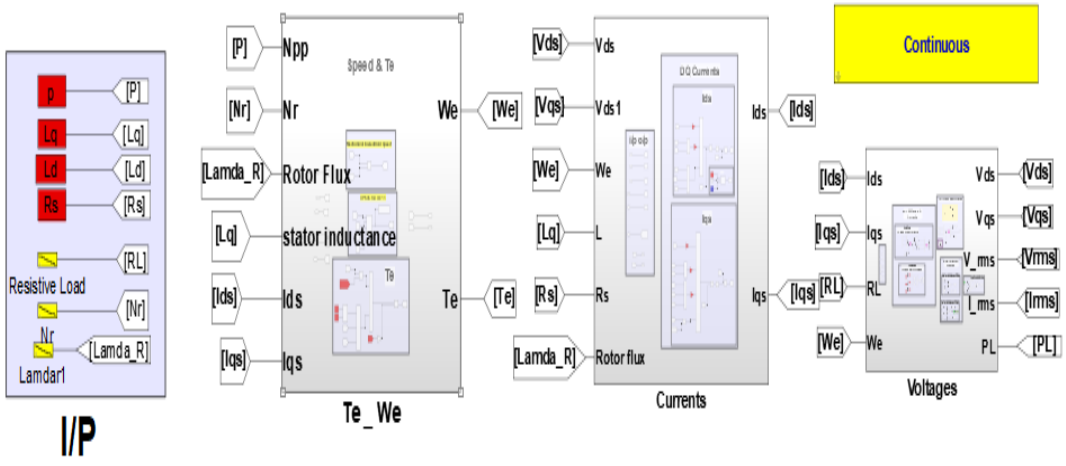

Figure 2. PMSG's dynamic model in Matlab/Simulimk

3. Results and discussion:

3.1 Model validation

The model was validated by comparing the results of (BinWu & Kouro, 2011) model, which is shown in Fig.(3), and the results of the created model, which is shown in Fig(4), for the same rating and operation conditions; the comparison showed that all results were identical.

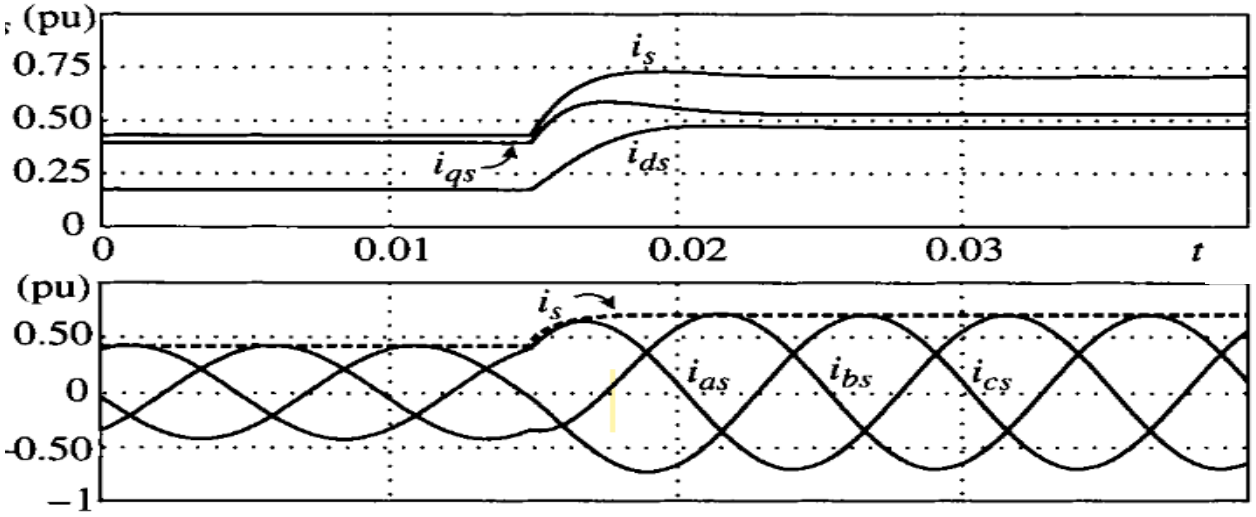

Time(sec)

Figure 3. Bin wu's two & three phase instantaneous & rms currents

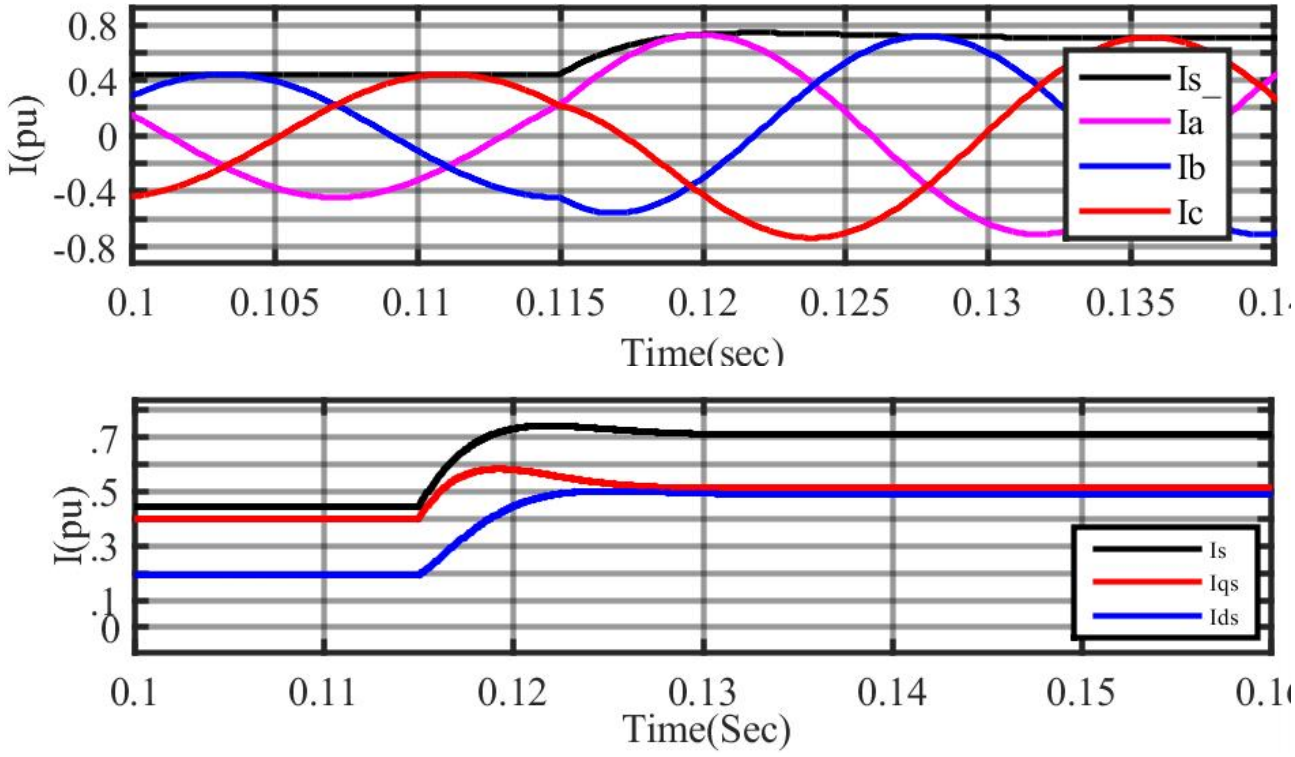

Figure 4. Proposed model's two & three phase instantaneous & rms currents

3.2 Operation at resistive load

3.2.1 Constant load, rotor speed, and flux

After the successful loading of the model with the aforementioned specifications as outlined in the introduction, it was operated with a rotor speed of 1500 rpm, a load resistance of 56 ohms, and a rated rotor flux. The results shown in Fig. (5) & Fig. (6) explain the instantaneous three-phase voltages and currents, which, in turn, have been obtained by using park transformation as a part of the proposed model. In contrast, the results in Fig. (7) were obtained from measurement models built depending on the basic law of power and torque. In Fig. (8), the sum of copper losses power and electromagnetic power equals the input mechanical power.

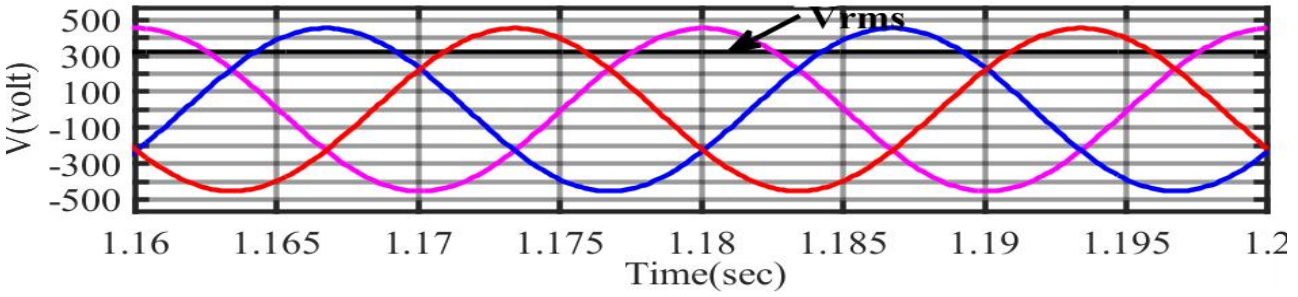

Figure 5. Three phase instantaneous & rms voltages

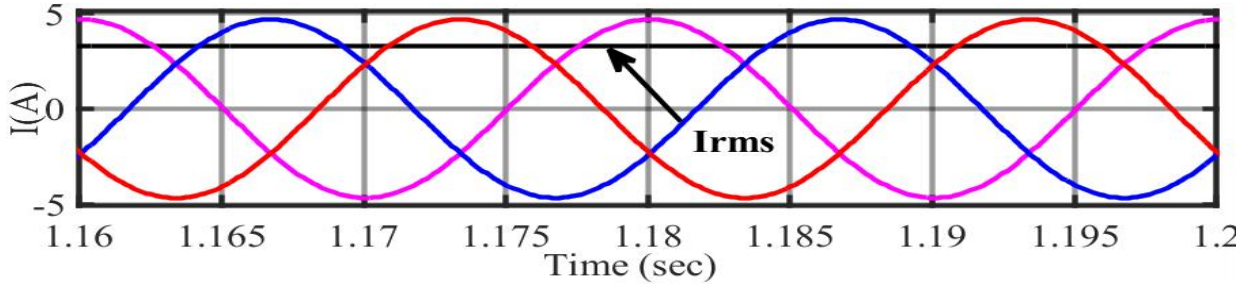

Figure 6. Three phase instantaneous & rms currents

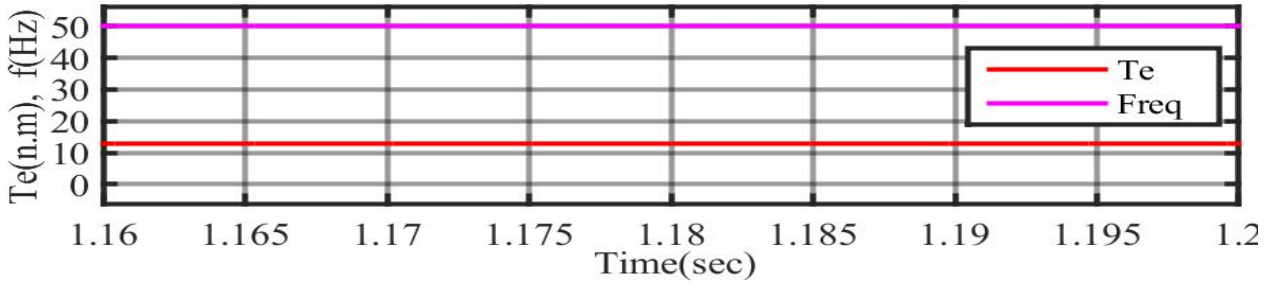

Figure 7. Measured electromagnetic torque and frequency

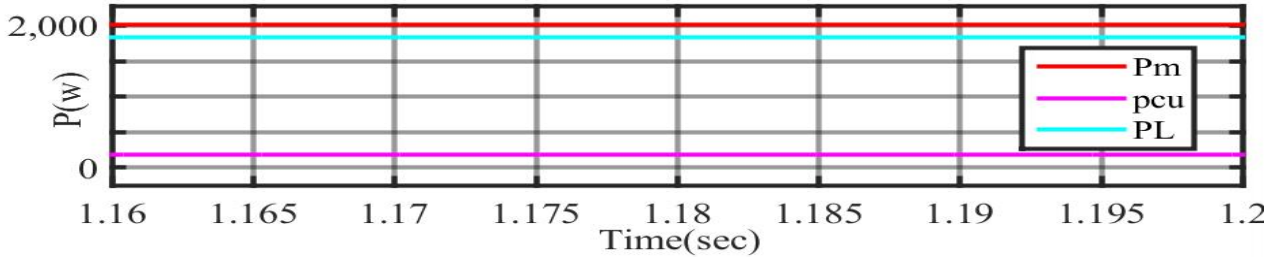

Figure 8. The power for the mechanical (Pm), copper loss (Pcu) & load power (PL)

3.2.2 Constant, speed, variable load & rotor flux

In this operation case, the speed was kept constant at 1500 rpm while both load and rotor flux was changed; Fig. (9) shows the effect of changing the last mentioned quantities on the power vs terminal voltage relation for different values of rotor flux. As a result of the demagnetizing impact caused by an excessive increase in rotor temperature or corrosion, the rotor flux may decrease, while the overrated case also falls under this study, where permanent magnets may be redesigned to greater values to overcome voltage drops due to armature resistance with increased load currents.

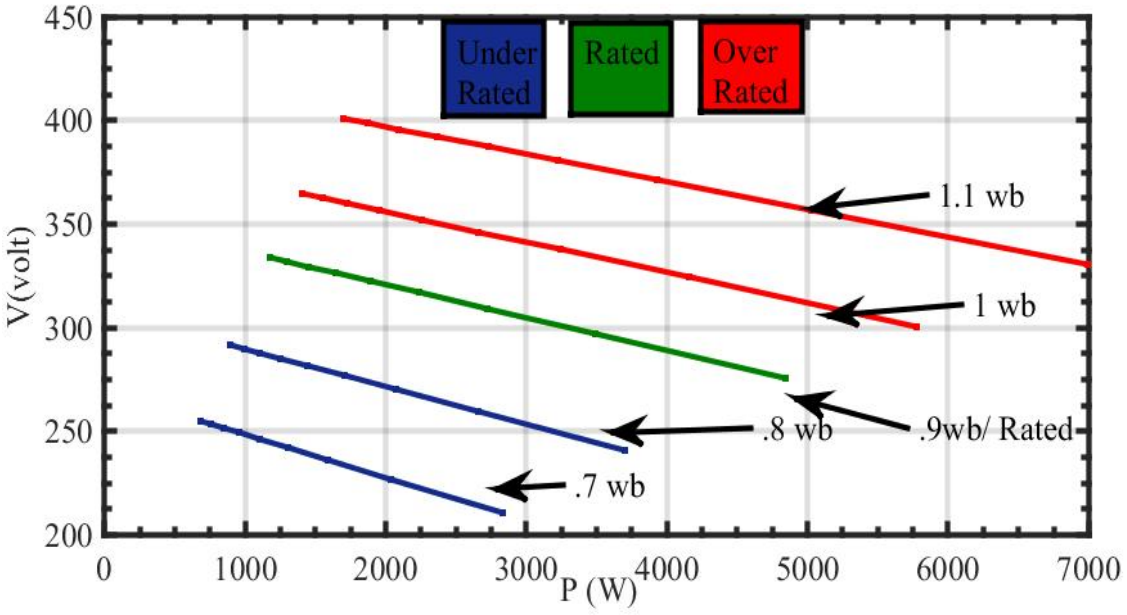

Figure 9. Terminal voltage vs generated power for multiple values of rotor flux

3.2.3 Constant load, variable speed & constant rotor flux

Here, the only variation is due to rotor speed, Fig. (10) shows how the voltage and output power behave with the changing in the mechanical input rotation.

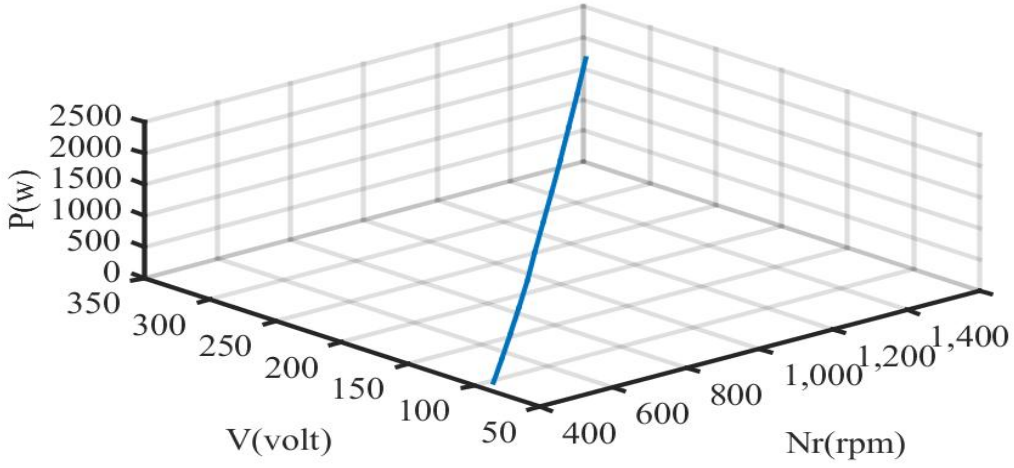

Figure 10. Terminal voltage, generated power vs Rotor speed

3.2.4 Variable load constant speed & rotor flux:

Fig(11) shows the relation between terminal voltage and output power for various load values at constant rotor speed and flux.

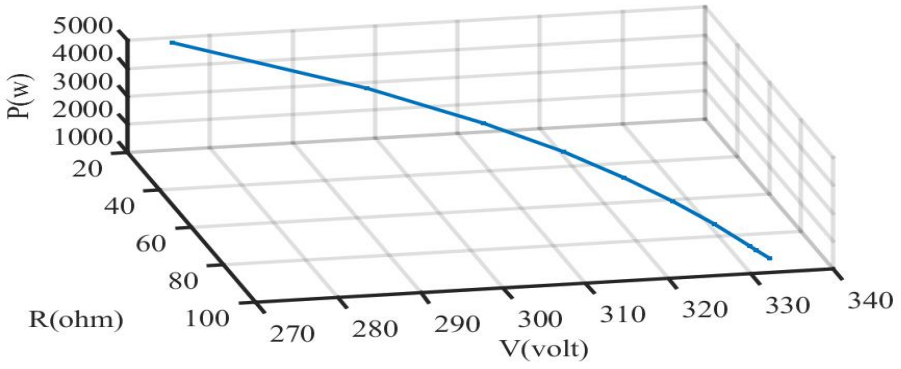

Figure 11. Terminal voltage, generated power vs variable load

4. Conclusions:

Different simulations cases performed with the proposed model show that the disturbances in performance are either constrained externally by changes in mechanical input/ output or internally by changes in rotor flux caused by demagnetizing effects, which results in a factor of time, high temperatures at faults or corrosion effects. These results have indicated the importance of exciting control systems to set the magnitude and frequency of the generated voltage at the rated limits to meet the consumer's needs. The proposed model provides a successful environment to predict the machine's behavior to develop these control algorithms or to modify the machine design, all of that were done by a simple, robust, and understandable model.

Acknowledgements

The authors would like to thank the University of Mosul for their assistance with this work.

Conflict of Interest

Authors declare that there is no conflict of interest.

References

Anbarasan, P., Venmathi, M., & Krishnakumar, V. (2021). Modeling and Simulation of Standalone PMSG based Wind Energy Conversion System with Common Mode Voltage Suppression. *2021 7th International Conference on Electrical Energy Systems (ICEES)*, 85–88. https://doi.org/10.1109/ICEES51510.2021.9383728

Binwu, & Kouro, Y. L. N. Z. S. (2011). Power Conversion And Control Of Wind Energy Systems. A John Wiley & Sons, Inc., Publication. https://ieeexplore.ieee.org/servlet/opac?bknumber=6047595

Bisoyi, S. K. (2013). Modeling and Analysis of Variable Speed Wind Turbine equipped with PMSG. *International Journal of Current Engineering and Technology*, *2*(2), 421–426. https://doi.org/10.14741/ijcet/spl.2.2014.78

Chandran, V. P., Murshid, S., & Singh, B. (2018). Voltage and Frequency Control with Load Levelling of PMSG Based Small-Hydro System. *India International Conference on Power Electronics, IICPE*, *2018-Decem*, 1–6. https://doi.org/10.1109/IICPE.2018.8709475

Denny, M. (2004). The efficiency of overshot and undershot waterwheels. *European Journal of Physics*, *25*(2), 193–202. https://doi.org/10.1088/0143-0807/25/2/006

Eduardo, R., & Palomo, Q. (2019). *Wrocław University of Science and Technology Faculty of Electrical Engineering PhD Thesis*.

F. AL Kababjie, P. D. M., & H. Hamdon, W. (2013). Performance Evaluation study of Hybrid Generation System (Microhydro + Diesel) in Iraqi Remote Rural Electrification_ENG. *AL-Rafdain Engineering Journal (AREJ)*, *21*(2), 32–41. https://doi.org/10.33899/rengj.2013.72823

Fateh, L., Ahmed, O., Amar, O., Abdelhak, D., & Lakhdar, B. (2016). Modeling and control of a permanent magnet synchronous generator dedicated to standalone wind energy conversion system. *Frontiers in Energy*, *10*(2), 155–163. https://doi.org/10.1007/s11708-016-0410-1

Fukami, T., Hayamizu, T., Matsui, Y., & Member, S. (2010). *Steady-State Analysis of a Permanent-Magnet- Assisted Salient-Pole Synchronous Generator*. *25*(2), 388–393.

Ghanim, A. S., Alnaib, I. I., & Bassamaziz, A. (2022). *DQ Model of Three Phase Isolated Induction Generator using Matlab DQ Model of Three Phase Isolated Induction Generator using Matlab*. *October*.

Ghanim, A. S., & Alsammak, A. N. B. (2020). Modelling and Simulation of Self-Excited Induction Generator Driven By a Wind Turbine. *Eastern-European Journal of Enterprise Technologies*, *6*(8), 6–16. https://doi.org/10.15587/1729-4061.2020.213246

Hossain, E., Hossain, J., Sakib, N., & Bayindir, R. (2017). Mdelling and simulation of permanent magnet synchoronous generator wind turbine: A step to microgrid technology. *International Journal of Renewable Energy Research*, *7*(1), 1–8. https://doi.org/10.20508/ijrer.v7i1.5615.g7013

Kamruzzaman Khan Prince, M., T. Arif, M., Gargoom, A., M. T. Oo, A., & Enamul Haque, M. (2021). Modeling, Parameter Measurement, and Control of PMSG-based Grid-connected Wind Energy Conversion System. *Journal of Modern Power Systems and Clean Energy*, *9*(5), 1054–1065. https://doi.org/10.35833/MPCE.2020.000601

Mohan, M., & Vittal, K. P. (2018). Modeling and Simulation of PMSG-Based Wind Power Generation System. *2018 3rd IEEE International Conference on Recent Trends in Electronics, Information & Communication Technology (RTEICT)*, *1*, 57–62. https://doi.org/10.1109/RTEICT42901.2018.9012620

Murali Krishna, V. B., Duvvuri, S. S., Yadlapati, K., Pidikiti, T., & Sudheer, P. (2022). Deployment and performance measurement of renewable energy based permanent magnet synchronous generator system. *Measurement: Sensors*, *24*(August), 100478. https://doi.org/10.1016/j.measen.2022.100478

Praptodiyono, S., Maghfiroh, H., Nizam, M., Hermanu, C., & Wibowo, A. (2021). Design and Prototyping of Electronic Load Controller for Pico Hydropower System. *Jurnal Ilmiah Teknik Elektro Komputer Dan Informatika*, *7*(3), 461. https://doi.org/10.26555/jiteki.v7i3.22271

Quintal-Palomo, R. E., Flota-Banuelos, M., Bassam, A., Peon-Escalante, R., Penunuri, F., & Dybkowski, M. (2021). Post-Fault Demagnetization of a PMSG Under Field Oriented Control Operation. *IEEE Access*, *9*, 53838–53848. https://doi.org/10.1109/ACCESS.2021.3070531

Quintal-Palomo, R. E., Gwozdziewicz, M., & Dybkowski, M. (2019). Modelling and co-simulation of a permanent magnet synchronous generator. *COMPEL - The International Journal for Computation and Mathematics in Electrical and Electronic Engineering*, *38*(6), 1904–1917. https://doi.org/10.1108/COMPEL-12-2018-0501

Uršič, L., & Nemec, M. (2019). Permanent magnet synchronous machine demagnetisation prevention and torque estimation control considering rotor temperature. *IET Power Electronics*, *12*(9), 2161–2169. https://doi.org/10.1049/iet-pel.2018.6162

Wang, C.-N., Lin, W.-C., & Le, X.-K. (2014). Modelling of a PMSG Wind Turbine with Autonomous Control. *Mathematical Problems in Engineering*, *2014*, 1–9. https://doi.org/10.1155/2014/856173

Williamson, S. J., Griffo, A., Stark, B. H., & Booker, J. D. (2017). Modeling and simulation of a pico-hydropower off-grid network. In *Modeling and Dynamic Behaviour of Hydropower Plants* (Vol. 100, pp. 225–253). https://doi.org/10.1049/pbpo100e_ch11

Zainuddin, H., Yahaya, M. S., Lazi, J. M., Basar, M. F. M., & Ibrahim, Z. (2009). Design and development of pico-hydro generation system for energy storage using consuming water distributed to houses. *World Academy of Science, Engineering and Technology*, *59*(December 2015), 154–159.